STRUCTURAL ANALYSIS OF AN ALUMINUM PEDESTRIAN BRIDGE IN CONFORMITY TO AASHTO SPECIFICATIONS FOR HIGHWAY BRIDGES & THE ALUMINUM ASSOCIATION DESIGN MANUAL

A Thesis

Presented to

The Graduate Faculty of The University of Akron

In Partial Fulfillment

of the Requirements for the Degree

Master of Science

Ramon Ortiz-Morgado

August 2006

STRUCTURAL ANALYSIS OF AN ALUMINUM PEDESTRIAN BRIDGE

IN CONFORMITY TO AASHTO SPECIFICATIONS FOR HIGHWAY BRIDGES &

THE ALUMINUM ASSOCIATION DESIGN MANUAL

Ramon Ortiz-Morgado

Thesis

Approved:	Accepted:
Advisor Dr. Craig Menzemer	Dean of the College Dr. George K. Haritos
Co-Advisor Dr. Teresa Cutright	Dean of Graduate School Dr. George R. Newkome
Department Chair Dr. Wieslaw Binienda	Date

ABSTRACT

This thesis project was developed with the main objective to present the results obtained from a structural analysis performed on a bridge system patented and produced by PML LOGIS Bridge System Company from Singen, Germany. Its design is intended primarily for pedestrian or bicycle traffic, however it could also be conceived for any possible equestrian or snowmobile passage. In general, the target of the designer is to introduce this bridge concept into the ongoing expanding market for aluminum transportation facilities in the United States. In view of such prospective applications, the groundwork for such structural evaluation consist of the specifications provided by the governing agency which is the American Association of State and Highway Transportation Officials and in consideration of those design provisions stipulated by the Aluminum Association. Its distinctive design, although incorporates simple structural features from a conventional, sturdy and well-built half-through truss, it does show various deficiencies which may possibly put at risk the overall integrity of the system under certain loading and geometric conditions. Therefore, the subject matter of this evaluation is to examine the system response to a set of prescribed load combinations considering the applicable standards and to identify the areas with such potential deficiencies with the intention to delineate appropriate corrective actions.

TABLE OF CONTENTS

LIST OF TABLES

LIST OF FIGURES

CHAPTER I

INTRODUCTION

1.1 General Information

An innovative and modern bridge system for pedestrian, bicycle, and conceivably equestrian or snowmobile traffic has been patented and produced by PML LOGIS Bridge System Company from Singen, Germany. This distinct design is the bridge's second generation (see Figure 1), which assimilates structural features from the conventional design and whose creators are attempting to introduce into the expanding market for transportation facilities in the United States. The overall construction integrity of this system is the subject matter of this evaluation accounting for all applicable federal, state, and local standards and design specifications. As such, the specifications of the governing agency – the American Association of State and Highway Transportation Officials – in conjunction with those stipulated by the Aluminum Association would be the set of rules delimiting the comprehensive assessment of this pedestrian overpass. As illustrated, the PML system bridge incorporates modular construction as typically resembled by Pratt Trusses. A parallel top and bottom chord connected to vertical posts and diagonal members depicts its fundamental layout having the entire framework made of extruded aluminum profiles. These structural sections have been designed and standardized in conformity to the non-rigid nature of the assembly. Prefabricated welded platform units are used to make up the bridge walkway surface, which in turn is supported at each panel joint by double hollow floor beams attached to the lower tension chord of the structure. Conclusively plain hollow square extrusions are used as the remaining elements that include diagonal components and vertical posts all bolted together to form the lateral trusses which in succession function as the handrails of the pony truss bridge.

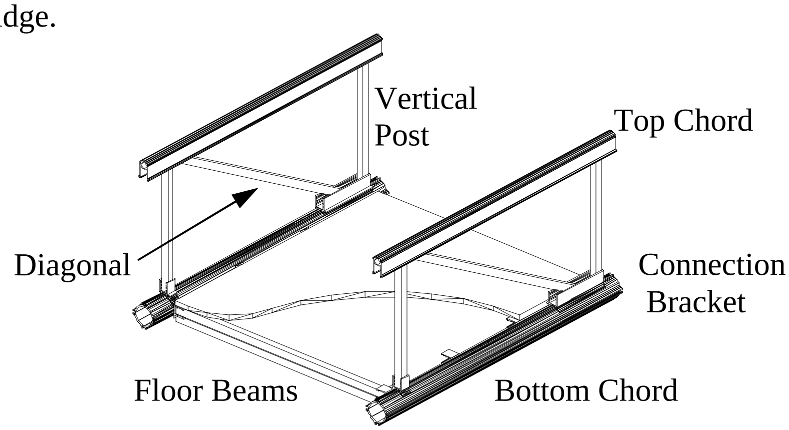

Figure 1: PML System S – Second Generation
Conventional Modular Construction (Pratt Trusses)

1.2 Study Background and Objectives

One of the major shortcomings for half-through type bridges is the development of adequate lateral bracing to the top chord as a compression member. The nature of the end restraints of this frame element promotes an intermittent elastic behavior of each lateral support. Furthermore, its adverse effects on the member's effective length represent the primary factor influencing its load carrying capacity. This is further affected by any potential imperfection of the column material once extruded in the manufacturing shop. As it happens, the overall dimensions of the member - especially minimum cross-sectional thickness and width - in conjunction with the existing support configuration ought to be evaluated due to the direct effect each of these parameters have on the buckling strength of this aluminum component. For that reason, it is the foremost intent of this evaluation to determine the level of structural stability this member has in view of the correlation of every influential aspect previously stated following the aluminum design specifications and to concisely recommend any desirable upgrading if needed be.

An additional consideration that must be accounted for in the analysis is the potentiality of induced combined stresses to the top-chord, which results either from any floor deflections imposed across the walkway surface plus any possible initial crookedness in the flooring system. This specific scenario in conjunction with the impending likelihood of imposed bending moments in the floor beams under minimum design loads has also the means to produce a detrimental effect in the member's capability to sustain prescribed compressive forces. In consequence two prospective alternatives would be considered in this investigation, the heavier bridge-type where the upper compression chord consists of the same tower profile as in the bottom chord, and the lighter version where the upper chord comprise a tubular extrusion with side-flat plates (Figure 2).

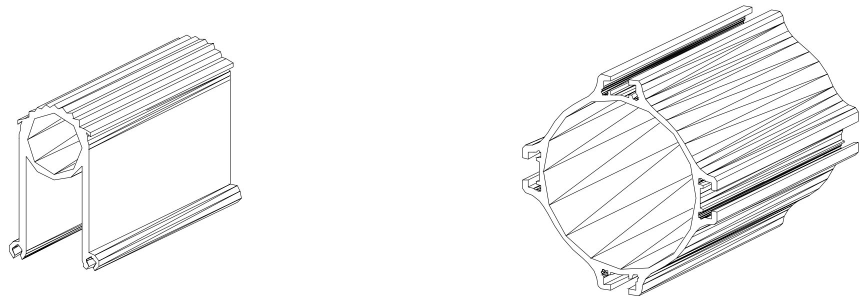

(a) (b)

Figure 2: PML System S – Second Generation
Top Chord Profiles: (a) Tubular Section with Side-flat Plates
(b) Tower Profile

One more disadvantage on the subject of aluminum applications is the adverse effect welding has on the mechanical properties of heat treatable alloys. The structural design of welded connections is a function of several factors such as the prescribed certified welding process, the joint geometry, but specially the filler wire used in the welds. Therefore, in this evaluation the aluminum alloy AA6061-T6 would be regarded as the bridge base material and the alloys AA4043 and AA5356 as the selected filler wires due to is widely spread availability within the structural industry in the United States. Considering the weld design of the supports in this structure (Figure 3), its capacity must be assessed in concordance with the seismic design requirements prescribed by AASHTO. In essence, all mechanical connections on a single-span bridge which joint the superstructure and the foundations must be designed to resist longitudinally and transversely the gravity reaction force at this location multiplied by the acceleration coefficient matching the bridge's geographic location. Specifically, the transverse welded joints at these connections represent the weakest link, even in areas of relatively low stress.

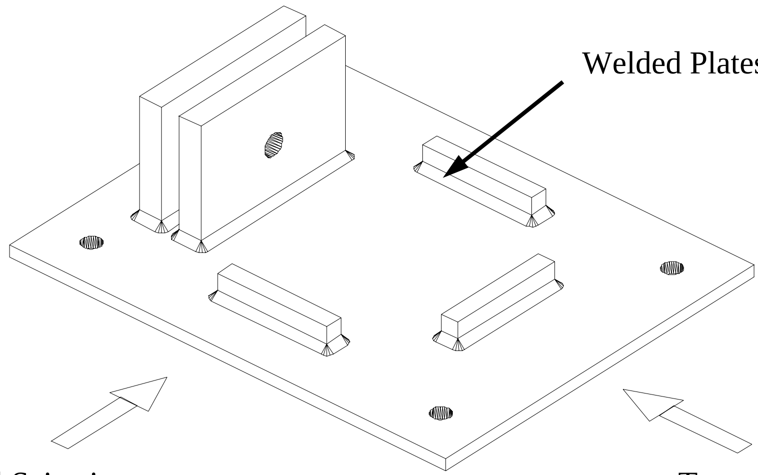

Figure 3: PML System S – Second Generation
Typical Foundation Support

For the reasons previously stated, it is also the aim of this investigation to examine the weld design of this particular connection as well as the effects of welding on its overall strength. The analysis would be conducted bearing in mind the orientation of the weld group with respect to the geometry of the connection and the line of action of the apply seismic reaction forces at the joint. In addition, a set of fundamental recommendations would be integrated as part of the analysis to supplement the understanding of the behavior of aluminum under such design conditions.

One more aspect that would be contemplated in the study is the tensile capacity of one of the primary connections of the truss assembly, a splice joint at the bottom chord. The splice joint design incorporates a riveted connection, which fastens together the two sections of the bottom chord by means of an inner tubular section. In this type of joint there are several factors having an impact on the load carrying capacity in pure tension. The subject matter to keep in mind is the load path and the way design forces are transferred between via the mechanical connection. This riveted joint is designed under the assumption that the connected parts can slip in relation to each other. Hence, the joint is basically a bearing type connection having the rivets bearing on the side of each hole once the primary connection elements have slipped under the prescribed design loads. Once displacement occurs along the longitudinal axis of the bottom chord and the rivets bear against each hole, then the design tensile forces are transmitted from the bottom chord into the inner tubular section by means of shearing forces imposed across the cross section of each rivet. That is the load path to follow in between the connected parts (Figure 4).

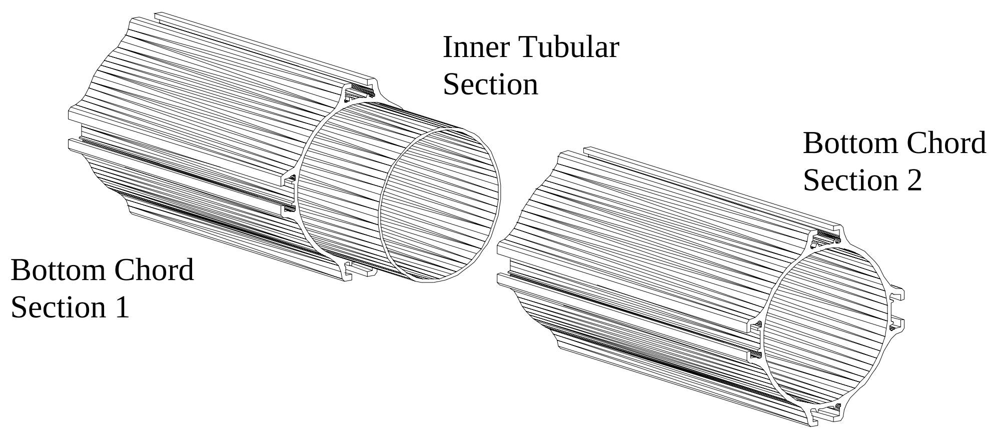

Figure 4: PML System S – Second Generation
Bottom Chord Splice Joint

Thus, the bearing capacity of the bottom chord as well as the inner tubular section ought to be evaluated in addition to the overall shear strength of the rivet group in this connection. What's more, the aluminum design specifications state that the yield tensile strength on the gross area and the ultimate tensile strength at the net section on all the primary members – bottom chord and inner tubular section – must also be accounted for in the analysis. And so, it is also our goal to evaluate each of these elements distressing this specific connection and assess potential modifications to the structural design in order to fulfill fundamental structural standards (Figure 5).

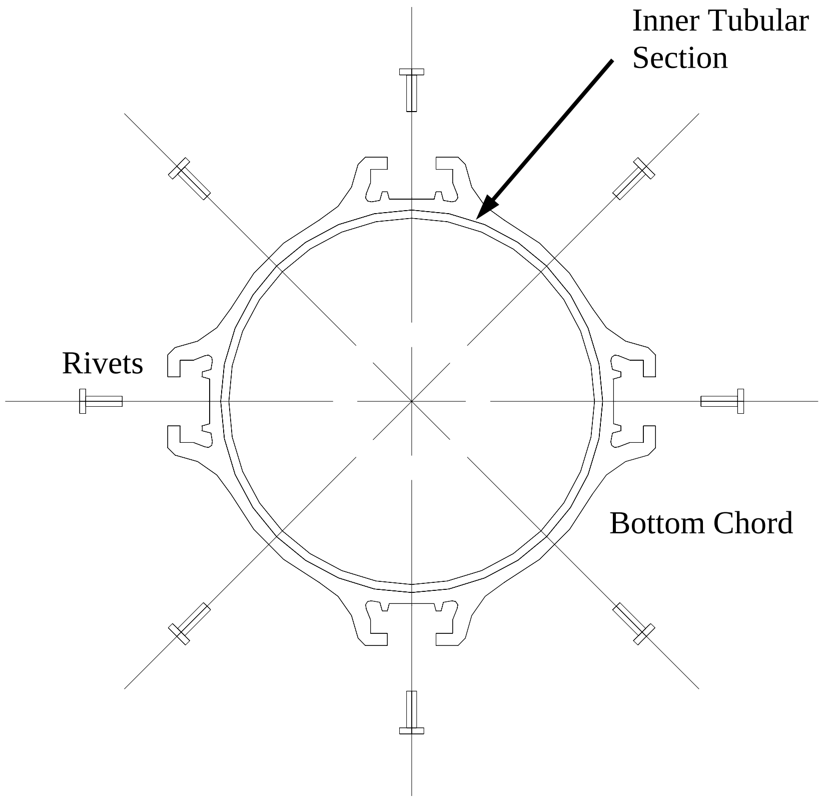

Figure 5: PML System S – Second Generation
Cross Section of Bottom Chord Splice Joint
Riveted Connection

The last concern to be analyzed has to do with the vibration performance, likely to be unstable, on half-through truss bridges having relatively low structural stiffness as well as low specific weight, such as those structures made of aluminum alloys. As one would expect, the floor deflections could represent a problem for aluminum bridges having spans and effective widths large enough to produce a structure with a low natural frequency. Physical structures such as this type of bridges clearly can vibrate during cyclical loadings such as those imposed by a large group of people crossing the bridge at any single time, any seismic activity or possibly because of a hurricane wind forces. In turn this could cause the structure to vibrate with large and/or increasing amplitudes if the loading conditions facilitate such behavior. This cyclical flexing could potentially put undesired stresses at specific locations on the structure. The main concern is that back and forth behavior in the same place, which could exceed the allowable capacity of the bridge weakening in turn the structures at these flexing points and resulting in potential damage or failure. However, there are cases when these types of bridges have been determined to be relaxed enough by the consideration of high damping values. Damping refers to the dissipation of vibration energy, which in turn could reduce the overall motion or acceleration of the framework system under this kind of critical cyclical loading.

The Light Metal Structures division at the Technical University of Munich, Germany, has been carrying out a series of experimental and field studies pertaining to the bridge structural integrity, vibration behavior, and its service life performance. In concurrence with the German DIN 4113 specification and the European ENV 1999 Design Codes, the AASHTO Guide Specification for Pedestrian Bridges, and the Aluminum Design Manual provided by the Aluminum Association, a comparative design analysis focusing on these structural issues will be presented. Further an examination of the conformity to governing U.S. design guidelines will be offered for the purpose of providing the necessary alternatives to improve the required structural functionality and the service life reliability of this bridge system.

CHAPTER II

LITERATURE RIVIEW

2.1 Aluminum Systems – General Findings

The design of aluminum structures for civil engineering applications is significantly different from conventional construction materials, such as for steel or reinforced concrete. This distinctive nature emerges from the physical and mechanical properties inherent to these types of metal alloys [1]. Indisputably, the freedom designers have to place the material where it is mostly needed on the member's cross section by means of the extrusion process represents the foremost benefit in aluminum design. Along with the capability to create detailed and precise cross sectional shapes for optimized extrusion design, the assortment of possible uses is relatively unlimited in the construction industry. The freedom attained by conceiving any necessary extrusion profile to fulfill a particular need is the key to achieve the most advantageous structural shapes and consequently practical and cost efficient aluminum structures. In spite of everything the overall design does not merely rely on structural mechanics alone, but also on the efficiency of the manufacturing processes, the erection techniques available as well as maintenance constraints, governing design restrictions, and the constant human tendency to use traditional construction materials, which are all major factors to consider in any particular application. The use of aluminum in the design of such bridge structures has been documented worldwide. As well many countries favor its use given the material's physical and mechanical properties. Despite the potential advantages, the tendency in structural designs is to avoid its widespread use in the field of construction.

The dilemma of countless engineers having not sufficient knowledge and experience in aluminum design remains an ongoing influential fact. It is common in the construction industry that structural designs tend to be traditional, repetitive, and conservative in view of the limited time and restricted budgets for detailed calculations. In specific situations where design restrictions are questionable, the loading conditions might be exceedingly severe, the mechanical behavior is in doubt, or the architectural demands are beyond measure, is then that the mechanical behavior of such required structures is considered more thoroughly. On the other hand, it is a fact that ever-increasing demands on the infrastructure will result in the need to optimize the existing structural systems by means of using high performance materials like aluminum alloys.

It was a reality that 50 years ago aluminum production and its applications in construction were priced significantly higher than customary materials like steel and reinforced concrete. These past days, material manufacturers, extruders, and designers in the United States and Canada have continually searched for attractive, potentially viable, and economically feasible production methods and construction techniques to promote the increasing use of aluminum alloys. This is particularly true for construction materials used in special applications in civil engineering, as is the case for pedestrian bridges. The derived benefit from the use of aluminum is promoted in structures where dead loads and increasing live loads remain a primary concern. In such diverse cases like large clear-span dome roofs and bridges, tractor-trailer frames, and even crane booms, the reduced dead loads allows for the consideration of a much higher minimum design live load. Decreased dead weight, in any case, is the key aspect in possible future renovations by enhancing the simplification of assembly, erection, transportation costs, in addition to the service performance of any particular structure.

Furthermore, the consideration of aluminum alloys is favorable for civil engineering applications because of its good strength and toughness properties, excellent workability and durability, relatively low maintenance, and high corrosion resistance. These are intrinsic properties suitable for special applications in aggressive environments. On the other hand, consideration must be given to its relatively low modulus of elasticity, just about one third that of steel, in addition to its low melting point and low strength at higher temperatures. The susceptibility to fatigue and buckling is much higher than that of other comparable structural materials and it is a aspect that could not be overlooked during the design process.

2.2 Historical Perspective of Aluminum Bridges in the United States

Most of the existing aluminum bridges in the United States were built within the last forty years [2], and they were in fact structural designs conceived for experimental purposes. It has been the past experience that these bridges had safely withstood the stresses induced by the continuously increasing traffic loads throughout their service life and yet required relatively low maintenance or retrofitting. It has been establish that these structures remain strong enough to uphold the latest minimum design loads as prescribed by the governing codes by firmly supporting the unexpected boost in the applied stresses. They have been ranked as functional, yet aesthetically pleasing. It's essential characteristics including high-strength, lightweight, corrosion resistance, and ease of production and construction have fulfilled the prescribed serviceability and strength requirements.

It is of great significance to recognize though that neither in the United States nor in Canada there is a single federal authority that provides specific design data on constructed aluminum bridges. The only resources for statistics on structural performance have been technical journal articles from either international or local conference meetings, as well as the different U.S. State Departments of Transportation. These sources in fact show and make reference only to the large highway structures along which various deck restoration projects had been performed by the use of aluminum structures. It has been concluded that their records – which are extracts from the inspection database – provide only from time to time information about the structural performance and long-term behavior of these structures [3].

The first application in the United States of aluminum in bridges took place in 1933, when Alcoa succeeded with the city of Pittsburgh in replacing a timber and steel floor system on the Smithfield Street Bridge. As an expected result, the bridge whose construction took place originally in 1882 was subjected to an increase in its live load carrying capacity as the lightweight of the aluminum alloys used in its replacement reduced the dead load on its foundations. In 1946, the first aluminum bridge conceived and constructed using aluminum plate girders had a deck span of 100 feet and it was a railroad line serving an Alcoa smelter. This span was one out of seven others rebuilt in an effort to restore the existing bridges crossing the Grass River near the city of Massena in the state of New York. The first aluminum highway bridge was designed and built with a span of 290 feet over the Sanguinity River near Arvida, Canada, and it design incorporated a riveted box arch having multiple 20 feet approach spans. Seven additional highway bridges of this type were manufactured and put together for public service between 1958 and 1963 using structural aluminum. One reason for the application was the shortage of prefabricated structural steel at that time.

After 1963 an increase in the use of aluminum bridges took place all around the United States, as well as in some locations in Canada. In the state of Colorado, for instance, three additional aluminum bridges extending over 20 feet were designed and built using hollow rectangular box girders [3]. These aluminum-deck overpasses were conceived to carry vehicular traffic on regional areas having a relatively small average daily traffic counts. In contrast, the state of Georgia commissioned two bridge designs, one that incorporated an aluminum plate arch to function concurrently as a culvert to carry traffic on Mt. Zion Road in Rockdale County, and the other aluminum multi-beam stringer bridge to service a highway overpass on top of the Dry Creek in Walker County. Frequent state bridge inspections revealed that the structural operation and functionality of these structures was adequate. The state of New Mexico, on the other hand, is one location that has a high concentration of aluminum bridges in the western United States.

There are a total of fourteen single-span aluminum bridges in the state, some of which consists of through-type trusses and others single deck-beam type of bridge. These all serve highways that cross over water.

With these thoughts in mind it should be recognize there is not much information available on pedestrian bridges made of aluminum alloys in the USA. In contrast, the general aptitude in the industry has been changing considering that the state of Michigan took the initiative in using aluminum bridges for pedestrian applications during the early seventies. In 1972, a five span pedestrian bridge was constructed in the city of Saginaw to cross over the C&O Railroad. Some corrosion was detected during its last inspection, as well as cracking on some welded stiffeners and other truss members. The Michigan Department of Transportation has two other pedestrian bridges in their inventory, both of which are located in Wayne County. These bridges consist of a through-type and an arch-type truss, which were built in the late sixties and early seventies respectively. All members in both bridges consisted of aluminum wide flange beams made up by welding two T-sections together. Stainless steel fasteners in turn fastened all these members in this bridge. In the city of Anchorage in Alaska, a pedestrian bridge made of aluminum spans 170 feet over the Glen Highway and it was built in 1974.

2.3 PML Half-through Bridges: System Description & Design

Footbridges and stairways produced by PML are of a traditional modular construction completely engineered and designed using extruded aluminum (6061-T6) profiles [4]. The basic building unit is a truss panel. Its standardized construction is derived from the precise structural design of these aluminum-extruded sections. This inventive bridge system, primarily conceived for pedestrian, bicycle, and most likely also equestrian or snowmobile traffic, was developed in 1996 and patented by PML LOGIS Bridge Systems Company from Germany. The bridge system was produced and is intended to be consistent with the design specifications and minimum design loads requirements as prescribed by the German DIN 4113 and the Eurocode ENV 1999. Two generations of the bridge - system Type-L and Type-S - were initially conceived and are set apart from each other by design features. Such distinctive features are the extent of their maximum free spans in conjunction with variable effective widths.

The first generation - System Type-L - uses a prefabricated rod-connected walking platform that functions as the lower tension chord of the structure. These units consist of aluminum hollow extrusions having their male-female edges shop welded together to form composite panels; all joined to one another at panel points by sliding a solid steel rod through a Y-shape bracket and end hollow extrusion across the floor platform. One versatile feature of this bridge is that the height of the truss panels can vary with the number of basic decking elements that are welded to form the walkway platform units (Figure 6). As such, an assortment of structural dimension, free span lengths, and related loading capacities could be accounted for in the overall design of the bridge structure. The bridge effective width may vary as the basic extruded elements come in any desired lengths. The bridge may be constructed as a “through-type bridge” or with a closed frame section by integrating into the design overhead lateral bracing between each truss panel. These features provide for an enhanced stiffness and higher load carrying capacity, hence allowing longer free spans lengths.

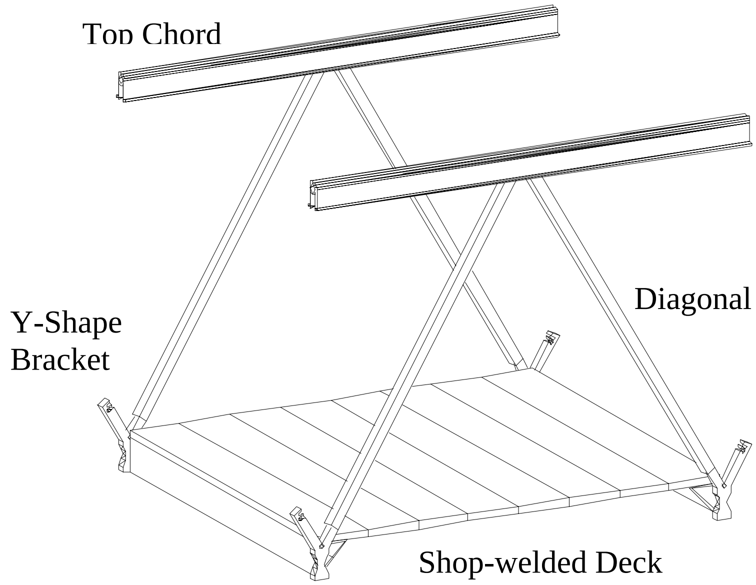

Figure 6: “System L” of First Generation

The System-S, or the so-called tower-profile type bridge is the structural system to be evaluated in this particular evaluation. It does incorporate into a typical Pratt truss a set of independent tubular sections fabricated by means of extrusion shapes (Figure 1). Unique profiles outline the main framework of the truss providing to the system a distinct but conventional approach to achieve redundancy when the load transfer takes place. That is quite a different scheme as compared to its first generation. All together as designed in this second generation, these longitudinal tubular shapes are all joined together by extruded double floor beams which subsequently are bolted to the modified shop welded floor units as used in the System Type-L. The prefabricated rod-connected walking platforms, Y-Shape brackets, and sliding steel rods system are replaced by a more conventional design. Special tubular extruded shapes enable easy on-site assembly. In addition, vertical posts and attached stiffeners yield higher structure stiffness. The upper truss member of this pedestrian bridge functions as both a handrail as well as the top compression chord, and is either the identical “tower profile”, or a lighter tubular extrusion with flap-plates (Figure 7).

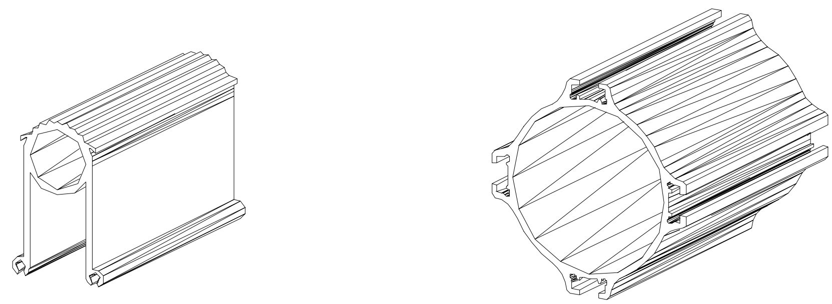

(a) (b)

Figure 7: Top-chord Profiles
(a) Tubular Section with Flat Plates (b) Tower Profile

Both bridge systems consist of aluminum structural parts weighting less than 110 pounds (50 kilograms) each. The system allow for repetitive construction and rapid assembly. In general the system is designed to withstand a surface load of around 103 psf (500 kg/m^2) and corresponds to the controlling guidelines provided in the German loading and latest European design specifications. AASHTO design guidelines and the corresponding provisions of the Aluminum Design Manual [5] have also been accounted for in the system’s development. It has been known that AASHTO Specifications ask for a lower live load capacity as compared to European codes. On the other hand, there are certain discrepancies with regards to allowable stresses for welded joints, particularly where seismic design provisions are a concern. However, these aspects represent some of the structural issues to be assessed and corresponding code requirements compared in the bridge design.

2.4 AASHTO Minimum Design Loads and Specifications

These applicable design specifications are intended primarily for pedestrian and pedestrian/bicycle bridges, which function as a fundamental part of highway facilities and therefore designed in conformance to AASHTO Standard Specifications for Highway Bridges. The term “primarily pedestrian and/or bicycle traffic” implies that the bridge does not carry a public highway or vehicular roadway, yet the design provisions allow for the passage of an occasional small maintenance or service vehicle. This specification allows for the use of both an Allowable Stress Design (ASD) and Load Resistance and Factor Design (LRFD) methods. The former approach is the one selected for this assessment.

A minimum design pedestrian live load for main supporting members shall be 85 pounds per square foot of walkway surface. The pedestrian live load must be applied to those areas of the deck so as to produce maximum loading response in the members being considered for design. This type of loading prescribes a loading effect equivalent to an average person occupying two square feet of decking surface. AASHTO has established that with the allowable stress design approach this loading ensures an ample overload capacity as well as reliable structural safety and performance. The loading provisions outlined in ASCE 7-98 [6], a possible reduction of the pedestrian live load may be applicable to areas exceeding 400 square feet, but it is subjected to the limitations stipulated for public assemblies that forbids possible reduction of live loads of 100 pounds of square feet or less. This is intended to account for the probability of a large influence area being simultaneously overloaded under special or critical circumstances.

Secondary members like the bridge decking, supporting floor systems, including stringers, floor beams, and their respective connections are required to be designed for a minimum pedestrian live load of 85 pounds per square foot with no allowable reductions. Requiring an 85-psf design load for these members is intended to foresee the likelihood of attaining maximum loads over small influence areas of the bridge walkway, which represents a rather critical loading case. Further, the bridge decking and floor systems design to be used on public or private facilities may also include possible loading condition as for equestrian or snowmobile traffic. This is planned to take into account a broad assortment of possible loading conditions that may be represented by a single concentrated load as high as 1000 pounds. This concentrated load is somewhat subjective and may be dependent upon the operating agency, but is intended to represent for instance a single horse or maybe a snowmobile crossing the bridge. However, this type of concentrated loading shall not be applied in combination with the uniformly distributed pedestrian live load.

In view of the vehicle load AASHTO requires also to consider an occasional single two-axle maintenance vehicle, mainly when a right of way is provided to the bridge. AASHTO specifies for bridges having effective deck widths between six and ten feet that an H-5 (10000 lbs.) [7] truck load (Figure 8). The nature of the loading condition shall be as to induce maximum stresses along the structure. It is also predictable the occurrence of both pedestrian and vehicular loading is quite unlikely and consequently it is not going to be considered in this evaluation. Further, AASHTO does not require vehicle impact be applied on the bridge.

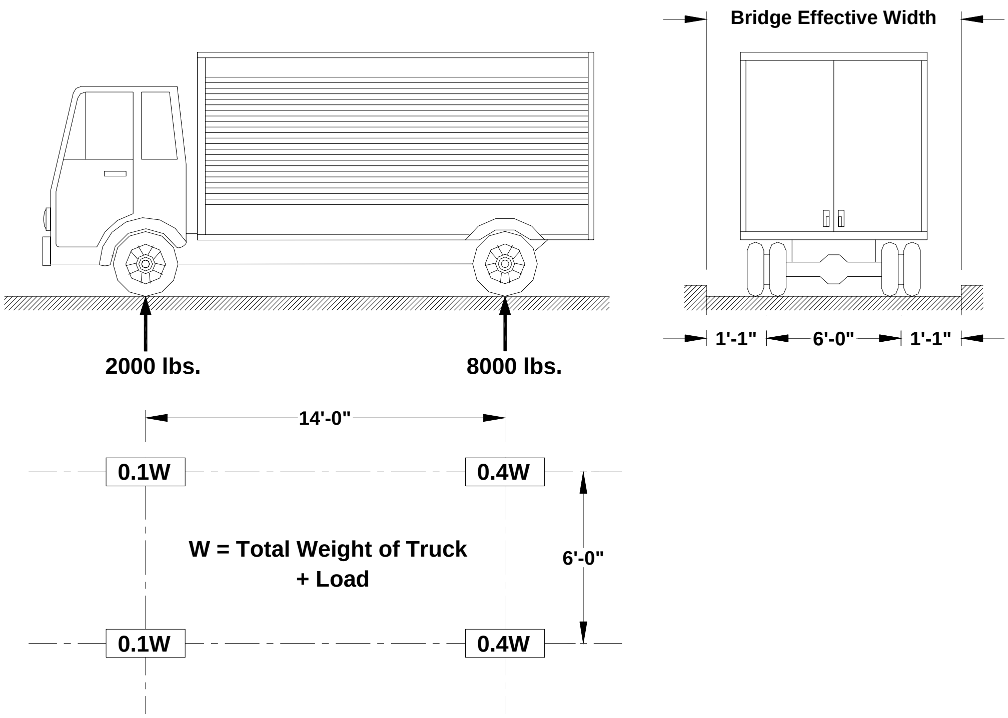

Figure 8: Standard H-Trucks Loading
W=10 Kips

AASHTO wind loads [8] shall be uniformly distributed across the exposed area of the structure. The exposed area is considered as the sum of the areas of all members, as seen in an elevation view and oriented at 90 degrees from the longitudinal axis of the bridge. AASHTO wind load provisions indicate that a wind force shall be equivalent to 75 pounds per square foot (366.2 kg/m^2) of superstructure and applied horizontally at right angles to such longitudinal axis. The total force shall not be less than 300 pounds per linear foot in the plane of the windward chord and 150 pounds per linear foot in the plane of the leeward chord for independent truss spans. AASHTO recognizes that open trusses where the wind can readily pass through the superstructure, the design forces shall be a minimum horizontal force of 35 pounds per square foot (170.9 Kg/m^2) on the full vertical area of the bridge and applied as if the structure is completely enclosed.

This alternative method is provided to simplify the design process and is intended to eliminate excess computations. AASHTO specifies these as full lateral wind forces that must be resisted by the whole superstructure. The specified wind pressures are for a base wind velocity of 100 mph (160.9 kph), and may be modified based on a maximum probable site-specific wind velocity in conformity with AASHTO Article 3.15, Wind Loads. Following these wind provisions and considering the applicable load combination groups, these wind-generated pressures may be reduced or increased based on the ratio of the square of the design wind velocity to the square of the base wind velocity. In order to do so the highest possible wind velocity has to be determined with reasonable correctness, or permanent topographic features must be present on the surrounding areas of the structure to make such adjustment reliable and not dangerous (Table 1).

Table 1: U.S. Hurricane Prone Regions – Site Specific Design Wind Speeds

Location	SSDWS MPH (KPH)	BWS MPH (KPH)	$\frac{SSDWS^2}{BWS^2}$
1. Hawaii	105 (169.2)	100 (160.9)	1.103
2. Puerto Rico	145 (234.0)	100 (160.9)	2.103
3. Guam	170 (273.6)	100 (160.9)	2.890
4. Virginia Islands	145 (234.0)	100 (160.9)	2.103
5. Florida Key	150 (241.2)	100 (160.9)	2.250
6. American Samoa	125 (241.2)	100 (160.9)	1.563

NOTES:

1. SSDWS correspond to Specific-Site Design Wind Speed.
2. BWS corresponds to Basic Design Wind.
3. Values are nominal design 3-second gust wind speed @ 33 ft (10 m) above the ground for Exposure Category C which refers to open terrain with scattered obstruction having height less than 33 ft (9.10. m) including flat open country, grasslands, and shorelines in hurricane prone regions.

AASTHO seismic forces do not require a detailed analysis for single span bridges. The connections between the superstructure and its foundation must be designed to resist a lateral seismic load equal to the gravity reaction at the foundation interface times its local acceleration coefficient. The coefficients act for the potential ground acceleration prescribed on contour maps of horizontal acceleration in rock with a 90% probability of not being exceeded in 50 years. However, it is of great significance that an earthquake engineer be consulted for sites located in the vicinity of actives faults (Table 2).

Table 2: AASHTO Coefficients for Ground Acceleration on Rock Type Soils

Location	Coefficient of Acceleration, A	Location	Coefficient of Acceleration, A
California	80, 70, 60, 50, 40, 30, 20, 10	Borderline between Missouri, Arkansas, & Tennessee	36, 30, 20, 10, 7.5
Alaska	80, 70, 60, 50, 40, 30, 20, 10	Hawaii	30, 20, 10, 5
Idaho	43, 40, 30, 20, 10, 5	South Carolina	12, 10, 7.5, 6
Nevada	42, 40, 30, 20, 10, 4	Ohio	7, 6, 5
New York	18, 15, 10, 7.5	Puerto Rico & The Virgin Islands	20

In turn further loading conditions must be accounted for in the analysis of the bridge system. The railing framework of the bridge must resist a lateral load of to 50 pounds per linear foot, which is applied all at once transversely and vertically to all railing members. The loads are going to be applied to the entire top chord of the truss frame. However, design loads for rail members located more than 54 inches (1.37 m) above the walkway surface shall be determined by the design engineer. The minimum height of a railing to protect a bicyclist are these 54 inches measured from the top of the walkway surface on which the bicyclist rides to the top side of the top rail. In addition, the vertical posts shall be designed for a transversely applied uniform distributed load equivalent to (W X L), where "L" is the post spacing between panel points and W is equivalent to 50 pounds per linear foot. Since railing components must be proportioned accounting for any expected pedestrian or bicycle traffic, strong consideration to safety is as essential as any structural requirement is in the design of these members.

As a final note on load combinations and allowable stress percentages for service load design, the guide specifications for pedestrian bridges accounts for several modifications. AASHTO considers it is improbable that wind forces and live loads, such as those induced by pedestrian traffic, would occur with the occasional maintenance vehicle. Moreover, because the longitudinal forces that might be induced by pedestrian or bicycle traffic are relatively small, it is rather unrealistic to take into consideration these forces in the bridge design. The standard specifications states that each single component of the structure, including the foundations on which it rests, to be properly design and proportioned to withstand safely all group loading combinations that are applicable to this type of bridge and it represents the overall objective of this evaluation.

CHAPTER III

ANALYTICAL APPROACH AND METHODOLOGY

3.1 AASHTO Standard Specifications for Highway Bridges

The compilation of these design guidelines was intended to serve as a model or set of guiding rules for the preparation of State specifications and as reference to bridge engineers in the construction industry. For the most part, these specifications outline minimum design requirements in agreement with recent practices; then again some modifications may be necessary to accommodate local design restrictions. The point of these Specifications is to produce “safe” structures to serve the general public by means of providing structural integrity under the estimated minimum design loads, along with small or no damage or with no injury or loss of life because of any possible failure. These apply to ordinary highway bridges, yet supplemental specifications are available for unusual type of structures. Members of the Association are the fifty State Highway or Transportation Departments, the District of Colombia, and Puerto Rico. Each member has a vote, yet the U.S. Department of Transportation is a non-voting member.

3.2 Guide Specifications for Aluminum Highway Bridges

Distinct design provisions stipulated in these specifications are intended to transcend Section 11.2, Aluminum Design of Bridges, in Division I of the existing AASHTO Standard Specifications for Highway Bridges. AASHTO in this section designates design requirements for aluminum structures as issued by the Aluminum Association to serve as the standard protocols to be applied to “Bridges and Similar Type Structures”. Engineers and fabricators of aluminum bridges and railing structures using the alloys registered with the Aluminum Association consider these guiding principles as the primary reference. The objective of these procedures is to enable designers, who may not know much about aluminum alloys, to more assertively design and construct aluminum structures. These design provisions attain this objective by simplifying the selection of materials and by specifying those alloys and corresponding tempers whose performance has already been proven in the construction of aluminum highway bridges.

3.2.1 Top Compression Chord: Members with Elastic Lateral Restraints

Following the AASHTO design guidelines for aluminum bridges, the top compression chords in half-through trusses are considered as columns elastically restrained by intermittent lateral supports at each truss-panel connection. In trusses with floor systems in the plane of the lower tension chords and where vertical clearance requirements may forbid direct lateral bracing, each panel point will provide both vertical support and elastic lateral restraint for the top chord. The overload buckling response of this compression members falls between two limiting extremes [9]. Exceedingly stiff elastic restrains could produce nodal points at each restraint location. In contrast, if restraints were too flexible the buckling response could occur in the shape of a single half-wave over the full member length. The overall buckled shape of the column will include a number of half-waves not larger than the total number of spaces at the lateral supports.

The analysis and design of these type of elastically restraint compression members is be based on the so determined critical buckling force, which shall exceed the maximum force produced by the controlling combined forces by not less than 50 percent; given that vehicle impact allowance is not required for pedestrian bridges [10]. As a result of any initial crookedness and because of moments induced by bending of the floor beams, the design of this compression chord must also account for the possibility of combined stresses. As such, the design will then incorporate the effects produced by these potential induced deflections across the floor system. These current provisions are based on a semiempirical theory in which satisfactory stiffness of the lateral supports on the compression-chord is achieved by designing them for a fictitious horizontal load. The point of application shall be at each panel points of the top-chord and normal to the plane of each truss. The overall design of each truss transverse frames – floor beams, truss verticals, and connecting bracing – will have a direct effect on the general behavior and structural performance of these members and it is essential for the overall safety and reliable serviceability of any half-through structure.

3.2.2 Buckling of Top Compression Chords in Half-through Bridges

The cornerstone of column theory goes back to the work of the Swiss mathematician Leonard Euler, who in 1744 published his famous column formula for a mathematically straight, prismatic, and centrally loaded compression member, which in fact was slender enough to buckle at a stress below the materials proportional limit. Toward the end of the nineteen-century, the failure of several pony-truss bridges by lateral buckling of their compression top-chords placed attention on the structural behavior of these compression members. The buckling reaction of these members in half-through trusses is distinguish as that of a column braced at intervals or panel joints by elastic springs whose rigidity corresponds to the stiffness of the truss transverse frames (Figure 9). From panel to panel, both the top-chord axial compression force and the member's stiffness vary. Furthermore, the stiffness of the transverse frames also changes from panel joint to panel joint.

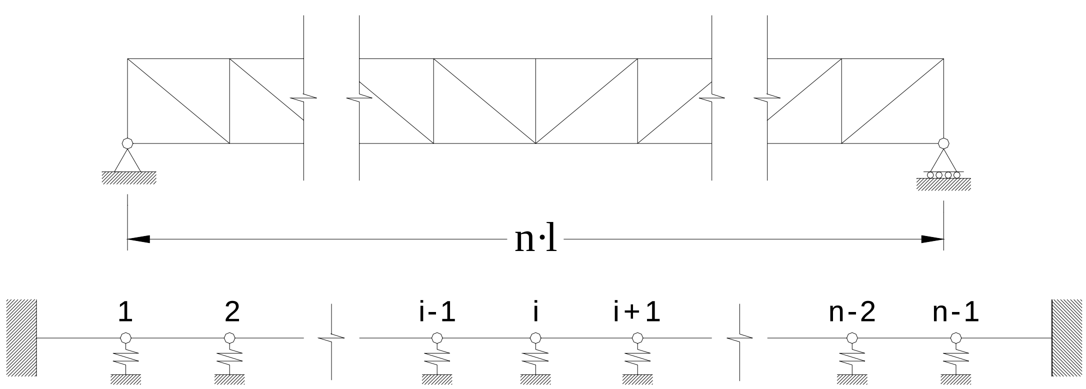

Figure 9: Pony Truss and Analogous Top-chord

Engesser in 1884 was the first to present a straightforward and approximate formula for the required stiffness - C_{req} - for elastic lateral supports that are equally spaced between the ends of a hinged-end column of prismatic cross section. Engesser's solution incorporated the following simplifying assumptions. First, he assumed that the top-chords and the end posts were completely straight from top to bottom having a uniform cross section. Secondly, ends restraints were conceived as pin-connected and rigidly supported. And lastly, the equally spaced elastic lateral supports were conceived having the same stiffness in addition to the constant axial compressive force through the chord's length. Engesser's approach can be applied with reasonable accuracy in any case where the lateral support is supplied by equally spaced springs, provided that the half-wavelength of the buckled shape of the continuously supported member is at least 1.8 times the spring spacing. Also, Engesser's formulation is accurate if the compression members are stable as two-hinge columns carrying the same axial load and with a member length no less than 1.3 times the spring spacing. Engesser's solution for the required stiffness of a half-through truss transverse frame is given as:

$$C_{req} = P_c^{\,2} \bullet l \,/\, 4\ E\ I$$

where C_{req} is the required elastic stiffness of the transverse frame at each panel point. This stiffness will ensure that the overall chord, having panel length "l" and flexural rigidity "EI", will attain the buckling force, P_c. It is important to recognize that if the proportional limit of the column member is exceeded upon the imposed external loading, the modulus of elasticity "E" should be replaced by the tangent modulus "E_t".

Engesser's simplifying statement, which assumes the top chord end restraints as pin-connected, may result in notably unsafe errors in the estimation of C_{req} for short trusses. Holt (1952-56) instead provided an alternate design procedure not requiring Engesser's simplifying assumptions. His research is the guiding principle for design incorporated in the guide specifications for pedestrian bridges and made available by AASHTO [11]. Holt's solution for the buckling load of the compression chord on pony trusses is based on the following postulations. Holt's theory states that transverse frames at all panel points have identical stiffness. He assumes the top-chord and end post having the same radii of gyration and the top-chord members with the same allowable unit stress, hence their areas and moment of inertia are proportional to the compressive forces.

The connections between the top-chord and the end posts are pinned, and each end posts act as cantilever springs supporting the ends of the top-chord. A uniformly distributed force is the basis for the analysis. The results of Holt's studies provide the reciprocal of the effective length factor "K" as a function of "n" – the number of truss panels in the frame – and Cl/P, where C is the stiffness at the top of the least stiff transverse frame. In determining an effective length for compression member the entire structure needs to be considered. The characteristics of the joints and the resistance of the structure to rotation and translation of the column-ends have a large effect on the compressive strength of the compression member (Figure 10). Conservative values of the slenderness ratio should be chosen even though calibration factors empirically introduced in the column formulas provided in the Aluminum Design Manual compensate for the reduction of strength due to crookedness of the top chord material.

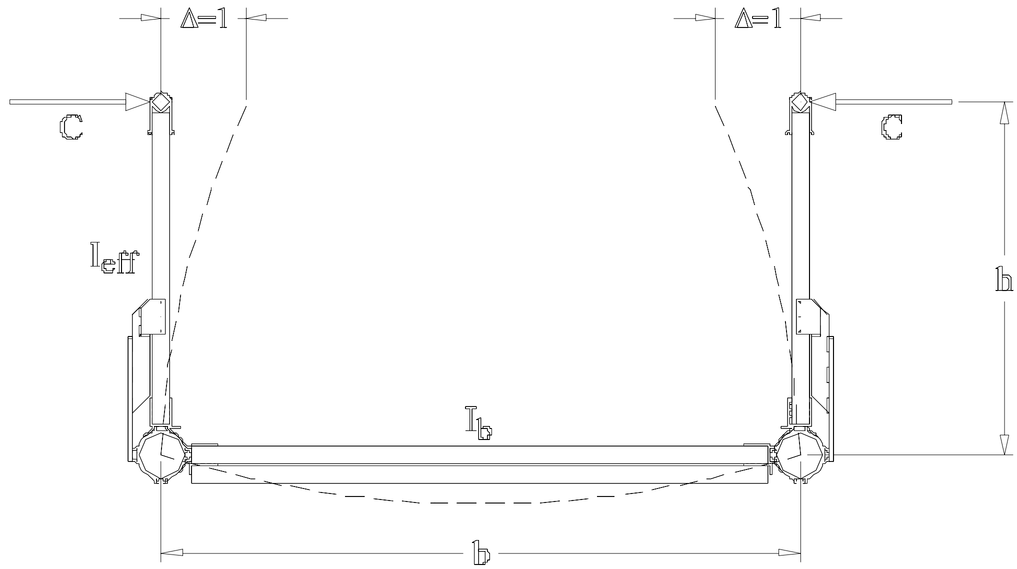

Figure 10: Resistance of Structure to Rotation and Translation of the Column-ends

The spring constant "C" can be determined for the loaded frame by means of either one of the expressions, Equation A or B. The first term within the denominator represents the contribution of the truss verticals, and the second term represents the contribution of the floor beams. Thus, the contribution of the top chord torsional strength and the web diagonal bending strength to the frame stiffness are neglected in this equation, and as a result the frame stiffness will represent a lower bound (Figure 11).

$$C = \frac{E}{h^2\,[(h / 3I_{eff}) + (b / 2I_b)]} \qquad \text{(Eq. A)}$$

$$C = \frac{E}{h^2\{h / [3I_{eff} + 3I_d\,(h / L_b)^3\,] + (b / 2I_b)\}} \qquad \text{(Eq. B)}$$

Figure 11: Transverse Frame Spring Constant "C" for Half-Through Trusses

3.2.3 Additional Requirements for Top-chord in Half-trough Bridges

AASHTO stipulates as supplementary design requirement that for structural component of individual trusses connected by either by welds, rivets, and/or bolts consideration must be given in avoiding laterally unsupported hip joints. Preference should also be given to trusses whose members are symmetrical about the central plane of the truss. Furthermore, each panel should have inclined end posts. If the overall shape of the structure permits, compression chords shall also be continuous. With regard to secondary stresses, the design and structural details shall be such that secondary stress levels will be as small as practicable. Secondary stresses due to any truss distortion or induced deflections on the floor-beams usually need not to be considered in any member, the width of which, measured parallel to the plane of distortion, is less than one-tenth of its length. If the secondary stresses exceed 4 ksi for tension members and 3 ksi for compression members, the excess shall be treated as primary stresses. Stresses induced by flexural dead load moments of the member shall be taken into consideration as an additional secondary stress.

3.3 Aluminum Welded Members

Though on occasion aluminum alloys are regarded as a challenging material to weld. The designer shall be aware that aluminum is one of the most readily weldable of all metals, including steel. It has in contrast certain intrinsic characteristics that should be thoroughly understood. One of the most crucial factors in welding aluminum is oxidation, a transparent layer of aluminum oxide that forms on the surface almost instantaneously upon experiencing contact with the surrounding atmosphere [12]. Though aluminum gains its corrosion resistance from this oxide film, it has to be completely removed before sound welding can be made on the parts to be joined. Its removal can become a very difficult task to accomplish, just by the fact that the oxide film has a much higher melting point than that of the base metal. Unless this oxide film is properly removed preceding or broken up during welding, the temperature differential produced in the heated affected zone can allow the aluminum base metal to melt before the oxide film does, therefore precluding suitable coalescence between the deposited filler metal and the base material.

Furthermore, the overall cleanness of the areas to be welded is critical considering that moisture, grease, oil films, and any other foreign substance sitting on the edges to be joined can cause welds to be of poor quality. The difficulty arises when the contaminants breakdown into hydrogen and other gases that become entrapped in the weld deposit. These trapped gases produce porosity that affecting adversely the weld strength and its ductility. Welding aluminum members also reduces the strength of the base material. Most structural alloys attain their strength by heat treatment and/or strain hardening or cold work. Welding causes local annealing, which introduces a zone of lower strength along both sides of the weld. Because of its apparent weakness at high temperatures, many aluminum alloys are partially molten over a wide range of temperature if enough care is not taken during the manufacturing process. When temperatures are reached during welding at which partial melting occurs, the aluminum alloy will show a tendency to collapse. However, the proper selection of filler material should overcome this concern.

It is important to realize that the range of temperatures achieved in welding aluminum is not within the visible light range. In consequence, it is very difficult to conclude that any component of the piece of metal being welded has melted down adequately reaching suitable fusion. It is therefore an unquestionably critical safety issue that must not be overlooked during the fabrication process considering the design requirements of the welded detail. This is contrary to the circumstances in welding of most other metals, such as steel, where welders know the temperature by the color of the heated piece; therefore they can heat to any desire range. This condition also necessitates precaution to avoid subjecting the hot metal to shrinkage and reaction stresses because of the high thermal conductivity of aluminum in view of the high thermal conductivity of these types of alloys.

3.3.1 Metallurgical Effects of Welding

The characteristics of aluminum parts are to a great extent influenced by microstructural changes that take place during welding. An understanding of these changes is necessary to predict the mechanical properties and ultimate performance of weldments. When a fusion weld is made in aluminum, two basic types of materials must be considered [13]. These are the weld metal having a cast structure and the base metal that may be wrought or cast. The properties of the cast aluminum in the welded zone are affected by the composition and rate of solidification. The rate of solidification of the welded metal depends on the welding process plus the factors affecting the heat input and transfer away from the molten pool. A higher rate of solidification rarely produces a finer microstructure and an enhanced strength. The effects of welding on aluminum-base metals change with the distance from the weld and may be divided into areas that reflect the temperature attained by the metal during welding. The widths of these areas and their distances from the welds vary with the welding process, the thickness or geometry of the part, and the speed at which welding is performed. Within each area certain microstructural changes take place upon welding that largely determine the as-welded properties of the alloy.

The heat-treatable aluminum alloys contain elements that exhibit a marked change in solubility with temperature changes. These elements are quite soluble in aluminum at high temperature, despite the fact they have low solubility at room temperatures. They have a tendency to break up as various microconstituents in the base metal structure. The high strength of the heat-treatable alloys is due to the controlled solution and precipitation of some of these microconstituents. Conversely most of the difficulties in welding these alloys are due to the uncontrolled melting, solution, and precipitation of these elements. These alloying ingredients are dissolved into the aluminum at very high temperatures by means of solution heat-treatment. These are maintained in solid solution by rapidly quenching from these elevated temperatures governing the strength of these alloys in the as-quenched temper.

Additional increases in the strength of welded parts are affected by the precipitation of portions of the soluble elements in a finely divided form. This precipitation may take place at room temperature after quenching or accelerated by a thermal treatment at a fairly elevated temperature, usually in the range of 210 - 350 °F. Heat-treatable alloys may be reheated after welding to bring the base metal in the heat-affected zone back to nearly its original strength. The strength achieved in the weld metal after reheat-treatment will depend on the filler metal used. In cases where filler metal of other than base metal composition is used, the overall strength of the joined parts will depend upon the percent dilution of filler metal within the base metal. In situations where complete reheat-treatment of weldments is not practical and realistic, parts can be welded in the solution heat-treated condition and then artificially aged after the welding process. The properties and performance of weldments are greatly influenced by factors such as composition, form and temper of the base material, the filler alloy, and the welding techniques including the rate of cooling and the weld design. These effects and other variables must be considered in any particular application.

3.3.2 Cracking

Cracking in the heat-affected zone is a primary structural deficiency for any welded component in aluminum alloys. However, these deficiencies could be overcome if adequate fabrications techniques are applied. The cracks in welded metals are usually in the shape of either a crater or of an elongated form. Crater cracks often occur when the welding is quickly broken. Crater cracks are certainly detrimental considering the strength of the weld and especially when these are located in highly stressed areas. The defect may be prevented by proper torch handling or by a buttoning technique or current control devices used to the fill craters. Longitudinal cracks are usually the result of improper filler metal choice or poor welding procedures. High stresses imposed during welding, mainly in restrained joints, may also produce longitudinal cracks by exceeding the strength of the metal when the weld bead is small enough or the filler metal is of poor strength. Cracking in the heat-affected zone of base metals takes place primarily with heat treatable alloys. Usually, it is related to the precipitation of brittle constituents at the grain boundaries within the weld structure. To prevent this it is necessary to use a higher welding speed to diminish heat input to the base metal and employ filler alloys with lower melting points than the base metal. To reduce heat-affected zone cracking attention to lessen the restraint imposed during welding and cooling is important. High welding speeds are advantageous as well as the selection of the filler alloy, which may be critical. Heat-treatable alloys welded in the solution-treated condition are slightly less subject to this cracking when they are in the fully heat-treated and aged condition.

3.3.3 Porosity

Gas pockets or voids in the welded metal are often observed in cross sections of fusion-welded joints in aluminum applications. A slightly small amount of porosity spread uniformly throughout the welds has little or no influence on the strength of joints in these metals. If clusters or gross porosity are present, they can have an adverse effect on the performance of the welded joints. Numerous welding codes regulate the amount and allocation of porosity in aluminum-welded joint. Hydrogen is a main source of porosity as it is very soluble in molten aluminum but has low solubility in solid aluminum. In consequence, hydrogen can be easily picked up by the molten weld pool during welding and be released upon solidification during the cooling process. The presence of foreign substances such as moisture, oil films, grease, or heavy oxides in the area during welding can produce porosity within the weld structure. Other contributing items that could produce gross porosity are improper voltage or arc length and an improper or erratic wire feed in gas metal welding. Filler wire contaminated either during its manufacture or shop handling, a leaky torch, and moist or contaminated inert shielding gas or insufficient shielding gases when employed are all sources of porosity. Since welding speeds in combination with good quality arc transfer are also linked with metal soundness, it may require selecting a welding process with a proper solidification rate to aid in the reduction of porosity.

3.3.4 Incomplete Fusion

Incomplete fusion is depicted as a failure to fuse adjacent layers of weld metal or weld metal to base metal. In aluminum weldments the two most common causes are incomplete removal of the oxide film prior to welding or unsatisfactory cleaning among passes at some stage in welding. The applied weld bead will, on average, have a dirty gray appearance when the pre-weld or inter-pass weld cleaning is not properly done. Not enough bevel angles or back-chipping, or unsuitable amperage or voltage often plays an important part in incomplete fusion. This type of defect may be identified by means of radiographic or ultrasonic inspection. However, if the incomplete fusion is not oriented in a plane parallel to the X-ray beam, it may be perceived by the method of radiography.

3.3.5 Inadequate Penetration

Inadequate penetration comes about when the weld does not penetrate the full depth of a prepared joint or it does not penetrate to the indicated depth. In both groove and fillets welds, inadequate penetration can be the result of low welding current, improper filler metal size, improper joint preparation, or excessive welding speeds for the amount of amperage or voltage used during the welding process.

3.3.6 Inclusions

Weld inclusions in aluminum alloys are of two types: metallic and non-metallic. In gas tungsten arch welding (GTAW) too much current for a given electrode size will trigger melting and the resulting deposit of tungsten within the weldments. If rectification of the alternating current and the required adjustments for the high frequency are improperly set, this may also result in tungsten inclusions. Tungsten inclusions can be credited to welds starting with a cold electrode, also by dropping the electrode into the weld pool, or by touching the filler rod to the electrode. Fine widely scattered particles of tungsten do not have too much of an effect on the mechanical properties of the gas tungsten arch weld, however, code specifications may call for welds that are free of these types of defects. Copper inclusions are possible in gas metal welding as a consequence of a burn back of the electrode to the contact tube. Copper inclusions will produce a brittle weld structure and can lead to a serious corrosion problem and should be removed from the weld deposit as much as possible. Inappropriate use of wire brushes during cleaning the weld groove or between passes also results in metallic inclusions if the bristles from the wire brush become entrapped in the weld. Nonmetallic inclusions are often the result of poor base metal cleaning when using soldering or brazing procedures or when flux shielded metal-arc welding is improperly employed.

3.3.7 Additional Requirements for Welded Members

AASHTO specifies that the aluminum alloy to be welded, the filler alloy, and the corresponding welding details conform to the requirements of the latest edition of AWS D1.2, Structural Welding Code – Aluminum. It is also important that welding symbols as well as fabrication processes conform to these specifications. With regard to end returns, fillet welds that are subjected to tensile forces not parallel to the axis of the weld, or which are proportioned to withstand repeated stresses, shall not terminate at corners of parts or members. Instead it is specified that end returns shall be turned continuously around the corner of the part being welded for a length equivalent to twice the weld size, where such return can be made in the same plane of the weld. The end returns shall also be specified and indicated on design and detail drawings. With respect to the required minimum effective size for fillet welds, these shall be such that the stresses induced in the adjacent base material do not exceed the allowable stresses presented by AASHTO [2]. It is specified also that the maximum size for fillet welds that may be used along edges of connected parts must be equal either to the thickness of the part being welded, if the part is less than 0.250 inches thick. In the case of edges of material 0.250 inches thick or more, the maximum size shall be 0.0625 inches less than the thickness of the material, unless is specially designated on the detail drawings to be built out to achieve full throat thickness.

3.4 Deflections

The term “deflection” as used herein shall be the deflection computed in accordance with the assumption made for loading when computing the stress in a member. AASHTO specifies that members with either simple or continuous spans should be proportioned so that the deflection due to the service live load on bridges in urban areas used in part by pedestrians do not exceeds L/1000, where L represents the clear span of the structure. In the case of cantilever systems, as is the case for the overhang side of this pedestrian bridge, the deflection due to the minimum service live load should be limited to L/375. It is also stipulated that when deflections of beams and girders are estimated, the moment of inertia of the gross cross sectional area be used.

CHAPTER IV

DISCUSSION OF ANALYSIS RESULTS

4.1 Analysis of Top Chord

Top chord of members are structural elements subjected primarily to axial compressive forces. At any time compression takes place in engineered structures instability concerns certainly become a design consideration. The member's overall dimensions – particularly the unbraced length, cross-sectional widths and thicknesses – and the actual nature of its end-restraints strongly influence the buckling response of these types of components. In half-through bridges (i.e. pony trusses), the top compression chords are idealized as laterally restrained by intermittent elastic supports at each panel point. Furthermore, these axially loaded members are vertically supported at the same locations by each truss post. It is well recognized in this type of bridge that the buckling behavior of these compression components is a function of the minimum lateral support provided by the members defining the transverse frames. This investigation examines an array of external bracing in conjunction with a set of combination of extrusion profiles to form the transverse frames. This structural evaluation is to be carried out in order to assess the contribution of elements to the elastic lateral support provided to the top chord necessary to resist the maximum design compressive force (Figure 12).

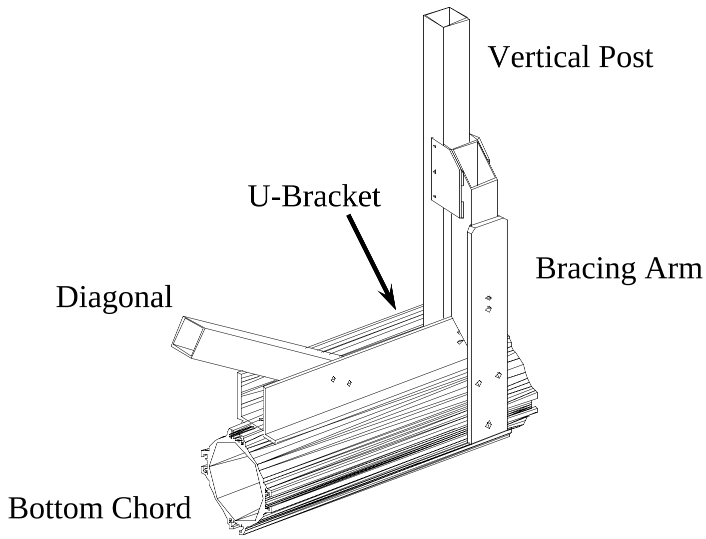

Figure 12: Typical Connection for External Bracing Arm

Based on the inherent geometric design of the bridge a portion of the required lateral support to its top chord is provided by means of an external bracing arm, which is rigidly connected from the bottom chord into each vertical post. This bracing arm was originally conceived to have an extrusion profile similar to that of the vertical posts and diagonals. Moreover, the actual design of the truss panels provided a particular location along the length of each post where these external bracing arms are connected. Given the actual geometry of these bracing members, a series of effective lengths were considered within the set of combinations previously incorporated into the analysis to further appraise its effect on the lateral stiffness induced by the transverse frames. By following the basic principles of beam theory an equivalent moment of inertia could be evaluated by considering each vertical post and their corresponding bracing arms working in unison as a composite member. By allowing the actual effective length of the external bracing arms to vary an equivalent moment of inertia for both members as a whole was found to be a function of each member's cross-sectional dimensions in addition to their relative lengths (Appendix 1).

The design of a compression member is clearly based on an estimated critical buckling load. The existing design principles employed in this analysis, as specified by AASHTO [7], are based on the semiempirical procedure completed by Holt and others. The method of analysis measures the required lateral stiffness made available to the top chord by the intermittent elastic supports. Holt presented a set of analytical guidelines that correlate these values to the magnitude of the critical buckling force. The elastic stiffness of the transverse frames was found to be directly dependent on the flexural rigidity (EI) of each panel member; especially the vertical posts in conjunction with the external bracing arms, the floor beams, and to some extent, the diagonals.

Knowing that aluminum alloys are homogeneous and isotropic, with a constant modulus of elasticity within the elastic range, the leading variables include the corresponding moments of inertia of each member outlining the transverse frames. In consideration of this fact, six different combinations were evaluated (Table 3). In each separate case, the contribution to the stiffness of the transverse frame was evaluated as a function of the effective lengths of the external bracing arms and each member's cross-sectional properties. As a result, the corresponding flexural rigidities of each combination as a function of the effective length of the external bracing arms were evaluated (Appendix 2).

Table 3: Frame Combinations Considered for Analysis

CASES	VERTICAL POST	BRACING ARM	FLOOR BEAM	DIAGONAL MEMBER	CONTRIBUTION FROM DIAGONAL
CASE I	HOLLOW	HOLLOW	HOLLOW	HOLLOW	NO
CASE II	HOLLOW	HOLLOW	HOLLOW	HOLLOW	YES
CASE III	SOLID	SOLID	HOLLOW	SOLID	YES
CASE IV	SOLID	SOLID	SOLID	SOLID	YES
CASE V	HOLLOW	SOLID	SOLID	HOLLOW	YES
CASE VI	HOLLOW	HOLLOW	SOLID	HOLLO	YES

4.1.1 Vertical Post/Bracing Arm: Effective Moment of Inertia

One of the main aspects to be analyzed is the simultaneous effect the vertical posts and each external bracing arm provide to the elastic lateral stiffness of each transverse frame. The magnitude of this effect is evaluated by considering the actual effective length of the external bracing arms relative to the overall length of the vertical posts. As derived from basic practices in beam theory – particularly the method of superposition as well as the moment area method – an equivalent moment of inertia was approximated for a composite section that consisted of each vertical post and it's corresponding external bracing arm.

Due to the rigid nature of the bolted connection between these two members, the response of the composite section can be regarded as a synchronized effect in relation to the lateral support provided to the truss top chord. In order to further evaluate this behavior, three distinct combinations of hollow and solid extrusions between these two members were incorporated in this part of the analysis (Figure 13). Based on the calculations performed it may be concluded that the maximum effect on the equivalent moment of inertia of the composite section is achieved either by setting both extrusions with solid profiles, as in Case B, or by allowing just the external bracing arm to have of a solid cross section, as in Case C (Appendix 1).

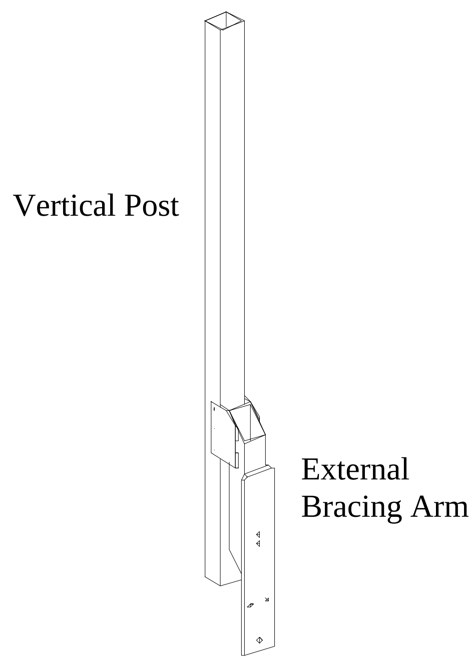

Figure 13: Typical Vertical Post Composite Member

Despite the results obtained, it was concluded from all three combinations that the greatest effect on the equivalent moment of inertia was induced by the external bracing arm, no matter the type of extrusion profiles chosen. Justifying this effect relies on the actual location of the bracing arm's cross-section with respect to the line of action of the forces applied to the vertical post and the top chord. In any case, the results obtained clearly indicate that the magnitude of the equivalent moment of inertia of the composite section is greatly altered by the degree of eccentricity between the geometric centroid of the external bracing arm and the vertical post. Regardless of the actual length of the external bracing arm and its cross-sectional dimensions, it is important to recognize that the equivalent moment of inertia of the "as-is design", does not exhibit a noticeable variation even by extending the effective length of the bracing arm all the way to the top of the vertical post (Case A on Appendix 11). This is due to the extrusion design of both members, particularly the external bracing arm, which translates into a smaller contribution to the lateral rigidity to the composite section.

4.1.2 Transverse Frame Spring Constant, C_{req}

In a truss providing support to a floor system in the same plane of the tension chord members, each panel point must provide both vertical support and elastic lateral restraint for the compression chord as a whole. In this type of bridge, the buckling behavior of the compression chord can be idealized as a column braced at each panel point (i.e. constant intervals) by elastic springs (Figure 9). The internal stiffness of these elastic springs represents the flexural rigidity provided concurrently by the members forming the transverse frames – the floor beams, the vertical posts, bracing members, and the diagonals. The required elastic stiffness of each transverse frame, C_{req}, may be derived at any of these locations from the analytical procedures designed by Holt as specified by the AASHTO Guide Specifications for Design of Pedestrian Bridges.

In view of the six frame-combinations incorporated into this study, the goal is to estimate an effective length factor that will correspond to the nature of the lateral constraint provided to the top chord by each of the frame combinations. As stated by Holt, there is an empirical correlation as a function of the reciprocal of the effective length factor (e.i. 1/K) between the ratio of the required transverse frame spring constant, C_{req}, and the ultimate buckling force applied to the top chord ($C_{req} \bullet l / P_{cr}$). This empirical correlation is dependent on the number of truss panels in the bridge, and in this particular case, it is clearly dependent upon the actual effective length of the external bracing arms relative to the height of the vertical posts. In consideration of the six cases reviewed, it was concluded that the longer the external bracing arm the stiffer the transverse frames. And this is the result of the actual contribution provided by the composite section to flexural rigidity of the transverse frames. This effect can be rationalized by evaluating Equations A & B designed by Holt to approximate the transverse frame spring constants (Figure 11). As previously explained, these two equations were evaluated as a function of the effective length of the external bracing arms relative to the constant length of the vertical post. As the external bracing member is extended upward from its original location the contribution made available by the composite section as a whole amplifies the resulting rigidity of the transverse frames.

What is concluded can be mathematically contemplated by evaluating the term related to the composite section (i.e. vertical post and external bracing arm) in the denominator of either Equation A or B. Following the prescribed range of effective lengths for the external bracing arms it may be inferred that the closer this member comes to the top chord the higher the transverse frame spring constant could become (i.e. frame flexural rigidity or elastic stiffness). This is expected because as the effective length of the external bracing members increases, the equivalent moment of inertia of the composite section increases as well. Accordingly, as the ratio of the equivalent moment of inertia and the overall height of the vertical post decreases, the lower the absolute value of the denominator. A higher elastic transverse spring constant, C_{req}, results.

Following this analogy, the fundamental effect that is achieved by increasing the effective length of the external bracing arm is an overall reduction in the effective length factor applied to the top chord. This is quite obvious since these values are inversely proportional to each other. Consequently, the longer the bracing arms, the higher the frame stiffness and the closer the nature of the lateral restraint on the top chord will be to that of an pin-ended column (Appendix 2). It may be concluded from the numerical results obtained in the analysis that the frame combinations – Cases IV through VI – were the most significant with regard to the estimated effective length factor and to the overall slenderness ratio for the truss top chord. Even though the contribution from the diagonals was incorporated in all Cases, the actual effect on the flexural rigidity of the transverse frames was not appreciable as you might expect.

4.1.3 Compressive Capacity of Top Chord

Extruded aluminum profiles that can be fabricated by standard practices in the industry may take practically any shape. In engineered aluminum components, their cross sections are considered to be made-up of one or more elements connected only along their edges to other elements. For design purposes these profile elements are characterized as plates, either rectangular or curved in cross section with diverse edge supports. It is well know that singly symmetric profiles subjected to compressive forces, such as the extrusion profile of the top chord, may be restricted in their design by flexural or flexural-torsional buckling, or by local buckling of a particular cross sectional element over a length about equal to the width of that specific element. Flexural or torsional – flexural buckling occurs over the length of the member or from panel to panel. For this main reason there are no buckling modes that can be dismissed without consideration in this particular type of axially loaded member. It is important to discuss the subject of local buckling behavior of slender plate elements for this specific type of extrusion profile (i.e. singly symmetric). Once a slender plate element with at least one edge supported on the cross section has buckled, in the elastic regime, this cross sectional component is capable of supporting additional load. This additional local load carrying capacity is referred to as post-buckling strength. However, post-buckling strength will only be acknowledged in singly symmetric compression members whose overall buckling-axis is an axis of symmetry.

Even though the actual overall buckling axis for the top chord is an axis of symmetry, the local buckling mode does not control the ultimate collapse behavior. Disregarding the weighted average allowable compressive stress due to inaccuracies in estimating cross sectional areas of individual plate elements, the flexural-torsional buckling response of this member controls its collapse behavior when subjected to its critical buckling force. Furthermore, in aluminum compression members an interaction may occur between overall and local buckling modes. This interaction may actually cause the actual overall buckling capacity of the member to be reduced if local buckling would be present. In this particular case however, since local buckling does not control the failure mode it is not necessary to account it for this interaction (Figure 14b).

Results of a numerical analysis of the compressive capacity of the top chord conducted for all six frame-combinations, is satisfactory only for Cases IV, V, and VI. In these specific cases however, there were a few instances where the overall factor of safety (i.e. P_{allow} / P_{cr}) was inadequate for a discrete number of effective lengths of the external bracing arms (Appendix 14). The entire evaluation of this compression member was a function of a prescribed range of effective lengths for the external bracing arms of

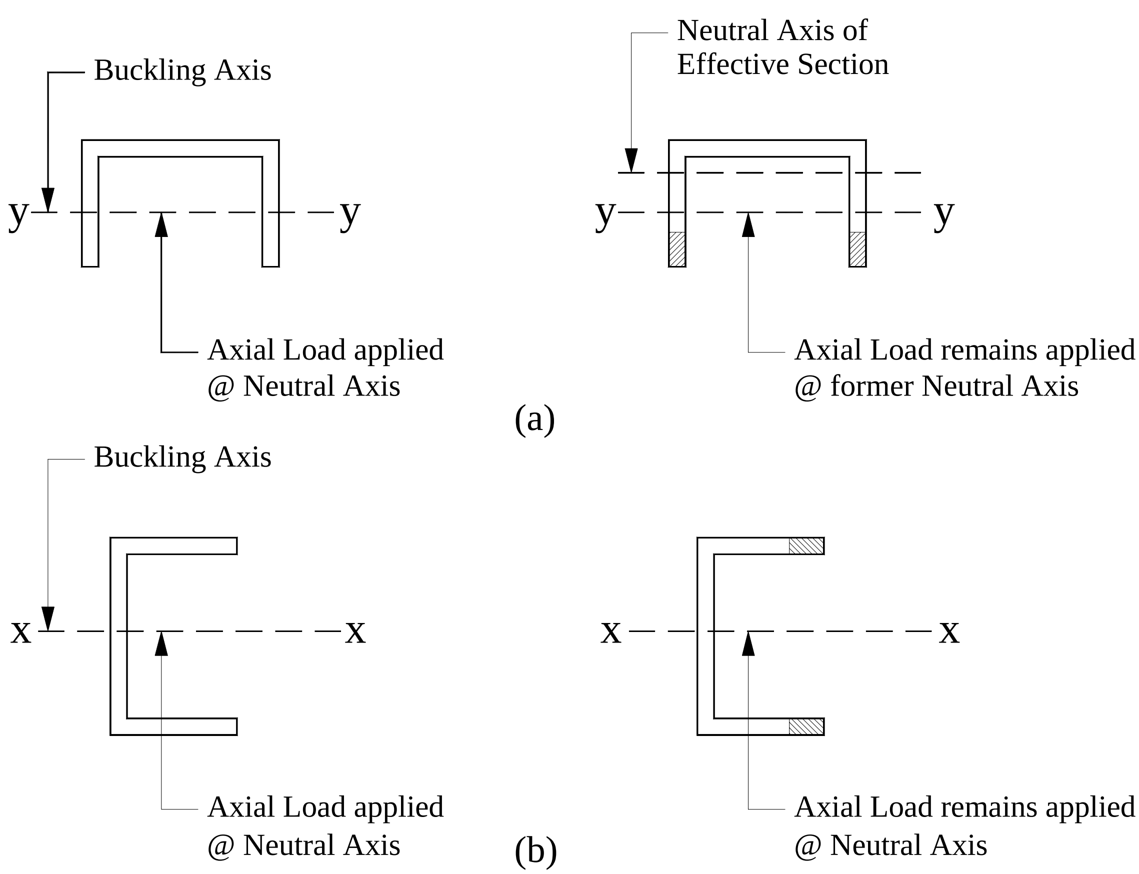

Figure 14: Comparison of Buckling Axis to the Axis of Symmetry for Equivalent Section of Top Chord (Post-buckling Strength)

the vertical posts. As the fundamental impediment to this type of structure (i.e. half-through bridges) is that of adequate lateral stability, enough lateral restraint needs to be provided by the transverse frames to enable of this compression chord be like that of a pin-ended column. It may be concluded, based on the minimum design loads and design specifications provided by the governing agencies, that this compression member is acceptable under specific loading and lateral restraint conditions.

Safety requirements will rely on the actual geometry of the external bracing arms in conjunction with the original profile of the top chord. Assumptions were made in this analysis regarding the extrusion profile of this compression member. It was decided at the early stages of this investigation that an equivalent channel shape would be chosen to a represent the lower bound behavior of the original extrusion profile for the top chord. It may be concluded, based on these assumptions, that some level of conservatism has been incorporated into this structural assessment. Nonetheless, the compressive load carrying capacity of the top chord will be adequate under the provided guidelines if strict restrictions are placed on the effective length of the external bracing arms and extrusion profiles of the members outlining the transverse frames.

4.1.4 Pedestrian / Bicycle Railing – Combined Stresses

AASHTO requires pedestrian and bicycle railings be sized for two uniformly distributed forces (50 plf each) imposed along the longitudinal axis of the top chord. These sets of forces are applied simultaneously in a vertical and horizontal plane and in combination with the maximum compressive axial force on the top chord. Thus, this design provision accounts for the effects imposed by combined stresses induced by the axial load as well as biaxial bending of the bridge railing. The Aluminum Specifications also states that if a member is subjected to bending moments in conjunction with axial compression, that the component be proportioned following two interaction equations. These must be evaluated when the average compressive stress is greater than 15% of its allowable compressive stress as for axially loaded columns. This is the actual case in this specific rail (Appendix 4).

The buckling strength of the top chord in this type of bridge is a function of the lateral support provided by the members comprising the transverse frames. Six different combinations for the transverse frames were chosen, and the lateral restrain provided by each was examined as a function of the effective length of the external bracing arms. The overall behavior of the bridge rail under combined stresses will rely upon the effective length of the external bracing arm as well. Given that three distinct stress conditions are evaluated, the load carrying capacity of the bridge rail in the case of biaxial bending will be controlled by two different failure parameters – one for each plane of bending. Examination of the bending strength about the strong axis of the rail, flexural buckling will govern the allowable compressive stress. In contrast, bending strength about the weak axis is controlled by local buckling strength of the plate elements.

Based on the numerical analysis performed for all combinations as specified by the Aluminum Specifications, the failure response of the rail varies with the effective length of the external bracing arms. Taking into account just a discrete range of effective lengths coming from these lateral support components, the failure mode of the rail is characterized by overall flexural buckling. Moreover, this failure response is restricted the member's bending strength given that the average combined compressive stress imposed on the top chord is greater than the allowable buckling stress, regardless of the overall slenderness considered in the analysis (Appendix 4). In order to achieve a reliable load capacity, the average compressive stress on the top chord needs to be restricted to values so it does not exceed its allowable compressive stresses. Given that the original design of the top chord, which uses the tubular profile with the side-plates, does not fulfill the load-carrying capacity required consideration must be given to use the tower profile as the top chord or redesign the former tubular profile.

4.2 Bottom Chord - Allowable Tensile Capacity at Splice Net Section

The main distinction between this type of axially loaded member and the top chord is the nature of the applied loads. Tension members are defined as structural elements that are subjected to axial tensile forces. For any material, the only significant factor under these loading conditions is the member's cross sectional area. In spite of this fact, it is important to recognize that if the cross section varies along the length. The induced stresses will be a function of the particular section under consideration. The actual presence of holes, as in the splice connection of the bottom chord, the load distribution and magnitude of the stresses developed across the cross section is affected (Figure 15). At any of these locations, the cross sectional area is reduced by an amount equal to area of the holes. This generates a more highly stressed section as compared to the gross cross sectional area in the member. Tension members may fail either by excessive deformation or sudden rupture. However, a check against the tensile fracture limit state must always be considered on the net area for aluminum tension members.

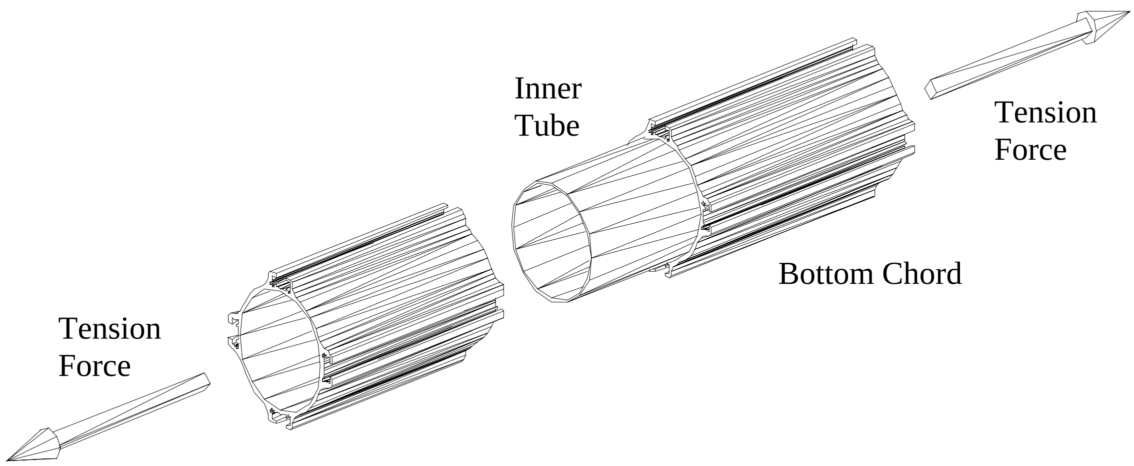

Figure 15: Splice Connection at Bottom Chord via Inner Tube

The design objective is to size an extrusion profile to have adequate cross sectional area so that the applied loads do not exceed the capacity of the member. The overall elongation under tensile forces is dependent on the portion of the structure's length that has yielded. In the case of bolted or riveted connections where the net section is restricted to discrete portions of the member, the limit state for yielding is applicable to the gross section instead. However, in the connected portions localized yielding would not result in an appreciable elongation of the member. The Aluminum Specifications however does not recognize this occurrence and it calls for the evaluation of both the ultimate and yielding capacity on the net section, however just for prismatic elements without any welds having axial tensile forces applied along the member's centroidal axis. Allowable stresses in these members are determined by dividing the minimum design strengths for a particular alloy by a factor of safety, which depend on the type of structure considered. Aluminum alloy 6061-T6 has the allowable tensile stresses governed by ultimate strength. The ratio of the factors of safety on yielding and fracture for bridges is 1.85/2.20 or about 0.84. Thus, the allowable tensile stresses for 6061-T6 are governed by tensile ultimate strength because the yield strength is greater that 84% of the ultimate strength (F_y = 35 ksi > 0.84 x F_u = 0.84 x 38 ksi = 31.96 ksi).

It may be concluded that the member allowable tensile capacity at the net section is controlled by the inner tube at the splice, and not the bottom chord. Considering the most critical case at the net section, where eight individual rivets are symmetrically installed (Figure 16), the member's load capacity is approximately 122 Kips. Given the actual location of the primary splice connections which is about 33 feet from either end of the bridge and based on the minimum design loads initially considered, the net tensile capacity of this member (i.e. inner tube) is higher than any resultant external tensile force applied to this member (Appendix 5).

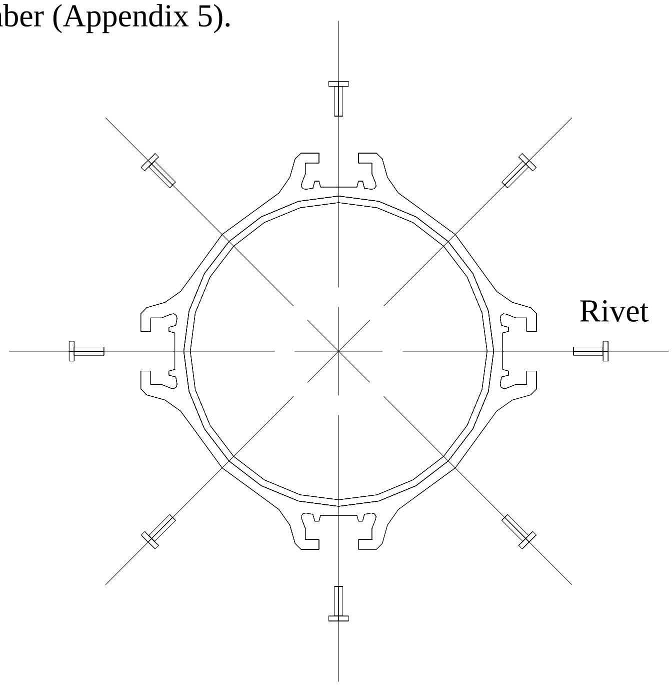

Figure 16: Rivet Pattern at Typical Splice Connection on Bottom Chord

4.2.1 Bottom Chord - Allowable Bearing Capacity at Splice Connection

Based on the intrinsic design of the splice connection in the tension chord, blind rivets are required. Since blind rivets can be installed from one side only without access to the inner side of the bottom chord, they are the fastener of choice. During installation of this type of rivet a special tool pulls the mandrel or pintail deforming the rivet sleeve material around the existing hole to form a head on the back side of the connection (Figure 17). One of the most important design factors in the selection of this type of fastener is the total thickness of the material to be joined (i.e. grip length) which is the wall thickness of the bottom chord plus the wall thickness of the inner tube. This total thickness defines the required length of the rivet necessary to achieve suitable construction of the rivet head.

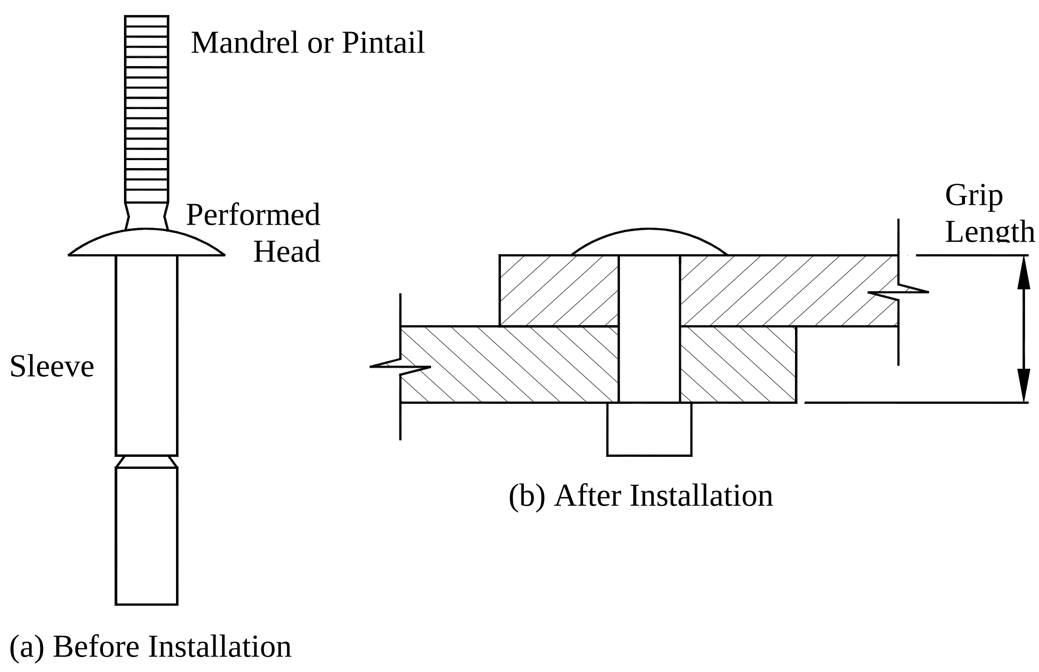

Figure 17: Blind Rivet

The Aluminum Specifications stipulates that blind rivets shall not be used except when the grip lengths and required rivet-hole tolerances are as those suggested by the rivet manufacturer. Furthermore, if the grip length of the rivets exceeds four and a half times the diameter, the allowable load per rivet should be reduced in accordance to a correlation between the grip length and the nominal diameter of the rivet. Since the total grip length in this particular connection (total thickness of metal being fastened is 0.590 inches), is less than the reduction requirement, this design provision does not apply to this splice connection. Additional design requirements called for by the Aluminum Specification are the minimum center-to-center spacing (defines as 3 times the nominal rivet diameter) as well as the edge distance (specified to be no more than 2 times the nominal rivet diameter). The latter is taken from the center of the rivet hole. Based on the overall geometry of the splice connection, the edge distance is again controlled by the dimensions of the inner tube, and evidently the center-to-center spacing remains the same for both members. The existing center-to-center spacing is about 1.97 inches, over 2-1/2 times the minimum required and is adequate. As to the actual edge distance, this dimension is about 0.87 inches, which exceeds 1-1/2 times the minimum edge distance specified, and is sufficient as well.

As to the bearing capacity of this member, the Aluminum Specifications defines the allowable bearing load per rivet as the product of the allowable stress for the material being connected times the effective bearing area of the fastener used. The allowable bearing stress is further defined as twice the ultimate tensile strength of the material divided by its corresponding factor of safety (i.e. $2 \times F_u / n_u$). It is important to point out the allowable bearing stress is used only for a ratio of edge distance to fastener diameter of 2 or greater. In cases where smaller ratios are contemplated, the calculated allowable bearing stress shall be reduced based on the following: edge distance/2 x fastener diameter. However, in this particular case, the reduction is not applicable. The effective bearing area is characterized by the specifications as the grip length times the effective rivet diameter. Moreover, the effective rivet diameter shall be taken as the actual diameter of the hole. Design specifications restrict the overall size of the rivet hole to not more than the actual nominal diameter of the rivet plus an additional 4%. As a result of our evaluation, the calculated bearing strength of this riveted joint at the splice connection is about 95 Kips. It may be concluded that this load carrying capacity exceeds the maximum tensile force induced by the minimum design loads in this member (Appendix 5).

4.2.2 Bottom Chord - Allowable Shear Capacity of Rivets at Splice Connection

Structural design of fasteners for any given material is based on the specifications for the alloy used to fabricate the fastener. Aluminum blind rivets are the type of fastener selected for this evaluation. The Aluminum Specifications call for shear stresses to be calculated on what is defined as the effective area of the rivets. This effective area shall be based on the effective diameter of the rivet. The design provision stipulate that the allowable shear loads on aluminum rivets shall be the product between the effective shear area of the rivet times the minimum shear strength of material divided by a factor of safety of 2.64 (i.e. bridges).

Following the analysis performed on this mechanical connection, the shear capacity was found to be inadequate upon the applicable resultant tensile forces and because of the limited number of rivets used to make up the joint. In order to achieve the required shear capacity two different approaches were chosen. The first approach was to determine the number of rivets required to effectively transfer the maximum applied force at the joint. The original design of the connection incorporated four rivets per row on either side of the splice connection. The analysis showed that more than twice the numbers of existing rivets are needed to transfer the shear at the joint. Thus, the number of rivets per row had to be increased from four to nine. Reference must be made to the actual row layout for rivets at the splice connection (Figure 10), which integrate eight individual rows. The second approach considered was to determine a rather larger effective diameter for the rivets on the original connection, which used four rivets per row. Based on the allowable shear stresses for the material chosen, the original effective diameter had to be increased from 0.256 inches to over 0.370 inches in order to keep the same number of rivets at either side of the splice connection. In either approach it can be seen that the require shear capacity could potentially be achieved and it is a matter of engineering judgment as to what method is more feasible or cost effective (Appendix 5).

4.3 Truss Diagonal Member - Allowable Tensile Capacity at Net Section

The fundamental design parameter for any member under tensile forces is it's cross sectional area. If discontinuities such as holes are present, the effect induced on the load distribution on the cross section must be accounted for concerning the magnitude of the stresses produced. Consequently, holes or discontinuities generate a more highly stressed section as compared to the gross area in these types of members. Since any tension component may fail by excessive yielding or sudden rupture, design checks against both the tensile fracture and yield limit states are considered. Once again, the overall design goal is to size a profile configuration with enough cross sectional area so that the induced ultimate tensile loads do not surpass the load carrying capability of the member. The unique design of the end-connections for these diagonal members incorporate two different bolt patterns (Figure 18). The specific use and location of either bolt configuration is strictly dependent on the magnitude of the applied tensile forces. A staggered pattern “A”, consisting of four individual bolts provided where the diagonal members are subjected to the largest tensile forces. In contrast, two aligned bolts are used in the remaining diagonals where the intensity of the tensile force is smaller.

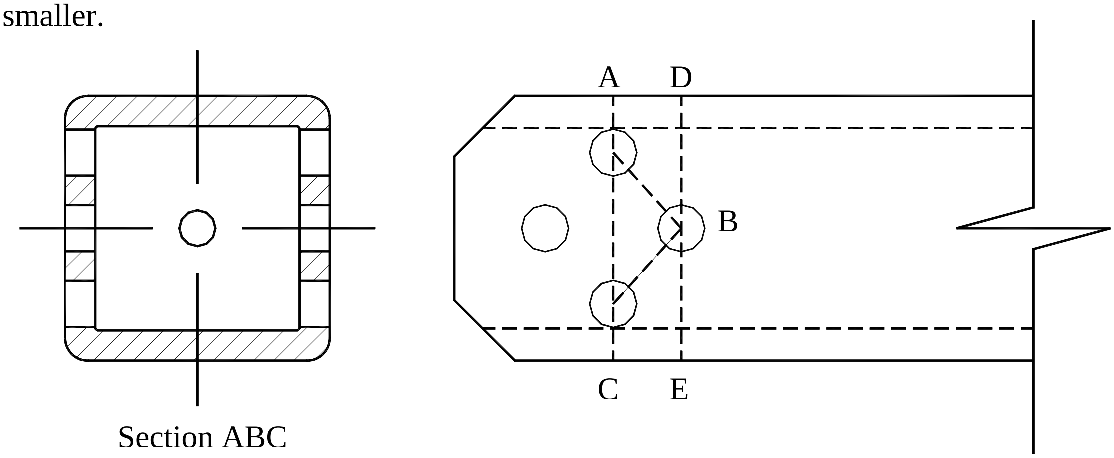

Figure 18: Diagonal Member
(Top Chord/Diagonal Bolt Pattern)

Therefore, three individual fractures paths were evaluated, and the load carrying capacity of each was compared to the applied tensile forces. Form the analysis it was concluded that fracture path AC, as for the heavier tensile loads, and fracture path DE, as for the lighter tensile loads, represent the critical paths. For this reason, the allowable tensile capacity derived from ultimate tensile strength at the net effective section was on the order of 40 kips for fracture path AC and 46 kips for the fracture path DE. As the induced maximum tensile forces are 24 kips for fracture path AC and 10 kips along fracture path DE, the overall allowable tensile strength in these typical diagonal members is considered to be adequate.

4.3.1 Truss Diagonal Member - Allowable Bearing Capacity

Considering both of the bolt configurations available for the diagonal members, the edge distance ratio was to be less than 2 due to the close proximity of the bolt group to the edge of the diagonal member. Therefore, the allowable bearing stress had to be reduced by multiplying its magnitude by the following: (edge distance / 2) x fastener diameter. The resulting reduction in the allowable bearing stress was on the order of 6%. Nonetheless, the arrangement provided an adequate bearing capacity for both bolted configurations considering the existing effective diameter of the bolts incorporated into the design. For bolt pattern “A”, the allowable bearing capacity was on the order of 42 kips as compared to the 24 kips induced in this member by the minimum design loads. Likewise, for bolt pattern “B”, the allowable bearing capacity was on the order of 21 kips as compared to the 10 kips produced in the member. Consequently, the bearing strength is certainly adequate (Appendix 5).

4.3.2 Truss Diagonal Member - Allowable Block Shear Rupture Strength

Another potential limit state for some bolted connections results when a portion of material tears out around the periphery of the bolt group. This limit state is based on a combination between shear and tension precipitating the failure. The failure process will induce fracture in some parts of the member, while at the same time other parts will experience yielding. The overall behavior of the connection upon failure is characterized by a sudden shear fracture accompanied by tension yielding, or by tensile rupture accompanied by shear yielding. However, both failure modes contribute to the strength of the mechanical connection. As a result, the total resistance to block shear will be the sum of the shear and tensile strengths of these two portions respectively.

The Aluminum Specification requires that the block shear rupture allowable force, P_{sr}, induced on the anticipated failure paths, shall be determined by comparing the ultimate strength of the net surfaces in tension versus the ultimate strength of the net surfaces in shear (Figure 19A and 19B). The most likely failure paths of the two diagonal member bolt group are shown. Examination of the geometry of bolt configuration "A" with respect to the line of action of the applied external forces, results in two-inclined failure surfaces (Figure 19). It is well known that these inclined surfaces will develop internally shear and tensile stresses that contribute concurrently to the overall resistance of the connection against block shear. Despite this fact, it was conservatively assumed that only tensile stresses would develop along the inclined surfaces.

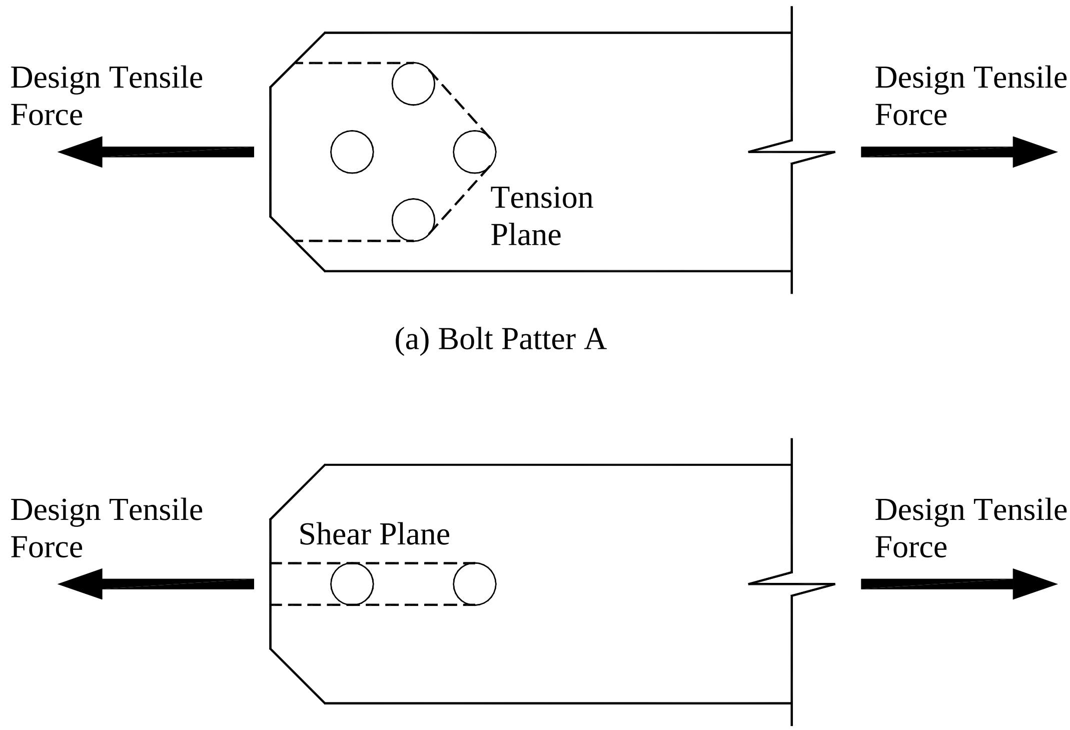

(b) Bolt Pattern B

Figure 19: Block Shear Failure Paths in Diagonal Member

Even so, it was concluded that the block shear behavior within the bolt group would be governed by tensile rupture accompanied by shear yielding (i.e. Fu x At > Fu x As). Based on calculations for bolt pattern "A", the block shear strength of this joint was estimated about 42 kips, in contrast to the 23 kips induced by the minimum design loads. For bolt pattern "B" however, the strength of this bolted connection was significantly of this bolted joint different from that of bolt pattern "A" as the overall capacity is derived solely from the net shear resistance of the failure paths. As such, only shear stresses are developed along the fracture paths without any tensile contribution. From the analysis, it was concluded that the block shear strength of the bolt group "B" was on the order of 35 kips. The 35 kip resistance was deemed satisfactory when compared with the applied design tensile forces of 10 kips applied in this particular member (Appendix 6).

4.3.3 Truss Diagonal Member - Allowable Shear Capacity of Bolt Group

In aluminum structures the selection of fasteners is a matter of choice, and the available options are rather varied. However, it is essential to realize the importance of selecting the appropriate material for the application. Typically, aluminum structures are considered when operating environments are hostile. In these cases, carbon steel fastener are not suitable unless properly coated or in the case that stainless steel materials are used. Furthermore, while different metals are used for fasteners and the members they join, the occurrence of galvanic corrosion is imminent. The difference in electrical potential between different metals gives riser to the possibility of corrosion. Depending on the type of environment and the difference in electrical potential, current will flow from one material (i.e. the anode) to the other material (i.e. the cathode), resulting in the physical deterioration or corrosion. This may be avoided by using fasteners with similar electrical potential. Since the electric potential of aluminum alloys is reasonably small, aluminum bolts do not undergo significant galvanic corrosion when used to joint aluminum members. Thus, aluminum alloy 6061-T6 is the material of choice in this evaluation to eliminate this design concern.

Besides galvanic corrosion, minimum mechanical properties for fasteners are another design consideration for any type of connection. Moreover, alloy specifications require that factors of safety be applied to the minimum design strengths for each fastener. For this particular type of structure (i.e. bridge) the factor of safety would be 2.64. Based on the alloy chosen, the shear strength per bolt in double shear is nearly 4.4 kips/bolt. As such, the overall capacity of bolt pattern “A” is about 17.6 kips, and inadequate when compared to the applied design tensile force of 24 kips. The overall shear capacity for bolt patter “B” is on the order of 8.8 kips and is inadequate as well when compared to the applied design tensile force of 10 kips. As a result, it may be concluded that the aluminum alloy 6061-T6 does not provided the required minimum shear resistance to overcome the applied tensile forces in these diagonal members. Thus, the total number of bolts in the connection group must have to be increased accordingly.

The Aluminum Specifications also provide allowable shear stresses for other aluminum fasteners, including those made of 2024-T4 and 7075-T73. In addition, bolts used in aluminum structures may be made of other material such as the 300 Series stainless steel as well as galvanized carbon steel fasteners. Considering all alternatives, only 2024-T4 would not develop the required shear resistance. Therefore, the remaining alloys 7075-T73, 300 Series Stainless, plated galvanized carbon steel, or even coated A325 carbon steel bolts could represent the feasible choices to provide adequate shear resistance in either bolt pattern (Appendix 6).

4.4 Floor Beams

Beams are structural members that support external transverse forces and primarily subjected to flexure or bending. Even though some degree of axial loading may be induced in beams, compressive effects often are negligible. As a result, internal bending moments give rise to two distinct types of internal stresses, tensile and compressive. It is well known that aluminum alloys are linear elastic materials up to a point, and regarded as homogeneous and isotropic. Thus, the bending stress distribution across any particular cross section is consider to be uniform, given that the strain varies linearly with the distance from the member's neutral axis. It is required that the member's cross-section to have a vertical axis of symmetry and the applied transverse forces to be aligned with this particular axis (i.e. no eccentric loading).

There are several limit states to consider for aluminum components subjected to flexure, and include yielding and fracture, overall buckling, and local buckling. It is essential to explain in detail the analytical approach considered for flexural members with respect to the applied loading conditions and the potential failure modes. Two distinct loadings were imposed on the floor beams as specified by AASHTO. Because of the overall clear width of this bridge, a pair of concentrated live loads produced by a maintenance vehicle was considered to be the first loading condition (Figure 4). This moving load was to act in conjunction with any uniformly distributed dead loads. The second loading condition was a uniformly distributed live load of 85 psf imposed on the full walkway area of the bridge, in addition to the dead loads.

Following a preliminary deflection analysis on the original floor, it was determined that the maximum allowable deflection as specified by AASHTO (i.e. L / 500 = 98.42 in. / 500 = 0.197 in.) was exceeded by either load case. The maximum deflection under the maintenance vehicle was Δ_{max} = 0.486 inch and Δ_{max} = 0.333 inch for the uniformly distributed load. Therefore, the original double-hollow profile did not provide adequate stiffness to properly sustain the prescribe live loads. As the deflection in members subjected to internal bending are a function of the moment of inertia of the cross section, an alternate solution to the original double-hollow profile included the use of a solid section instead. The imposed deflections produced by the two load cases were once again evaluated. It was determined based on the calculations that the deflections still exceeded the maximum allowable for the loads imposed by the maintenance vehicle.

It is important to recognize that structures must be safe, as well as serviceable. A serviceable structure is one that performs satisfactorily, not causing discomfort or perceptions of unsafe for the occupants or users. For a beam, being serviceable typically means that the induced deformations, primarily the vertical deflections must be limited. Too much deflection is always indicative of a rather flexible member, which may bring about problems if components connected to the beam can be damaged by the distortions. From this discussion it can be concluded that even though the overall clear width of the pedestrian bridge provides ample access for a maintenance vehicle to pass, this prescribed load condition exceeds the serviceability requirements for this member. Therefore, the alternate double-solid profile for the floor beams subjected only to the second load condition would be the only extrusion configuration to be considered for evaluation or the flooring system would have to be re-design.

4.4.1 Floor Beams - Bending Tensile Yielding and Fracture

The failure mode for bending tension in flexural members – either yielding or fracture – is to some extent alike to that anticipated for loaded components in axial tension. The similarity hinge on the overall behavior of the loaded material, which is limited by its excessive deformation or fracture strength. For that reason, it is the primary objective in the designing process of these components to determine what bending moments could produce such conditions. When aluminum alloys are loaded in flexure, its internal stress response is linear to some degree. However, once the imposed forces in the member provoke any permanent deformation of the material, this linear array of internal stresses is perturbed. Depending on geometry and how the material is distributed on the cross section of the member about its neutral axis, its response to any given loading condition may differ from any another member with a difference cross sectional distribution. This difference, in addition to the internal stress response of any member, is accounted for with shape factor. Unlike steel, which has a wide diversity of standard shapes, aluminum designs could incorporate any conceivable cross sectional shape so as to maximize the member's effectiveness in responding to any loading condition. Consequently, the corresponding shape factors for such out of the ordinary sections would have to be calculated accordingly since they are a function of the overall dimensions and geometry of the cross section.

For 6061-T6, the ratio of the corresponding factors of safety between the yielding and fracture is 1.85/2.20 or about 0.84. Allowable tensile stresses are strictly governed by the tensile ultimate strength of the material given that the yield strength is in fact greater that 84% of the ultimate strength (F_y = 35 ksi > 0.84 x F_u = 0.84 x 38 ksi = 31.96 ksi). For this reason, the tensile fracture capacity is more critical than yielding. Derived from the imposed loading condition in this flexural member – 85 psf imposed on the full walkway area of the bridge plus the tributary dead load – the actual bending stress at the extreme fiber in the tension side of the cross section is in the order of 1000 psi. It may be concluded that the allowable tensile strength is much larger than the induced bending stresses and is adequate.

4.4.2 Floor Beams - Flexural Buckling

When a beam bends as a result of the imposed external forces, the compression region just above the neutral axis behaves as a column. From a design standpoint, the member will buckle if in between its lateral supports it is slender enough. Unlike a column however, the tension portion just below the neutral axis restrains the compression portion of the beam’s cross-section. As a result, the overall response is an additional twisting about the longitudinal axis of the beam. This form of lateral instability is defined as Lateral Torsional Buckling and is dependent on the lateral bracing (i.e. unbraced length) provided to the compression zone of the beam. If the internal compressive stresses due to bending do not exceed the buckling capacity of the beam, then these stresses can be resolved in the same way as the tensile bending stresses previously discussed. However, if buckling is imminent the strength of the beam will depend on how is laterally braced along its compression flange. Naturally, one strength is also dependent on the cross sectional properties of the member, specifically the correlation between its moment of inertia and cross sectional area.

The Aluminum Specifications however do not provide a specific case to assess the allowable bending stresses for the alternate double-solid profile of the floor beams. As a result, an equivalent solid rectangular profile was considered for evaluation. For analysis purposes, the actual height of the equivalent rectangular cross section was restricted to that of the original double-solid profile of the floor beam (Figure 20). The equivalent width or thickness was derived from its actual moment of inertia (Appendix 3). Based upon the calculations, the allowable bending compressive stress at the extreme fiber of the gross section was on the order of 28 ksi. This is rather large as compared to the actual bending stress induced in the floor beams, which is about 4 ksi. It may be the actual flexural capacity against overall buckling is adequate enough.

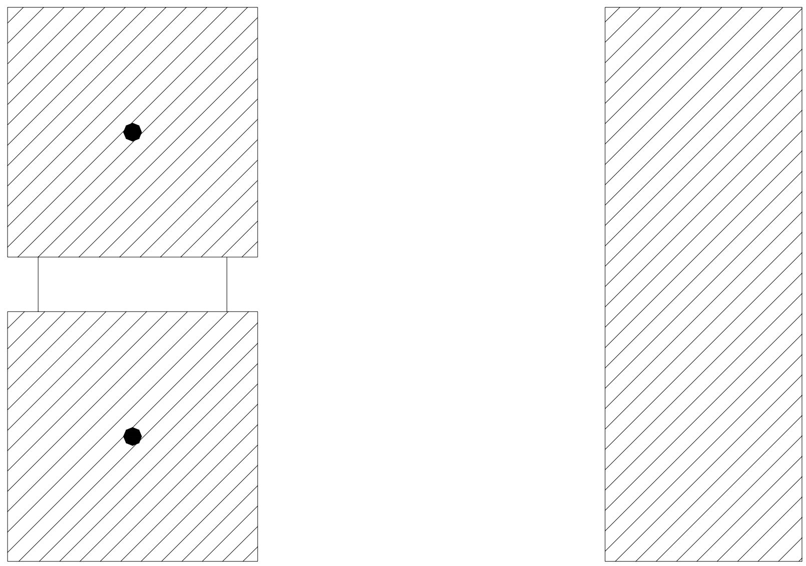

(a) (b)

Figure 20: (a) Double-solid Floor Beam and (b) Equivalent Rectangular Profile to evaluate Lateral Torsional Buckling

4.4.3 Floor Beams - Local Buckling

The Aluminum Specifications divide local buckling provisions for beam elements into two groups – beam elements under uniform compression and beam elements under in-plane bending. For design purposes cross-sectional elements in aluminum members are characterized as plate components, either rectangular or curved in cross section with diverse edge supports. For the double-solid configuration of the floor beam (Figure 14), its plate components are stocky enough to overcome local buckling and therefore this failure mode is not applicable.

4.4.4 Floor Beams Shear

In aluminum members, the bending shear corresponds to another buckling mode that may occur along a slender web of a beam. Based on mechanics, a web element oriented at 45 degrees from the longitudinal axis of a beam under pure bending is subjected to pure shear. However, just above the neutral axis, any portion of the cross-section is subjected to compressive stresses as a result of the bending. For this reason, if the compressive stress is too large then buckling might occur. However, the double-solid profile considered for the floor beams does not have a slender web. Therefore, buckling due to bending shear can be disregarded as a potential failure mode for this member. Nonetheless, the average shear stress across the beam's cross section was estimated to be about 921 psi (see Appendix 7) taking into account the imposed load condition previously chosen for analysis. As the design provisions give an allowable shear stress of 12 ksi as a lower bound for this particular cross section, it may be concluded that is overly conservative.

4.4.5 Floor Beam - Shear Strength of U-Bracket at Lower Standing Leg

The actual restraint provided by the beam's end-supports lends itself to a simply supported idealization. Based on the design of these end-connections, the alternate double-solid profile used for the floor beams is supported only at the top by an U-Bracket similar to that used to connect the vertical posts and diagonals to the bottom chord (see Figure 15). Due to the nature of the support provided by these connections, each U-

Bracket is subjected to an end-reaction of about 7000 Lbs. Therefore, the average shear stress induced across the lower standing leg of the U-Bracket is on the order of 3000 psi (see Appendix 7). However, the allowable shear strength for 6061-T6 alloys is 11000 psi. As such, the shear capacity across the net effective area of the standing leg in the end U-Bracket is adequate.

4.4.6 Floor Beam - Bearing Capacity of U-Bracket at Bottom Chord Connection

The design of these types of mechanical connections incorporates an extruded aluminum U-Bracket fastened to the Bottom Chord by means of a single bolt. There are two distinct material thicknesses however to be considered at this connection, given that the net thickness of the U-Bracket is different from the one of the Bottom Chord. The allowable bearing capacity per bolt in this connection is represented by the product between the allowable stresses for the material to be connected times the effective bearing area of the fastener used. The effective bearing area used from the fastener is the actual nominal diameter of the bolt times the net thickness of the part to be connected. Based on the dimensions provided for either extrusion profile, the thickness of the Bottom Chord is about 18% thinner than the thickness of the U-Bracket. Therefore, the Bottom Chord controls the bearing capacity of this mechanical connection. The allowable bearing force per connection is on the order of 8800 Lbs and is adequate as comparison to the end-reaction of 3000 Lbs produced by the load condition on the floor beams (Figure 21).

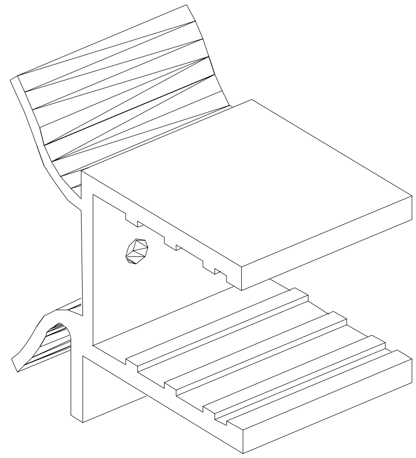

Figure 21: U-Bracket Beam Support

4.5 Vertical Post - Allowable Compressive Capacity

As described in Section 4.1, compression members are structural elements subjected primarily to axial compressive forces. Whenever compression takes place in engineered components, buckling instability is a concern that requires due consideration. The member’s overall dimensions, including the unbraced lengths and cross-sectional widths and thicknesses, in addition to the level of restraint provided by end supports influences the buckling response. In this specific case, the doubly symmetric profile of this member defines the type of buckling modes to be considered. These modes include torsional, flexural, and local buckling. For torsional buckling, this limit state is not applicable to closed cross-sections as the internal shear forces uniformly distributed over the thickness of the cross section counteract any induced twisting. It follows that overall flexural and local buckling modes may be the controlling limit states for the vertical posts considering their actual design spacing in the trusses being evaluated in this analysis.

4.5.1 Vertical Post - Overall Buckling versus Local Buckling

Based on the evaluation of the vertical post it was determined that overall flexural buckling governs its compressive design. However, there were two separate slenderness ratios considered in the analysis, each corresponding to the buckling modes considered. The first slenderness ratio (i.e. k x L / r) was used to assess the axial compression on the gross area of the vertical post. The second slenderness ratio (i.e. b / t) was necessary to measure the axial compression on the gross section of each individual plate component of the post cross-section and consequently, the allowable stress for local buckling. It was determined, that both global and local buckling response was characterized by inelastic behavior. Further, the stress analysis revealed that the allowable column-stress for global buckling was on the order of 13 ksi (Appendix 8). What's more, the effect of local buckling on the member performance is not applicable to this particular member since the slenderness ratios calculated for all the plate elements on the cross section do not exceed the limitations stipulated on the Aluminum Specifications. Given the values obtained form the analysis, the overall load carrying capacity of the vertical posts are larger than the imposed compressive forces induced by the minimum design loads.

4.5.2 Bearing Capacity on Bolted Connections – Vertical Post

The connections in this type of component are of significant importance considering it original design. In view of the applicable external compressive forces, the load transfer could cause a structural failure by excessive deformation of the joints if these are poorly design. Even though the spacing in between the holes is different, as compared to the bolt group at the ends of the diagonal members, the overall bearing capacity per bolthole remains the same in consideration of the same premises used before. It may be concluded that the bearing capacity of the connections in the vertical post is sufficient. The maximum compressive force in the vertical post is about 12 kips at the midspan of the bridge structure (Appendix 8).

4.6 Abutment Bridge Supports

AASHTO design specifications do not require a detail seismic analysis for single span bridges. However, there are some design parameters to be considered when sizing primary connections between the superstructure and substructure. In seismic prone regions, the bridge support connections and the abutments need to resist, both transversely and longitudinally, a seismic load of a prescribed magnitude. The earthquake load to be chosen for design shall be equivalent to the bridge support reaction induced by the self weight of the bridge times the coefficient of ground acceleration at the geographic site. Coefficients of horizontal acceleration are site-specific design values representing the fraction of dead load force to be imposed on these connections. Because of the intrinsic geometric design of these supports, the overall strength is a combination between the allowable bearing capacities of the weld-affected base material plus the allowable shear strength of the filler alloy chosen to weld these members. There are two distinct designs incorporated into these support connections (Figure 22).

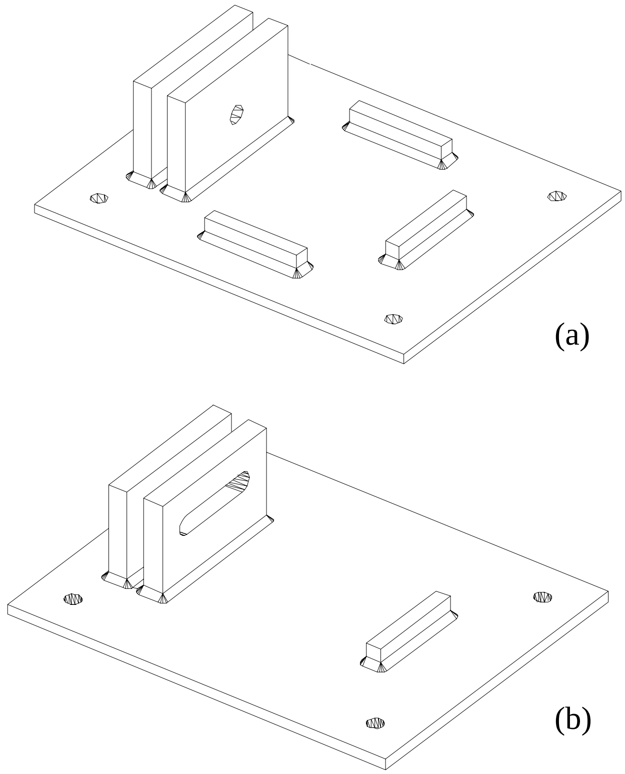

(a) (b)

Figure 22: (a) Bridge Support A (b) Bridge Support B

However, the bearing capacity needs to be considered for Support A only, given that Support B allows for some degree of longitudinal displacement along the slotted hole. As regards to the structural design of the welded members in these connections in conjunction with the load path, the allowable shear strength of the filler wire controls the load carrying capacity of the supports as compared with the allowable shear strength of the base metal affected by the welds. In consideration of the base alloy used for analysis in this bridge, 6061-T6, the Aluminum Specifications provides suitable filler alloys that are dependent on the based metal of the parts to be joined. The filler alloys selected for this specific application were alloys 4043 and 5356.

Based on the structural evaluation of these connections, it was concluded that they in fact are over designed. It is essential to state at this point that aluminum alloys possess a unit weight that is about one third that of typical carbon steels. For that reason, the gravity reaction force at each support induced by the self-weight of the bridge – which is about 2000 pounds – times the maximum coefficient of ground acceleration does not represent a critical loading condition in comparison to the overall strength of these connections, which is in the order of 24 kips.

4.7 U-Bracket Connector

These joint components are designed to connect each diagonal member, as well as the vertical posts to the bottom chord. In view of the reaction forces induced in the brackets, the maximum tensile forces produce by the truss diagonals imposes the most critical loading state. Therefore, the internal compressive forces imposed in these connections by the vertical posts may be disregarded from design. Based on the preceding discussion in Section 4.3, there are two distinct bolted connections at the ends of the diagonal members and their specific design depends on the magnitude of the tensile forces applied to these tension members. Consequently, the same assertion applies to these U-brackets (Figure 23).

With regards to the applicable limit states for the U-brackets, the allowable bearing capacity and block shear strength of the two bolted groups must be evaluated. In addition, the U-Brackets are mechanically fastened to the bottom chord and consequently, the allowable bearing strength must be evaluated as well. However, the load capacity of this connection to the bottom chord must be compared with the horizontal component of the maximum tensile forces on the diagonal. It was determined from the analysis performed on each U-Bracket that their respective allowable bearing capacities as well as the block shear strength of each bolt group were well above the imposed tensile forces in these members. Therefore, each individual U-Bracket provides adequate load capacity against block shear rupture or excessive hole deformation at every bolt group (Appendix 6).

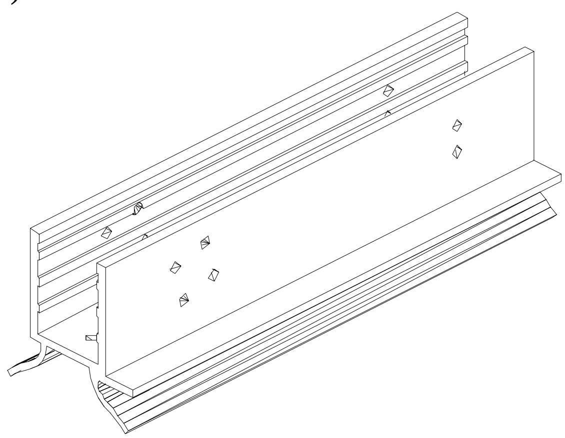

Figure 23: U-Bracket

CHAPTER V

CONCLUSION

The structural integrity of any engineered component as part of a system is a major design factor. A suitable design requires the appropriate selection of cross sections comprised of individual elements, and the determination of the overall proportions and dimensions of all supporting members. Structural safety, serviceability, and economic factors shall be accounted for so as to achieve a cost efficient and safe design. In order to achieve the anticipated service life or performance of a structure, some margin of safety must also be incorporated into its design. This may be attained either by proportioning the framework to factored external loads or by scaling down the stresses that represent the material strength to allowable values. Other than safety, a structure must be serviceable in the sense that it has to perform the intended function satisfactorily. A structure should not cause a perception of functional distress or produce uneasiness to the occupants or users. What's more, the engineer is required to select and assess in detail the overall structural system in order to generate an economical structure. That requires a well-organized and conscious use of construction materials and labor.

It is essential to recognize that any structure be design and constructed in agreement to provisions established by the governing building codes. These building codes embody legal records that consist of predefined requirements related to the structural reliability and serviceability that corresponds to that particular structure. These building codes have the capacity to impose governing laws. For that reason they are administered by governmental entities such as municipalities, cities, counties, and even states. On the other hand, however, these building codes do not furnish specific design procedures, but instead stipulate design requirements and constraints that must be satisfied. In contrast to building codes though, all design specifications provide detailed guidance for the proportioning of structural members and their connections. They present the foremost criteria to enable structural engineers to attain the primary objectives mandated by the governing building codes. These design specifications represent what are approved practices based on the latest advances in the industry.

During the evaluation of the second generation of PML LOGIS-Bridge System, several design specifications and codes were considered for its analysis. It is imperative to elucidate at this point the overall design of this pedestrian bridge was originally conceived at Singen, Germany. As such, its design was different as compared to those applicable in the United States. As a result, the primary objective of this investigation was to evaluate this bridge following the design specifications stated by the governing agency, the American Association of State Highway and Transportation Officials (i.e. AASHTO). In conjunction with the AASHTO Guide Specification for Design of Pedestrian Bridges, the leading design provisions for aluminum structures as established by the Aluminum Association were considered the core specifications for the structural analysis of this bridge. In addition to all these provisions, the latest version of the Minimum Design Loads for Building and Other Structures as provided by the American Society of Civil Engineers was considered as a supplementary reference for the estimation of all the applicable external loads for this structure.

The overall outcome of this structural evaluation is that of a rather sound pedestrian bridge, under well-defined restrictions. However, there are several limit states not fulfilled as based on the controlling design requirements provided by and The Aluminum Design Manual. A limit state is a condition that defines the limit of structural usefulness, and it may be categorized as that due to serviceability or allowable strength requirements. The primary concern for this type of structure (i.e. half-through trusses) is the lack of lateral stability of the top chord. Flexural-torsional buckling is the controlling limit state for the compressive design of this component. Nonetheless, its load carrying capacity in compression can exceed the maximum compressive force imposed provided the effective length of the external bracing arm is kept to a restricted range. Furthermore, AASHTO requires this particular member to be proportioned to sustain 50 pounds per linear feet applied both vertically and horizontally, as well as the maximum compressive force imposed by the estimated minimum design loads. Under these combined load conditions, this member does not provide adequate resistance against combined stresses, no matter the magnitude of the lateral support. This is one of the limit states not satisfied.

The interaction between the induced biaxial bending and the compressive force on the top chord needs to be of such magnitude not to exceed an interaction equation limit.

That was not the case in this particular structure, and the determining factor was the ratio of the average compressive stress on the top chord to the allowable compressive stress. There are several ways to overcome this, and these are all subject to engineering judgment. Either the effective width of the bridge may be reduced, or the height of the trusses increased in order to reduce the imposed compressive force on the top chord. Furthermore, the extrusion profile may be modified, and it's cross sectional area increased so as to further reduce the average compressive stress in this member. These are all reasonable alternatives that need further evaluation.

In the case of the floor system, AASHTO requires that bridges over a certain width to be design for a moving load, as produced by a passing maintenance vehicle. Based on the double-hollow design of the floor beams, the allowable deflection for this component is exceeded and therefore, this beam profile does not provide suitable stiffness to overcome this serviceability requirement. However, strength wise, this member provides adequate bending resistance against the induced stresses imposed by the load combination. As previously assumed, if a double-solid profile with similar geometry were selected, this serviceability requirement would not be a concern.

The load carrying capacity of the bottom chord was governed by the shear strength of the blind rivets at the splice connection. The single shear strength of the rivets themselves was not sufficient enough to sustain the maximum tensile force induced in this joint. Two approaches may be followed to solve the problem. The first approach was to increase the quantity of rivets to be a function of the maximum tensile force imposed in the bottom chord. The second approach was to estimate a new diameter.

Since the other applicable limit states of this component were adequate, the shear capacity of the riveted connection is the weak link. In regards to the remaining members outlining the trusses of this bridge and their corresponding connections, their load carrying capacities were greater than any anticipated external loads. Based on the numerical evaluation performed on each particular component, the imposed internal forces in each member are in well below the allowable stresses as defined by the Aluminum Design Manual.

For structural engineers, the issue of structural reliability is strictly dependent on the applicability of available techniques to carefully design structures, so that the chance of exceeding a prescribed limit state is acceptably small. However, the likelihood for a limited or total collapse in well-designed structures due to catastrophic events such as earthquakes, severe windstorms, or accidental overloads cannot be overlooked. The sole intent should be to limit human loss not necessarily property. The correct determination of the applicable limit state is crucial, given that instability might frequently come about with no preceding warning. It may even bring on a catastrophic collapse, as it has been exemplified by classic failures in the history of structural engineering.

The limit states for structural instability are affected by many variables including material properties, geometry, the magnitude and nature of the applied forces, structural imperfections, the assumptions underlying the theory, the assessment of boundary conditions, and so on. Each of these effects may be random in nature, however this randomness is not completely arbitrary since design rules and prescribed tolerances limit the extent of this variability. However, the reliability of the final overall design rests on the care taken through the whole process of analysis and design. Identifying the limit of a structure's usefulness and providing adequate safeguards against reaching that limit states are what design specifications are about.

BIBLIOGRAPHY

[1] Kissel, J.R & Ferry, R.L., Aluminum Structures: A Guide to their Specifications Design, 1st ed., John Wiley and Sons, 1995.

[2] Aluminum Association, Aluminum Now: Bridges Aluminum High's Strength and Durability Offers New Structural Possibilities, www.aluminum.org/aluminumnow.

[3] Plecher, Robert, Aluminum Applications in the United States, 2000.

[4] Kosteas, D., Aluminum Bridges: Comparative Design Cases, Proceedings Alumitech '97, 2nd International Conference and Trade Exposition, May 1997.

[5] Aluminum Design Manual, Specifications and Guidelines for Aluminum Structures, The Aluminum Association, 2000.

[6] ASCE 7-98 Minimum Design Load for Building and Other Structures, Article 4.8.4 Special Occupancies, pp. 9.

[7] AASHTO, Guide Specifications of Pedestrian Bridges, 1997.

[8] AASHTO Standard Specifications for Highway Bridges, 15th ed., 1992.

[9] Galambos, T.V., Guide to Stability Design Criteria for Metal Structures, 4th ed., 1966.

[10] AASHTO Guide Specifications for Aluminum Highway Bridges, 1991.

[11] AASHTO Guide Specifications for Design of Pedestrian Bridges, Section 1.3.6 Half-through Truss Spans, August 1997.

[12] Welding Aluminum and Aluminum Alloys, American Welding Society, 5th ed., 1966.

[13] Evans, Fernard M., Stress Analysis of Shear Panels in Design of a Semi-Monococue Aluminum Highway Bridge, June 1960

APPENDICES

APPENDIX A

EFFECTIVE MOMENT OF INERTIA FOR COMPOSITE SECTION

CONSISTING OF VERTICAL POST & BRACING ARM

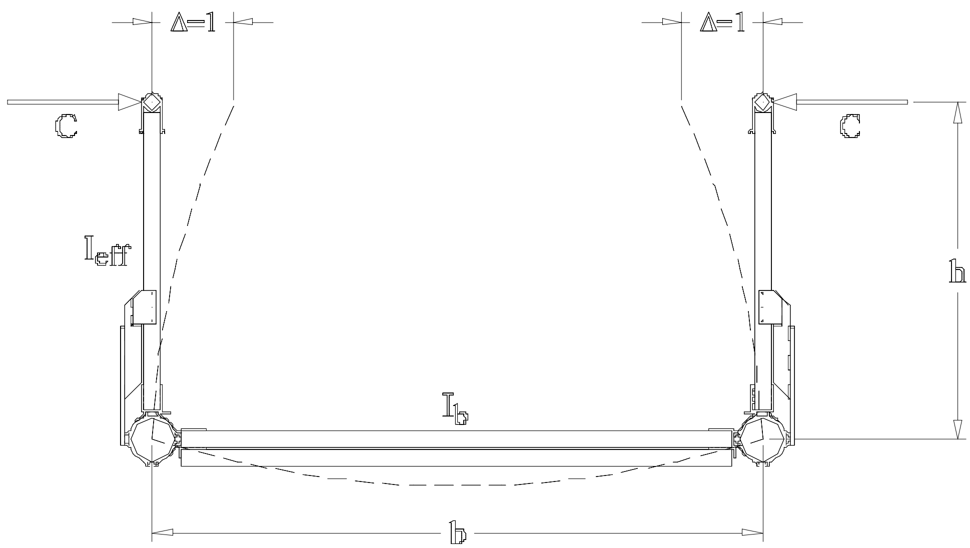

Figure 24: Bridge Typical Cross Section

It is the intent at this point to assess the simultaneous effect each vertical post in conjunction with the external bracing arms provided to the elastic lateral stiffness on each transverse frame. The magnitude of this effect is evaluated by considering the actual effective length of the external bracing arms relative to the overall length of the vertical posts. An equivalent moment of inertia was estimated for a composite section that consisted of each vertical post and it’s corresponding external bracing arm.

Part I: Equivalent Moment of Inertia of Composite Section

Case A - Hollow Vertical Post with Hollow Bracing Arm

Given Data:

1. Vertical Post Cross Sectional Area, A_{vp} = 3.028 in^2

2. Vertical Post Moment of Inertia, I_{vp} = 3.021 in^4

3. Bracing Arm Cross Sectional Area, A_{ba} = 3.028 in^2

4. Bracing Arm Moment of Inertia, I_{ba} = 3.021in^4

Find:

1. Equivalent Moment of Inertia of Composite Section, I_{eq}

$$I_{eq} = I_{vp} + [I_{ba} + A_{ba} \text{ x } e^2]$$

$$= 3.021 \text{ in}^4 + [3.021 \text{ in}^4 + (3.028 \text{ in}^2)(3.346 \text{ in})^2]$$

$$= 3.021 \text{ in}^4 + 36.920 \text{ in}^4$$

$$= 39.94 \text{ in}^4$$

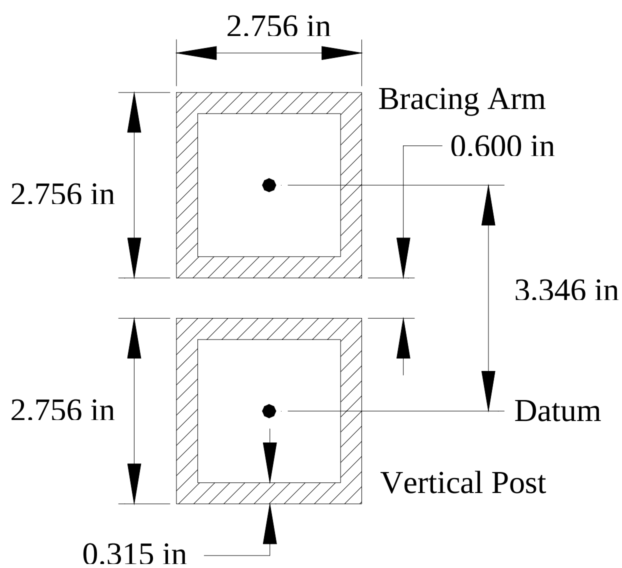

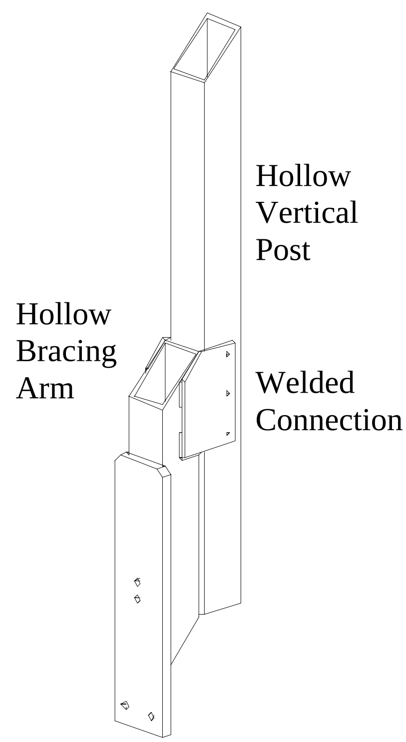

Figure 25: Vertical Post Composite Section – Hollow/Hollow

Case B - Solid Vertical Post with Solid Bracing Arm

Given Data:

1. Vertical Post Cross Sectional Area, $A_{vp} = 7.596 \text{ in}^2$
2. Vertical Post Moment of Inertia, $I_{vp} = 4.808 \text{ in}^4$
3. Bracing Arm Cross Sectional Area, $A_{ba} = 7.596 \text{ in}^2$
4. Bracing Arm Moment of Inertia, $I_{ba} = 4.808 \text{ in}^4$

Find:

1. Equivalent Moment of Inertia of Composite Section, I_{eq}

$$I_{eq} = I_{vp} + [I_{ba} + A_{ba} \text{ x } e^2]$$

$$= 4.808 \text{ in}^4 + [4.808 \text{ in}^4 + (7.596 \text{ in2})(3.346 \text{ in})^2]$$

$$= 4.808 \text{ in}^4 + 89.85 \text{ in}^4$$

$$= 94.65 \text{ in}^4$$

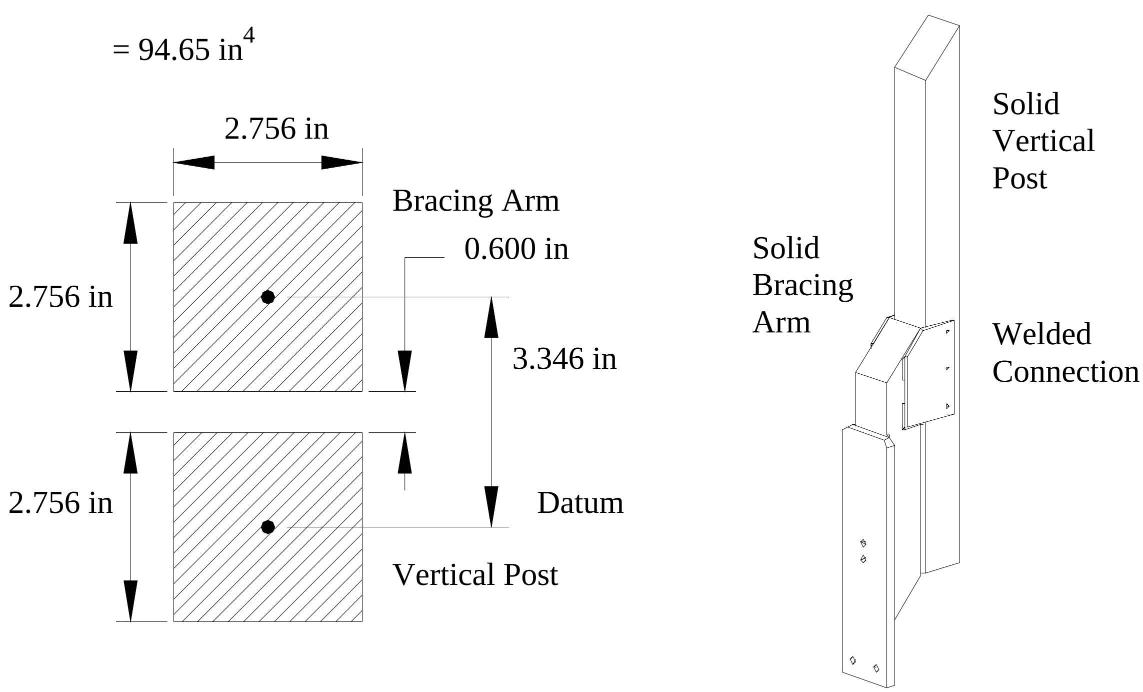

Figure 26: Vertical Post Composite Section – Solid/Solid

Case C - Hollow Vertical Post with Solid Bracing Arm

Given Data:

1. Vertical Post Cross Sectional Area, $A_{vp} = 3.028\ in^2$

2. Vertical Post Moment of Inertia, $I_{vp} = 3.021\ in^4$

3. Bracing Arm Cross Sectional Area, $A_{ba} = 7.596\ in^2$

4. Bracing Arm Moment of Inertia, $I_{ba} = 4.808\ in^4$

Find:

1. Equivalent Moment of Inertia of Composite Section, I_{eq}

$$I_{eq} = I_{vp} + [I_{ba} + A_{ba} \text{ x } e^2\ ]$$

$$= 3.021\ in^4 + [4.808\ in^4 + (7.596\ in2)(3.346\ in)^2]$$

$$= 3.021\ in^4 + 89.85\ in^4$$

$$= 92.87\ in^4$$

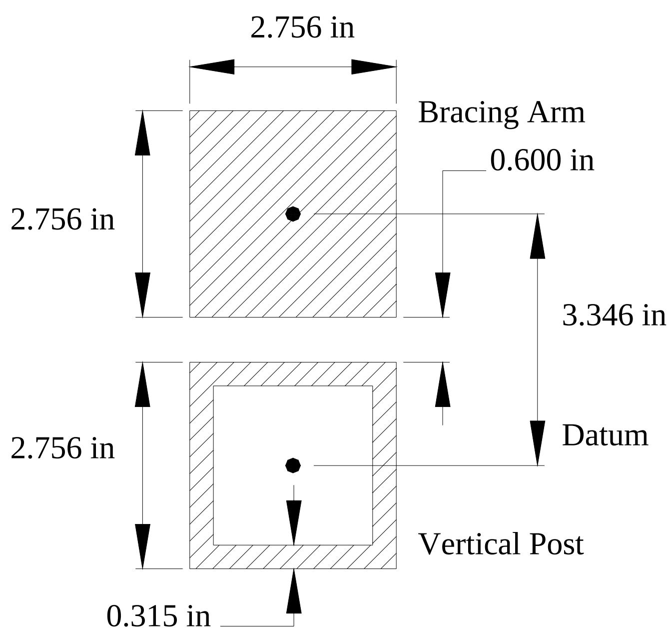

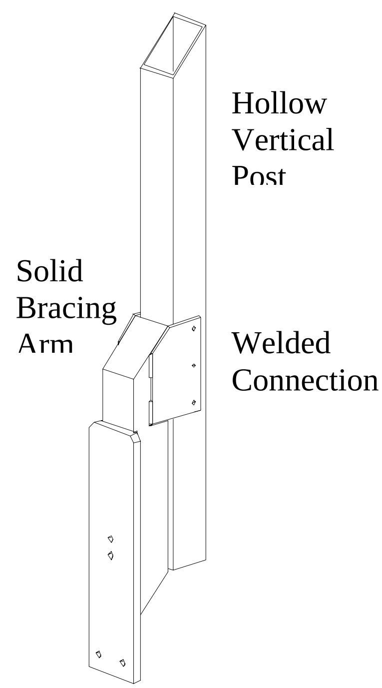

Figure 27: Vertical Post Composite Section – Hollow/Solid

Part II: Formulation of Typical Equation for the Effective Moment of Inertia for a Non Prismatic Member by the Moment Area Method

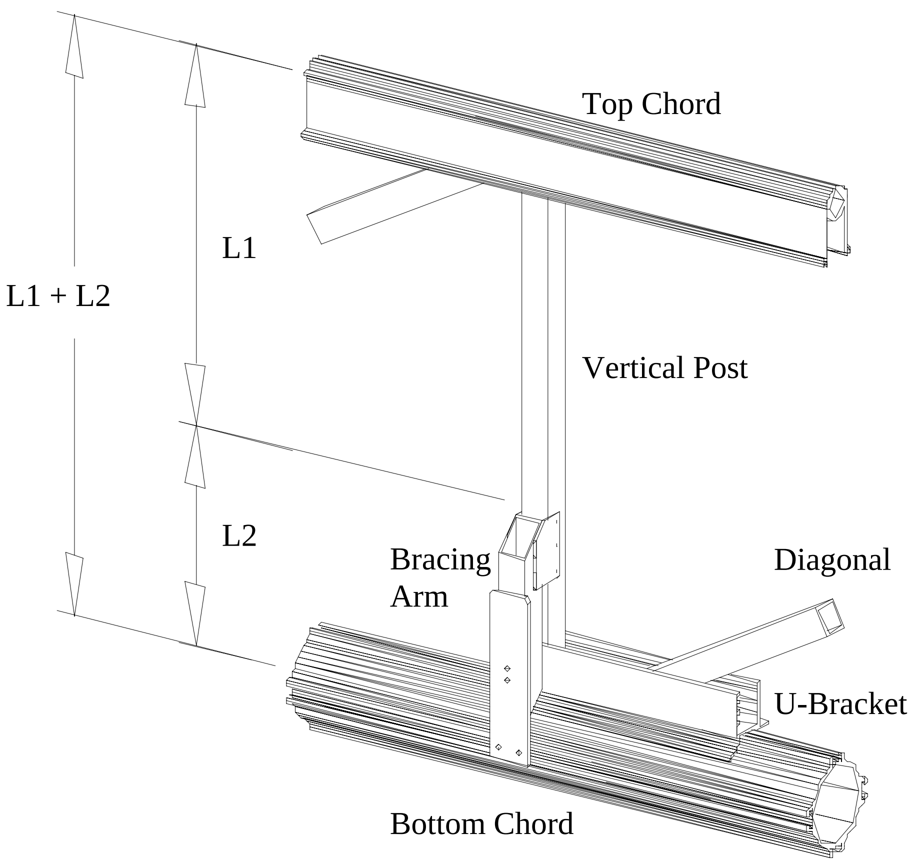

Figure 28: Typical Arrangement for Composite Member
(Vertical Post and Bracing Arm)

Procedure:

Figure 29: Analogy Diagram for Composite Member

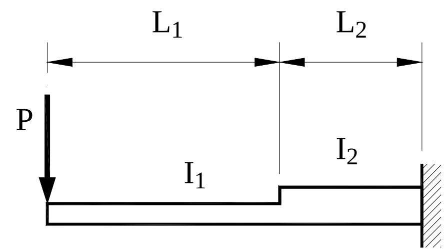

1. Δ = 1st Moment of Area about Fixed End

2. Areas:

$A_1 = ½\, l_1[(P \text{ x } L_1) / (E \text{ x } I_1)]$

$= (P \text{ x } L_1^2) / (2E \text{ x } I_1)$

$A_2 = [(P \text{ x } L_1 \text{ x } L_2) / (E \text{ x } I_2)$

$A_3 = \{[P(L_1 + L_2) / (E \text{ x } I_2)] – [(P \text{ x } L_1) / (E \text{ x } l_2)]\} \text{ x } (L_2 / 2)$

$= (P \text{ x } L_2^2) / (2E \text{ x } I_2)$

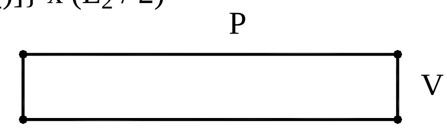

3. Deflections:

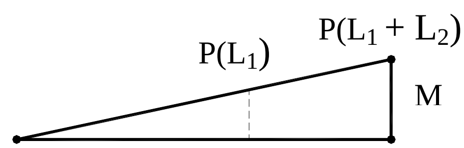

$\Delta_{end} = (A_1 \text{ x } r_1) + (A_2 \text{ x } r_2) + (A_3 \text{ x } r_3)$

$= \{[P \text{ x } L_1^2][L_2 + (L_1 / 3)] / [2E \text{ x } I_1]\} +$

$\{[P \text{ x } L_1 \text{ x } L_2][L_2 / 2] / [E \text{ x } I_2]\} +$

$\{[P \text{ x } L_2^2][L_2/3] / [2E \text{ x } I_2]\}$

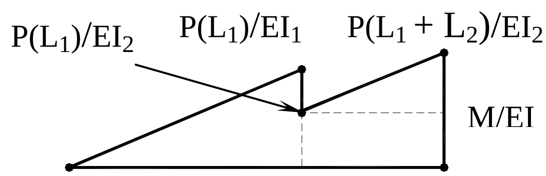

$\Delta_{end} = \Delta_{eff} = [P \text{ x } (L_1 + L_2)^3] / (3 \text{ x } E \text{ x } I_{eff})$

$$\therefore\ I_{eff} = \frac{(L_1 + L_2)^3}{[3L_1^2 \text{ x } L_2 / I_2] + [L_1^3 / I_1] + [3L_1 \text{ x } L_2^2 / I_2] + [L_2^3 / I_2]}$$

Notes:

1. Reference Figure 18 above for the general arrangement of a typical composite member consisting of a vertical post and bracing arm.
2. Formulation of Typical Equation for the Effective Moment of Inertia for a Non Prismatic Member by the Moment Area Method is based on a Cantilever System.

Part III: Application of Typical Equation for the Effective Moment of Inertia of a Non Prismatic Member

Example Calculation for Case A
"AS-IS Design" Hollow Vertical Post and Hollow Bracing Arm

Given:

1. $L_1 = 27.12$ in
2. $L_2 = 28.00$ in
3. $I_1 = 3.021\ in^4$
4. $I_2 = 40.00\ in^4$

$$I_{eff} = \frac{(L_1 + L_2)^3}{[3L_1^2 \times L_2 / I_2] + [L_1^3 / I_1] + [3L_1 \times L_2^2 / I_2] + [L_2^3 / I_2]}$$

$$I_{eff} = \frac{(27.12in + 28.00in)^3}{[3(27.12in)^2 \times (28.00in) / (40.00\ in^4)] + [(27.12in)^3 / (3.021in^4)]} + \frac{(27.12in + 28.00in)^3}{[3(27.12in\ )^2 \times (28.00in) / (3.021in^4)] + [(28.00in)^3 / (40.00in^4)]}$$

$$I_{eff} = \frac{(167466in^3)}{[6602.70 / in] + [1544.50 / in] + [1594.70 / in] + [548.80 / in]}$$

$I_{eff} = [167466\ in^3] / [10290 / in] = \underline{16.27\ in^4}$ CHECK!

Note: See Tables 4, 5 & 6 for all remaining results.

Table 4: Effective Moment of Inertia of a Non Prismatic Member – Case A

CASE A								
E (ksi)	10100	Both the Vertical Post and the Bracing Arm cosist of Hollow Profiles						
$I_1 (in^4)$	3.021							
$I_2 (in^4)$	40							
L_1 (in)	L_2 (in)	I	II	III	IV	V	VI	$I_{eff} (in^4)$
33.25	21.87	167466.38	12172.53	1813.50	1192.46	261.37	15439.86	10.85
33.12	22.00	167466.38	12025.97	1809.94	1202.26	266.20	15304.37	10.94
31.12	24.00	167466.38	9976.27	1743.22	1344.38	345.60	13409.47	12.49
29.12	26.00	167466.38	8173.79	1653.55	1476.38	439.40	11743.12	14.26
27.12	28.00	167466.38	6602.65	1544.54	1594.66	548.80	10290.65	16.27
25.12	30.00	167466.38	5246.97	1419.78	1695.60	675.00	9037.35	18.53
23.12	32.00	167466.38	4090.84	1282.88	1775.62	819.20	7968.54	21.02
21.12	34.00	167466.38	3118.39	1137.44	1831.10	982.60	7069.54	23.69
19.12	36.00	167466.38	2313.73	987.05	1858.46	1166.40	6325.65	26.47
17.12	38.00	167466.38	1660.97	835.32	1854.10	1371.80	5722.18	29.27
15.12	40.00	167466.38	1144.21	685.84	1814.40	1600.00	5244.45	31.93
13.12	42.00	167466.38	747.57	542.22	1735.78	1852.20	4877.77	34.33
11.12	44.00	167466.38	455.16	408.06	1614.62	2129.60	4607.44	36.35
9.12	46.00	167466.38	251.09	286.95	1447.34	2433.40	4418.79	37.90
7.12	48.00	167466.38	119.48	182.50	1230.34	2764.80	4297.11	38.97
5.51	49.61	167466.38	55.49	113.12	1017.65	3051.71	4237.96	39.52

Table Legend:

- Item I = $(L_1 + L_2)^3$
- Item II = $[L_1^3 / I_1]$
- Item III = $[3L_1^2 \times L_2 / I_2]$
- Item IV = $[3L_1 \times L_2^2 / I_2]$
- Item V = $[L_2^3 / I_2]$
- Item VI = (Item II + Item III + Item IV + Item V)
- I_{eff} = (Item I / Item VI)

Table 5: Effective Moment of Inertia of a Non Prismatic Member – Case B

CASE B								
I_1(in^4)	4.808	Both Vertical Post and Bracing Arm consist of Solid Profiles						
I_2 (in^4)	94.7							
L_1 (in)	L_2 (in)	I	II	III	IV	V	VI	I_{eff} (in^4)
33.25	21.87	167466.38	7648.34	766.00	503.68	110.40	9028.42	18.55
33.12	22.00	167466.38	7556.25	764.49	507.82	112.44	8941.00	18.73
31.12	24.00	167466.38	6268.37	736.31	567.85	145.98	7718.50	21.70
29.12	26.00	167466.38	5135.82	698.44	623.60	185.60	6643.46	25.21
27.12	28.00	167466.38	4148.63	652.39	673.56	231.81	5706.39	29.35
25.12	30.00	167466.38	3296.81	599.70	716.20	285.11	4897.82	34.19
23.12	32.00	167466.38	2570.39	541.87	750.00	346.02	4208.28	39.79
21.12	34.00	167466.38	1959.37	480.44	773.43	415.04	3628.28	46.16
19.12	36.00	167466.38	1453.78	416.92	784.99	492.67	3148.36	53.19
17.12	38.00	167466.38	1043.63	352.83	783.15	579.43	2759.03	60.70
15.12	40.00	167466.38	718.94	289.69	766.38	675.82	2450.82	68.33
13.12	42.00	167466.38	469.72	229.03	733.17	782.34	2214.26	75.63
11.12	44.00	167466.38	285.99	172.36	682.00	899.51	2039.86	82.10
9.12	46.00	167466.38	157.77	121.20	611.34	1027.84	1918.15	87.31
7.12	48.00	167466.38	75.07	77.09	519.68	1167.81	1839.65	91.03
5.51	49.61	167466.38	34.87	47.78	429.84	1289.00	1801.49	92.96

Table Legend:

- Item I = $(L_1 + L_2)^3$
- Item II = $[L_1^3 / I_1]$
- Item III = $[3L_1^2 \times L_2 / I_2]$
- Item IV = $[3L_1 \times L_2^2 / I_2]$
- Item V = $[L_2^3 / I_2]$
- Item VI = (Item II + Item III + Item IV + Item V)
- I_{eff} = (Item I / Item VI)

Table 6: Effective Moment of Inertia of a Non Prismatic Member – Case C

CASE C								
$I_1 (in^4)$	3.021	Vertical Post consist of a hollow profile with bracing arm solid						
$I_2 (in^4)$	93							
L_1 (in)	L_2 (in)	I	II	III	IV	V	VI	$I_{eff} (in^4)$
33.25	21.87	167466.38	12172.533	780.001	512.886	112.415	13577.836	12.33
33.12	22.00	167466.38	12025.974	778.470	517.099	114.495	13436.038	12.46
31.12	24.00	167466.38	9976.266	749.771	578.230	148.645	11452.912	14.62
29.12	26.00	167466.38	8173.788	711.204	635.004	188.989	9708.986	17.25
27.12	28.00	167466.38	6602.651	664.318	685.874	236.043	8188.885	20.45
25.12	30.00	167466.38	5246.965	610.659	729.290	290.323	6877.237	24.35
23.12	32.00	167466.38	4090.843	551.777	763.706	352.344	5758.670	29.08
21.12	34.00	167466.38	3118.394	489.221	787.572	422.624	4817.810	34.76
19.12	36.00	167466.38	2313.731	424.538	799.339	501.677	4039.286	41.46
17.12	38.00	167466.38	1660.965	359.277	797.461	590.022	3407.724	49.14
15.12	40.00	167466.38	1144.207	294.986	780.387	688.172	2907.753	57.59
13.12	42.00	167466.38	747.568	233.214	746.570	796.645	2523.998	66.35
11.12	44.00	167466.38	455.160	175.509	694.462	915.957	2241.088	74.73
9.12	46.00	167466.38	251.093	123.420	622.514	1046.624	2043.650	81.94
7.12	48.00	167466.38	119.478	78.495	529.177	1189.161	1916.311	87.39
5.51	49.61	167466.38	55.494	48.653	437.697	1312.562	1854.406	90.31

Table Legend:

- Item I = $(L_1 + L_2)^3$
- Item II = $[L_1^3 / I_1]$
- Item III = $[3L_1^2 \times L_2 / I_2]$
- Item IV = $[3L_1 \times L_2^2 / I_2]$
- Item V = $[L_2^3 / I_2]$
- Item VI = (Item II + Item III + Item IV + Item V)
- I_{eff} = (Item I / Item VI)

APPENDIX B

EFFECTIVE LENGTH FACTOR FOR COMPRESSIVE MEMBERS, K

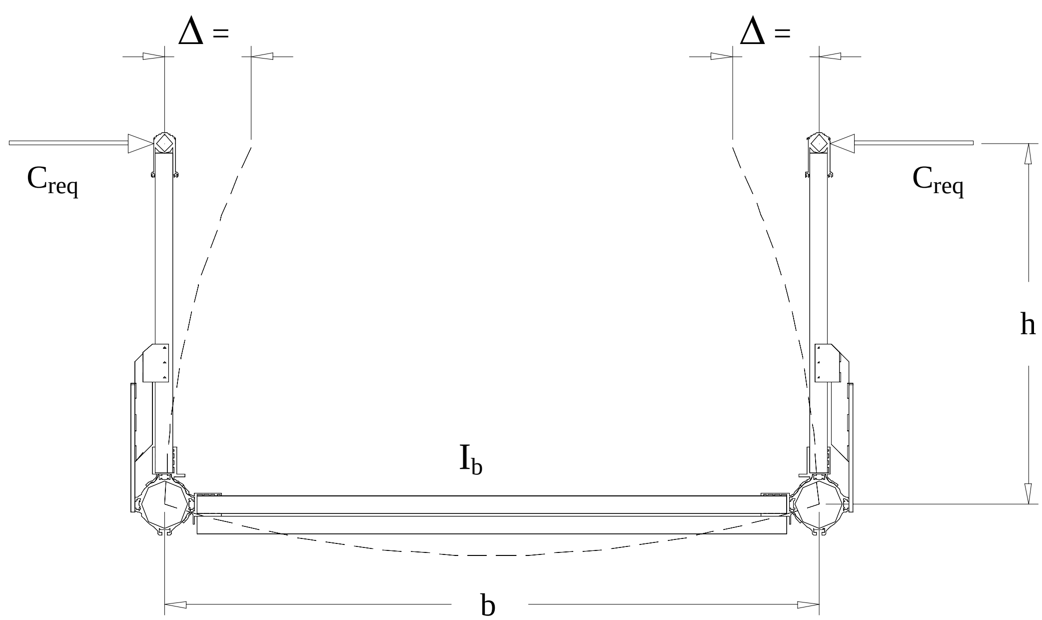

Figure 30: Transverse Frame Spring Constant

The design of a compression member is based on a calculated critical buckling force. The presented design principles in this structural evaluation, as specified by AASHTO [7], are based on a semiempirical method by Holt and others. Such method for analysis computes the required lateral stiffness made available to the top chord by the intermittent elastic supports. Holt presented a set of analytical guidelines that correlate these values to the magnitude of the critical buckling force. The elastic stiffness of the transverse frames was found to be directly dependent on the flexural rigidity (EI) of each panel member; especially the vertical posts in conjunction with the external bracing arms, the floor beams, and to some extent the diagonal members. Knowing that aluminum alloys are homogeneous and isotropic, with a constant modulus of elasticity within the elastic range, the leading variables include the corresponding moments of inertia of each member outlining the transverse frames. In consideration of this fact, six different combinations were evaluated. In each separate case, the contribution to the stiffness of the transverse frame was evaluated as a function of the effective lengths of the external bracing arms and each member's cross-sectional property.

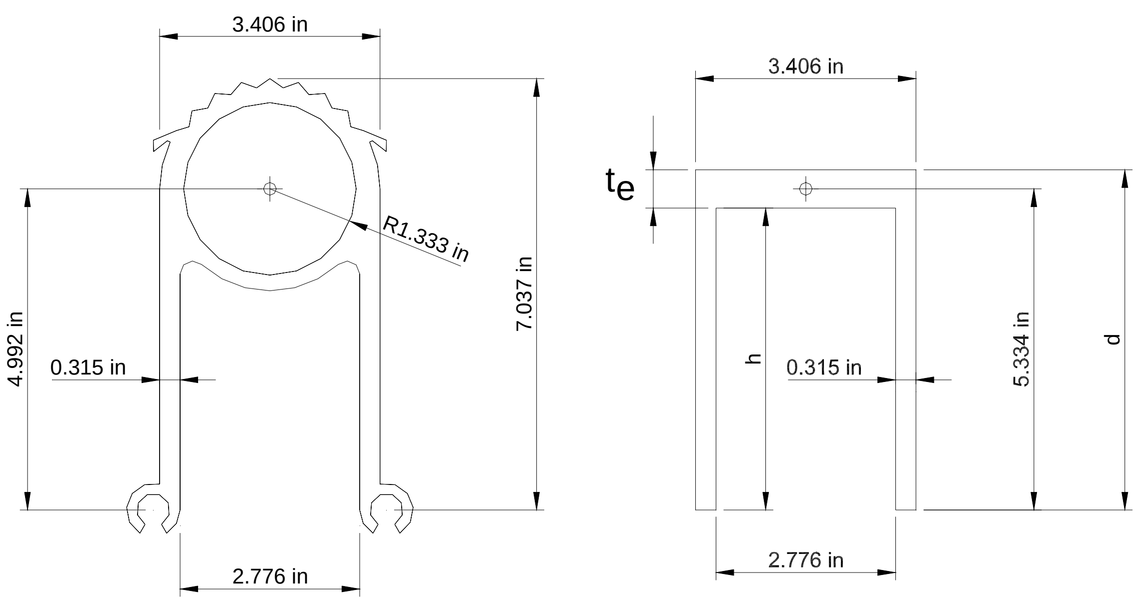

Figure 31: Top Chord Sectional View
(a) Original Section (b) Equivalent Section

Transverse Frame Spring Constant, C_{req}

(Effective Length Factor for Compression Members, k)

Description of Cases Evaluated:

Case I - All frame members are hollow extrusions (as-is design).

Note: Contribution form diagonal members not incorporated into analysis.

Case II - All frame members are hollow extrusions (as-is design).

Note: Contribution form diagonal members are incorporated into analysis.

Case III - Vertical Post and Bracing Arm consist of solid extrusions, however Floor Beams remain hollow.

Note: Contribution form diagonal members not incorporated into analysis.

Case IV - All frame members consist of solid extrusions.

Note: Contribution form diagonal members are incorporated into analysis.

Case V - Bracing Arm and Floor Beam consist of solid extrusions, however the vertical post remain hollow.

Note: Contribution form diagonal members are incorporated into analysis.

Case VI - Frame members consist of solid extrusions, except Floor Beams.

Note: Contribution form diagonal members are incorporated into analysis.

Truss Top Chord Lateral Support: Half-through Bridge

Overall Slenderness Ratio for Flexural Buckling

Equivalent Channel Cross Section

American Association of State Highway and Transportation Officials:

A. Section 1.3.6 Guide Specifications for Design of Pedestrian Bridges

1. Vertical posts, floor beams, and their connections shall be proportionate to resist a lateral force applied @ the top of the vertical post that is not less than 0.01/k times the average design compressive force in the two adjacent top chord members.
2. "k" is the effective length factor for the individual top chord member supported between the truss vertical post and it represents the nature of the lateral restraint against rotations and the resistance to lateral deflection at the end of the unbraced length of the top chord.
3. In no case shall the value for 0.010/k be less than 0.003 when determining the minimum lateral force regardless of the effective length factor used to determine the compressive capacity of the top chord.

B. Example Procedure: Case II (As-Is design)

1. Case Description - All members outlining the transverse frame consist of hollow extrusions (as-is design) and the contribution of the diagonal members is incorporated into the evaluation of the transverse frame spring constant.

2. As-is member dimensions and cross sectional properties:

a) Effective Length of Floor Beam = 102.91 inches

b) Moment of Inertia of Floor Beam = 22.94 in^4

c) Height of Vertical Post = 55.12 inches

d) Effective Moment of Inertia of Vertical Post = 26.47 in^4

e) Length of Diagonal Members = 112.81 inches

f) Moment of Inertia of Diagonal Members = 3.021 in^4

g) Modulus of Elasticity for 6061-T6 Aluminum Alloy = 10100 ksi

3. Transverse Frame Spring Constant, Creq

$$C_{req} = \frac{E}{h^2 \{h/[3 \text{ x } I_{eff} + 3 \text{ x } I_d \text{ x } (h/L_d)^3] + (b/2 \text{ x } I_{fb})\}}$$

$$C_{req} = \frac{10100 \text{ ksi}}{(55.12 \text{ in})^2\{55.12 \text{ in}/[3(37.9 \text{ in}^4) + 3(3.021 \text{ in}^4)(55.12 \text{ in}/112.81 \text{ in})^3]\}}$$

$$+ \quad \frac{10100 \text{ ksi}}{[102.91 \text{ in}/(2)(22.99 \text{ in\^{}4})]}$$

$$C_{req} = \frac{10100 \text{ ksi}}{(3038 \text{ in\^{}2})[(0.480/\text{in}) + (2.238/\text{in})]} = 1.223 \text{ k/in}$$

4. Estimation of the Effective Length Factor, k

Note: The top chord is considered for analysis purposes for this type of structures a column restraint by elastic lateral supports (elastic springs) @ each panel point. The critical buckling force of the column shall be determined in consideration of a factor of safety not less than 2 times the maximum design group loading.

- $(C_{req} \text{ x } L) / P_c$ = (1.223 k/in) (98.42 in) / 88 kips = 1.368

Table A provides the reciprocal of the effective length factor as a function of the transverse frame spring constant (C_{req}) and the total number of panels the bridge truss consist of.

- For (Creq x L)/Pc = 1.368 & by means of interpolation…

  1/k = 0.703 & k = 1.422

  Note: Make reference to Table A to estimate "k".

Table 7: 1/k for Various Values of (C x L)/L

N = NUMBER OF PANELS IN TRUSS							
1/K	4	6	8	10	12	14	16
1.000	3.686	3.161	3.660	3.714	3.754	3.785	3.809
0.980		3.284	2.944	2.806	2.787	2.771	2.774
0.960		3.000	2.665	2.542	2.456	2.454	2.479
0.950			2.595				
0.940		2.754		2.303	2.252	2.254	2.282
0.920		2.643		2.146	2.094	2.101	2.121
0.900	3.352	2.593	2.263	2.045	1.951	1.968	1.981
0.850		2.460	2.013	1.794	1.709	1.681	1.694
0.800	2.961	2.313	1.889	1.629	1.480	1.456	1.465
0.750		2.147	1.750	1.501	1.344	1.273	1.262
0.700	2.448	1.955	1.595	1.359	1.200	1.111	1.088
0.650		1.739	1.442	1.236	1.087	0.988	0.940
0.600	2.035	1.639	1.338	1.133	0.985	0.878	0.808
0.550		1.517	1.211	1.007	0.860	0.768	0.708
0.500	1.750	1.362	1.047	0.847	0.750	0.668	0.600
0.450		1.158	0.829	0.714	0.624	0.537	0.500
0.400	1.232	0.886	0.627	0.555	0.454	0.428	0.383
0.350		0.530	0.530	0.352	0.323	0.292	0.280
0.300	0.121	0.187	0.249	0.170	0.203	0.183	0.187
Reference: Galambos, T.V. Guide to Stability Design for Metal							
Structures, 4th ed.,1988. New York: John Wiley & Sons, Inc.							

APPENDIX C

EQUIVALENT SLENDERNESS RATIO FOR FLEXURAL TORTIONAL BUCKLING

For design purposes the slenderness ratio is a way to measure the tendency of compression member to buckle under a prescribed force. A clear advantage of extruded aluminum profiles however is that practically any shape can be fabricated by standard practices in the industry. Consequently, this buckling tendency could be restrained to some extent considering that by means of the extrusion process any cross section could be designed by putting the material where it is needed. However for singly symmetric profiles subjected to compressive forces, such as the extrusion profile of the top chord, their behavior is restricted by flexural, flexural-torsional buckling, or by local buckling. The intent in this particular section is to estimate the tendency of the top chord to buckle by means of flexural torsional buckling considering a representative channel shape with the equivalent cross sectional area from the original top chord. The evaluation of such buckling response of this member has been evaluated in conformity to the level of lateral restraint imposed onto the top chord by the external bracing arms.

Equivalent Slenderness Ratio for Flexural Buckling

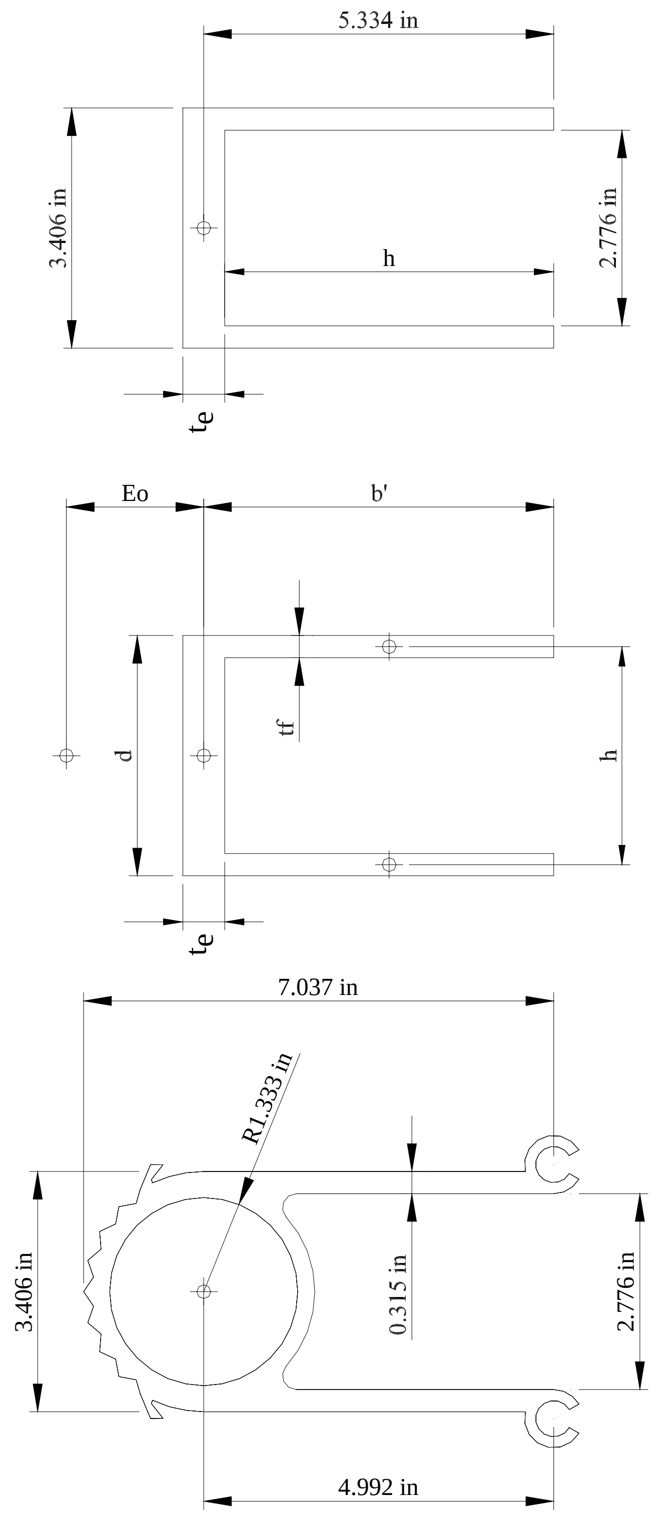

Figure 32: Top Chord Equivalent Channel Section

A. Total Cross Sectional Area of Original Extrusion Profile:

   1. At = 6.273 in^2

B. Find:

   1. Equivalent Web Thickness, t_e (in.)
   2. New Cross Sectional Properties for Equivalent Channel Section
      i. Centroid, y
      ii. Moment of Inertia, I_{xx} and I_{yy}
      iii. Warping Constant, C_w
      iv. Radius of Gyration, r_{xx} and r_{yy}
      v. Torsional Constant, J
      vi. Polar Radius of Gyration, r_o
   3. Equivalent Slenderness Ratio for Flexural Torsional Buckling

C. Procedure:

   1. Equivalent Web Thickness, t_e
      i. Atotal = (2)(A_{flange} + A_{web}) = 6.273 in^2

         = 2[(3.79 in + 1.535 in - t_e/2)(0.315 in)] + (3.406 in)(t_e)

         = (7.598 in + 3.069 in - t_e)(o.315 in) + (3.406 in)(t_e)

         = [2.393 in^2 + 0.967 in^2 - 0.315 x t_e]

         = (6.273 in^2 - 2.393 in^2 - 0.967 in^2)/(3.406 in - 0.315 in)

      ∴ t_e = 0.942 inches

2. New Cross Sectional Properties for Equivalent Channel Section

i. Centroid, y

Part	Area
1	3.406 x te
2	[5.334 -(te/2)] x (0.315 in)
3	[5.334 -(te/2)] x (0.315 in)

Part	M_x = Area • y
1	18.168 x te
2	{[5.334 -(te/2)] x (0.315 in)} x {[5.334 - (te/2)]/2}
3	{[5.334 -(te/2)] x (0.315 in)} x {[5.334 - (te/2)]/2}

Note: Part 1 corresponds to the Web & Part 2 & 3 to the Flanges.

$$y = \frac{18.168 \text{ x te} + 2\{[5.334 -(te/2)] \text{ x } (0.315 \text{ in}) \text{ x } [5.334 - (te/2)]/2\}}{3.406 \text{ x te} + 2\,[5.334 -(te/2)(0.315 \text{ in})]}$$

$$y = \frac{18.168 \text{ x te} +(1.680 -0.158 \text{ x te})(5.334 - 0.50 \text{ x te})}{3.406 \text{ x te} + 3.360 - 0.315 \text{ x te}}$$

$$y = \frac{18.168 \text{ x te} + 8.962 - 0.840 \text{ x te}^2 - 0.840 \text{ x te} + 0.079 \text{ x te}}{3.091 \text{ x te} + 3.360}$$

$$y = \frac{18.168(0.942 \text{ in}) + 8.962 - 0.840(0.942 \text{ in})^2}{3.091(0.940 \text{ in}) + 3.360}$$

$$\frac{-0.840(0.940 \text{ in}) +0.079(0.940 \text{ in})}{3.091(0.940 \text{ in}) + 0.360}$$

y = 3.925 in from Datum

ii. Moment of Inertia about Strong Axis, I_{xx}

$I_{xx} = I_{web} + 2 \text{ x } I_{flange}$

I_{xx} = (3.406 in)[(1/12)(0.942 in)^3 + (0.942 in)(5.344 - 3.799 in)^2] +

(0.315 in){(1/12)[5.334 in - (0.942 in)/2]^3 + [5.334 - (0.942 in)/2]} x

{3.799 in - [(5.334 in - (0.924 in /2))/2]}^{2}} x 2

I_{xx} = (6.764 in^4 + 6.608 in^4) = 11.969 in^4 = 12.0 in^4

iii. Moment of Inertia about Weak Axis, I_{yy}

$I_{yy} = I_{web} + 2 \text{ x } I_{flange}$

I_{yy} = [(1/12)(0.942 in)(3.406 in)^3] +

2 x {(1/12)[3.799 in + 1.535 in - (0.942 in /2)](0.315 in)^3 +

(0.315 in)[3.799 in + 1.535 in -(0.942 in/2)(1.545)^2}

I_{yy} = 3.102 in^4 + 7.338 in^4= 10.44 in^4

iv. Warping Constant, C_w

$h = d - t_f$ = 3.406 in -0.315 in = 3.091 in

$b' = b_f - (t_w/2)$ = 5.334 in

$E_o = (t_f \text{ x } b'^2)/[2 \text{ x } b' \text{x } t_f + (h \text{ x } t_w)/3]$

= [(0.315 in)(5.334 in)^2]/[2(5.334 in)(0.315 in) + (3.091in)(0.942in)/3]

E_o = 2.069 in

$C_w = \{(h^2 \times b'^2 \times t_w) \times [b' - (3 \times E_o)]/ 6.00\} + E_o^2 \times I_{xx}$

$= \{[(3.091\ in)^2(5.334\ in)^2(0.315\ in)] \times [5.334\ in - 3(2.069\ in)]]/6.00\}+$

$(2.069\ in)^2(12.0\ in^4) = 38.90\ in^6$

v. Radius of Gyration, r_{xx} & r_{yy}

$r_{xx} = (I_{xx} / A)^{0.50} = (12.0\ in^4 / 6.273\ in^2)^{0.50} = 1.383\ in$

$r_{yy} = (I_{yy} / A)_{0.50} = (10.44\ in^4 / 6.273\ in^2)^{0.50} = 1.290\ in$

vi. Torsional Constant, J

$J = \text{Sum } [(b_f \times t_w^3)/3 - 0.21 \times t_w^4]$ for Open Cross Sections

$= 2 \times \{[(5.334\ in - (0.942\ in /2))(0.315\ in)^3]/3 - 0.21(0.315\ in)^4\} +$

$\{[(3.406in)(0.942\ in)^3]/3 - 0.21(0.942\ in)^4\}$

$= 0.881\ in^4$

vii. Polar Radius of Gyration, r_o

$r_o = [y_o^2 + r_{xx}^2 + r_{yy}^2]^{0.50}$

$r_o = \{[E_o + (b' - y)]^2 + r_{xx}^2 + r_{yy}^2\}^{0.50}$

$r_o = \{[(2.069\ in + 1.401\ in)^2 + (1.383\ in)^2 + (1.290\ in)^2]\}^{0.50}$

$r_o = 3.959\ in$

3. Equivalent Slenderness Ratio

i. F_{et}

$F_{et} = \{[1/(A \text{ x } r_o^2)][(G \text{ x } J) + (3.14156)^2(E)(C_w)/(k_t \text{ x } L_t)^2]\}$

$F_{et} = \{[1/(6.273 \text{ in}^2)(3.959 \text{ in})^2][(3800 \text{ ksi})(0.881 \text{ in}^4) +$

$(3.14156)^2(10100 \text{ ksi})(38.9 \text{ in}^6)/((1.00)(98.42))^2]\} = 38.47 \text{ ksi}$

ii. B

$B = 1-(y_o/r_o)^2 = 1- [(2.069 \text{ in} + 1.401 \text{ in})/3.959 \text{ in}]^2 = 0.232$

iii. F_{ey}

$F_{ey} = [(3.14156)^2 \text{ x } E]/[(k_y \text{ x } L_b)/r_{yy}]^2$

$F_{ey} = [(3.14156)^2(10100 \text{ ksi})]/[k_y(98.42 \text{ in})/1.290 \text{ in})]^2$

$F_{ey} = (99683 \text{ ksi})/(5822) \text{ x } k_y^2$

Note: The equivalent slenderness ratio for flexural torsional buckling is a function of the effective length factor, k. The effective length factor is in turn dependent on the degree of restraint provided to the top chord by the members outlining the transverse frames. Therefore, the overall evaluation for flexural torsional buckling is in turn a function of the effective length of the external bracing arms. (REFERENCE WORKSHEET)

4. Example calculation: Equivalent Slenderness Ratio for Flexural Torsional Buckling (Equivalent Channel Section)

CASE I - L2 = 32 inches & ky = 1.59

(a) F_{ey}= 99683 ksi/(5822)$(1.59)^2$ = 6.80 ksi (CHECK)

(b) $F_{ey}+F_{et}$ = (6.80 ksi + 38.47 ksi) = 45.27 ksi (CHECK)

(c) $(F_{ey}+F_{et})^2$ = $(45.27 \text{ ksi})^2$ = 2049 ksi^2 (CHECK)

(d) $4B(F_{ey})(F_{et})$ = 4(0.232)(6.80 ksi)(38.47 ksi) = 242.76ksi^2 (CHECK)

(e) $[(F_{ey} + F_{et})^2 - 4B(F_{ey})(F_{et})]^{0.50} = [2049 \text{ ksi}^2 - 242.7 \text{ ksi}^2]^{0.50}$

= 42.49 ksi (CHECK)

(f) $(F_{ey} + F_{et}) - [(F_{ey} + F_{et})^2 - 4B(F_{ey})(F_{et})]^{0.50}$ = (45.27 ksi - 42.49 ksi)

= 2.76 ksi (CHECK)

(g) $(1/2B)\{(F_{ey} + F_{et}) - [(F_{ey} + F_{et})^2 - 4B(F_{ey})(F_{et})]^{0.50}\}$ = (2.76 ksi)/2(0.232)

= 5.948 ksi (CHECK)

(h) $(3.14156)[E/F_e]^{0.50} = (3.14156)[10100 \text{ ksi}/5.948 \text{ ksi}]^{0.50}$

= 129.30 (CHECK) ------------------ Equivalent Slenderness Ratio

Table 8: Overall Slenderness for Vertical Post – Case 1

CASE I: FLEXURAL TORSIONAL BUCKLING - OVERALL SLENDERNESS									
Bracing Arm Effective Length inches	ky	Fey	(Fey+Fet)	$(Fey+Fet)^2$	4B(Fey)(Fet)	$[(Fey+Fet)^2 - 4B(Fey)(Fet)]^{0.50}$	$(Fey+Fet) - [(Fey+Fet)^2 - 4B(Fey)(Fet)]^{0.50}$	Fe	$\pi[E/Fe]^{0.50}$
22	1.88	4.85	43.32	1876.26	173.00	41.27	2.05	4.41	150.32
24	1.82	5.14	43.61	1901.98	183.56	41.45	2.16	4.65	146.34
26	1.76	5.54	44.01	1937.18	197.90	41.70	2.31	4.98	141.48
28	1.70	5.92	44.39	1970.45	211.34	41.94	2.45	5.28	137.40
30	1.64	6.35	44.82	2008.85	226.70	42.22	2.60	5.62	133.20
32	1.59	6.80	45.27	2048.98	242.60	42.50	2.76	5.96	129.30
34	1.54	7.21	45.68	2086.82	257.46	42.77	2.91	6.28	126.00
36	1.51	7.53	46.00	2115.65	268.69	42.98	3.02	6.51	123.71
38	1.48	7.85	46.32	2145.30	280.15	43.19	3.13	6.75	121.51
40	1.46	8.03	46.50	2162.62	286.81	43.31	3.19	6.89	120.30
42	1.44	8.22	46.69	2180.21	293.55	43.44	3.26	7.03	119.12
44	1.43	8.34	46.81	2191.34	297.80	43.51	3.30	7.11	118.39
46	1.42	8.44	46.91	2200.33	301.23	43.58	3.33	7.18	117.82
48	1.42	8.51	46.98	2207.12	303.81	43.63	3.35	7.23	117.40
49.61	1.42	8.53	47.00	2209.39	304.67	43.64	3.36	7.25	117.26

Table 9: Overall Factor of Safety for Vertical Post – Case 1

CASE I: AS-IS TRANSVERSE FRAME (DIAGONALS NOT INCORPORATED INTO ANALYSIS)					
Effective Height of Bracing Arm	Effective Length Factor for Top Chord	Overall Slenderness (Flexural-Torsional)	Allowable Compressive Stress for Top Chord	Allowable Compressive Force for Top Chord	Overall Factor of Safety for Top Chord
Inches	k	$\left\{\frac{\pi \times E}{F_e}\right\}^{0.5} > S_2 = 66$	$F_c(\text{ksi}) = \frac{51000}{\left(\frac{\pi \times E}{F_e}\right)}$	P_c (kips)	$\frac{P_c \text{ (kips)}}{P_u \text{ (kips)}}$
22.00	1.88	143.80	2.47	15.47	0.35
24.00	1.82	139.62	2.62	16.41	0.37
26.00	1.76	134.49	2.82	17.69	0.40
28.00	1.70	130.17	3.01	18.88	0.43
30.00	1.64	125.72	3.23	20.24	0.46
32.00	1.59	121.55	3.45	21.65	0.49
34.00	1.54	118.02	3.66	22.97	0.52
36.00	1.51	115.55	3.82	23.96	0.54
38.00	1.48	113.19	3.98	24.97	0.57
40.00	1.46	111.88	4.07	25.56	0.58
42.00	1.44	110.60	4.17	26.16	0.59
44.00	1.43	109.81	4.23	26.53	0.60
46.00	1.42	109.19	4.28	26.83	0.61
48.00	1.42	108.73	4.31	27.06	0.61
49.61	1.42	108.58	4.33	27.14	0.62

L	Iy	A	ry	Pu
98.42	10.44	6.27	1.29	44 Kips

Table 10: Overall Slenderness for Vertical Post – Case 2

CASE II: FLEXURAL TORSIONAL BUCKLING - OVERALL SLENDERNESS									
Bracing Arm Effective Length inches	ky	Fey	(Fey+Fet)	$(Fey+Fet)^2$	4B(Fey)(Fet)	$[(Fey+Fet)^2 - 4B(Fey)(Fet)]^{0.50}$	$(Fey+Fet) - [(Fey+Fet)^2 - 4B(Fey)(Fet)]^{0.50}$	Fe	$\pi[E/Fe]^{0.50}$
22	1.87	4.92	43.39	1882.61	175.61	41.32	2.07	4.47	149.30
24	1.81	5.24	43.71	1910.21	186.92	41.51	2.19	4.73	145.15
26	1.75	5.62	44.09	1944.07	200.69	41.75	2.34	5.04	140.60
28	1.69	6.00	44.47	1977.63	214.22	41.99	2.48	5.34	136.58
30	1.63	6.41	44.88	2014.47	228.94	42.26	2.63	5.67	132.63
32	1.58	6.86	45.33	2054.86	244.92	42.54	2.79	6.01	128.77
34	1.54	7.26	45.73	2090.89	259.05	42.80	2.93	6.31	125.67
36	1.50	7.57	46.04	2119.84	270.31	43.01	3.04	6.55	123.39
38	1.48	7.82	46.29	2143.16	279.33	43.17	3.12	6.73	121.66
40	1.46	8.06	46.53	2164.80	287.65	43.33	3.20	6.91	120.15
42	1.44	8.25	46.72	2182.43	294.40	43.45	3.27	7.04	118.97
44	1.43	8.37	46.84	2193.58	298.66	43.53	3.30	7.13	118.25
46	1.42	8.46	46.93	2202.59	302.08	43.59	3.34	7.20	117.68
48	1.42	8.53	47.00	2209.39	304.67	43.64	3.36	7.25	117.26
49.61	1.41	8.56	47.03	2211.66	305.53	43.66	3.37	7.27	117.12

Table 11: Overall Factor of Safety for Vertical Post – Case 2

CASE II: AS-IS TRANSVERSE FRAME (DIAGONALS ARE INCORPORATED INTO ANALYSIS)					
Effective Height of Bracing Arm	Effective Length Factor for Top Chord	Overall Slenderness for Top Chord	Allowable Compressive Stress for Top Chord	Allowable Compressive Force for Top Chord	Overall Factor of Safety for Top Chord
Inches	k	$\left\{\frac{\pi \text{ x } E}{F_e}\right\}^{0.5} > S_2 = 66$	$F_c(\text{ksi}) = \frac{51000}{\left(\frac{\pi \text{ x } E}{F_e}\right)}$	P_c (kips)	$\frac{P_c \text{ (kips)}}{P_u \text{ (kips)}}$
22.00	1.87	142.73	2.50	15.70	0.36
24.00	1.81	138.36	2.66	16.71	0.38
26.00	1.75	133.56	2.86	17.93	0.41
28.00	1.69	129.30	3.05	19.14	0.43
30.00	1.63	125.10	3.26	20.44	0.46
32.00	1.58	120.98	3.48	21.86	0.50
34.00	1.54	117.66	3.68	23.11	0.53
36.00	1.50	115.21	3.84	24.10	0.55
38.00	1.48	113.35	3.97	24.90	0.57
40.00	1.46	111.71	4.09	25.63	0.58
42.00	1.44	110.44	4.18	26.23	0.60
44.00	1.43	109.66	4.24	26.61	0.60
46.00	1.42	109.04	4.29	26.91	0.61
48.00	1.42	108.58	4.33	27.14	0.62
49.61	1.41	108.43	4.34	27.21	0.62

L	Iy	A	ry	Pu
98.42	10.44	6.27	1.29	44 Kips

Table 12: Overall Slenderness for Vertical Post - Case 3

CASE III: FLEXURAL TORSIONAL BUCKLING - OVERALL SLENDERNESS									
Bracing Arm Effective Length (inches)	ky	Fey	(Fey+Fet)	$(Fey+Fet)^2$	4B(Fey)(Fet)	$[(Fey+Fet)^2 - 4B(Fey)(Fet)]^{0.50}$	$(Fey+Fet) - [(Fey+Fet)^2 - 4B(Fey)(Fet)]^{0.50}$	Fe	$\pi[E/Fe]^{0.50}$
22	1.63	6.43	44.90	2016.35	229.69	42.27	2.63	5.68	132.44
24	1.56	6.99	45.46	2066.72	249.59	42.63	2.83	6.11	127.71
26	1.52	7.46	45.93	2109.40	266.26	42.93	3.00	6.46	124.19
28	1.47	7.87	46.34	2147.45	280.98	43.20	3.14	6.77	121.36
30	1.44	8.25	46.72	2182.43	294.40	43.45	3.27	7.04	118.97
32	1.41	8.58	47.05	2213.94	306.40	43.68	3.38	7.28	116.98
34	1.39	8.85	47.32	2239.30	315.99	43.86	3.47	7.48	115.48
36	1.37	9.10	47.57	2262.83	324.84	44.02	3.55	7.65	114.15
38	1.36	9.30	47.77	2281.97	332.01	44.16	3.61	7.79	113.12
40	1.34	9.48	47.95	2298.96	338.35	44.28	3.67	7.91	112.24
42	1.33	9.63	48.10	2313.71	343.83	44.38	3.72	8.02	111.49
44	1.33	9.73	48.20	2323.63	347.50	44.45	3.75	8.09	111.01
46	1.32	9.81	48.28	2331.11	350.27	44.51	3.77	8.14	110.64
48	1.32	9.86	48.33	2336.13	352.13	44.54	3.79	8.18	110.40
49.61	1.32	9.89	48.36	2338.65	353.06	44.56	3.80	8.20	110.28

Table 13: Overall Factor of Safety for Vertical Post – Case 3

CASE III: TRANSVERSE FRAME VERTICAL POSTS, BRACING ARMS, & DIAGONALS CONSIST OF SOLID PROFILES EXCEPT FLOOR BEAMS (DIAGONALS ARE INCORPORATED INTO ANALYSIS)					
Effective Height of Bracing Arm	Effective Length Factor for Top Chord	Overall Slenderness for Top Chord	Allowable Compressive Stress for Top Chord	Allowable Compressive Force for Top Chord	Overall Factor of Safety for Top Chord
Inches	k	$\left\{\frac{\pi \times E}{F_e}\right\}^{0.5} > S_2 = 66$	$F_c(\text{ksi}) = \dfrac{51000}{\left(\frac{\pi \times E}{F_e}\right)}$	P_c (kips)	$\dfrac{P_c \text{ (kips)}}{P_u \text{ (kips)}}$
22.00	1.63	124.90	3.27	20.51	0.47
24.00	1.56	119.86	3.55	22.27	0.51
26.00	1.52	116.07	3.79	23.75	0.54
28.00	1.47	113.02	3.99	25.05	0.57
30.00	1.44	110.44	4.18	26.23	0.60
32.00	1.41	108.28	4.35	27.29	0.62
34.00	1.39	106.64	4.48	28.13	0.64
36.00	1.37	105.19	4.61	28.91	0.66
38.00	1.36	104.07	4.71	29.54	0.67
40.00	1.34	103.10	4.80	30.10	0.68
42.00	1.33	102.28	4.87	30.58	0.69
44.00	1.33	101.75	4.93	30.90	0.70
46.00	1.32	101.35	4.97	31.15	0.71
48.00	1.32	101.09	4.99	31.31	0.71
49.61	1.32	100.96	5.00	31.39	0.71

L	Iy	A	ry	Pu
98.42	10.44	6.27	1.29	44 Kips

Table 14: Overall Slenderness for Vertical Post - Case 4

CASE IV: FLEXURAL TORSIONAL BUCKLING - OVERALL SLENDERNESS									
Bracing Arm Effective Length	ky	Fey	(Fey+Fet)	$(Fey+Fet)^2$	4B(Fey)(Fet)	$[(Fey+Fet)^2 - 4B(Fey)(Fet)]^{0.50}$	$(Fey+Fet) - [(Fey+Fet)^2 - 4B(Fey)(Fet)]^{0.50}$	Fe	$\pi[E/Fe]^{0.50}$
inches									
22	1.14	13.08	51.55	2657.29	466.92	46.80	4.75	10.24	98.66
24	1.11	13.90	52.37	2742.56	496.21	47.40	4.97	10.73	96.39
26	1.08	14.65	53.12	2821.72	523.00	47.94	5.17	11.16	94.50
28	1.06	15.19	53.66	2879.74	542.40	48.35	5.32	11.47	93.23
30	1.05	15.52	53.99	2914.65	553.98	48.59	5.40	11.65	92.50
32	1.04	15.88	54.35	2953.73	566.85	48.86	5.49	11.85	91.73
34	1.03	16.14	54.61	2982.59	576.31	49.05	5.56	11.99	91.18
36	1.02	16.41	54.88	3011.84	585.84	49.25	5.63	12.13	90.63
38	1.02	16.51	54.98	3022.90	589.44	49.33	5.65	12.19	90.43
40	1.02	16.54	55.01	3026.60	590.64	49.36	5.66	12.21	90.37
42	1.02	16.61	55.08	3034.02	593.05	49.41	5.68	12.24	90.23
44	1.01	16.65	55.12	3037.74	594.25	49.43	5.68	12.26	90.17
46	1.01	16.68	55.15	3041.47	595.46	49.46	5.69	12.28	90.10
48	1.01	16.68	55.15	3041.47	595.46	49.46	5.69	12.28	90.10
49.61	1.01	16.68	55.15	3041.47	595.46	49.46	5.69	12.28	90.10

Table 15: Overall Factor of Safety for Vertical Post - Case 4

CASE IV: TRANSVERSE FRAME MEMBERS ARE ALL SOLID PROFILES (DIAGONALS ARE INCORPORATED INTO ANALYSIS)					
Effective Height of Bracing Arm	Effective Length Factor for Top Chord	Overall Slenderness for Top Chord	Allowable Compressive Stress for Top Chord	Allowable Compressive Force for Top Chord	Overall Factor of Safety for Top Chord
Inches	k	$\left\{\frac{\pi \times E}{F_e}\right\}^{0.5} > S_2 = 66$	$F_c(\text{ksi}) = \frac{51000}{\left(\frac{\pi \times E}{F_e}\right)}$	P_c (kips)	$\frac{P_c \text{ (kips)}}{P_u \text{ (kips)}}$
22.00	1.14	88.00	6.59	41.31	0.94
24.00	1.11	85.42	6.99	43.84	1.00
26.00	1.08	83.26	7.36	46.15	1.05
28.00	1.06	81.80	7.62	47.81	1.09
30.00	1.05	80.97	7.78	48.80	1.11
32.00	1.04	80.07	7.95	49.90	1.13
34.00	1.03	79.43	8.08	50.70	1.15
36.00	1.02	78.81	8.21	51.51	1.17
38.00	1.02	78.58	8.26	51.82	1.18
40.00	1.02	78.50	8.28	51.92	1.18
42.00	1.02	78.34	8.31	52.12	1.18
44.00	1.01	78.27	8.33	52.22	1.19
46.00	1.01	78.19	8.34	52.33	1.19
48.00	1.01	78.19	8.34	52.33	1.19
49.61	1.01	78.19	8.34	52.33	1.19

L	Iy	A	ry	Pu
98.42	10.44	6.27	1.29	44 Kips

Table 16: Overall Slenderness for Vertical Post - Case 5

CASE V: FLEXURAL TORSIONAL BUCKLING - OVERALL SLENDERNESS									
Bracing Arm Effective Length inches	ky	Fey	(Fey+Fet)	$(Fey+Fet)^2$	4B(Fey)(Fet)	$[(Fey+Fet)^2 - 4B(Fey)(Fet)]^{0.50}$	$(Fey+Fet) - [(Fey+Fet)^2 - 4B(Fey)(Fet)]^{0.50}$	Fe	$\pi[E/Fe]^{0.50}$
22	1.31	9.99	48.46	2348.75	356.78	44.63	3.83	8.27	109.81
24	1.23	11.37	49.84	2484.30	406.01	45.59	4.25	9.18	104.22
26	1.17	12.58	51.05	2605.60	448.93	46.44	4.61	9.93	100.18
28	1.13	13.50	51.97	2701.01	482.00	47.11	4.86	10.49	97.47
30	1.09	14.49	52.96	2804.96	517.36	47.83	5.13	11.07	94.89
32	1.06	15.13	53.60	2872.83	540.10	48.30	5.30	11.43	93.37
34	1.05	15.55	54.02	2918.18	555.14	48.61	5.41	11.67	92.43
36	1.04	15.94	54.41	2960.91	569.21	48.91	5.51	11.88	91.59
38	1.03	16.28	54.75	2997.17	581.07	49.15	5.59	12.06	90.90
40	1.02	16.48	54.95	3019.21	588.24	49.30	5.64	12.17	90.50
42	1.02	16.54	55.01	3026.60	590.64	49.36	5.66	12.21	90.37
44	1.02	16.61	55.08	3034.02	593.05	49.41	5.68	12.24	90.23
46	1.01	16.65	55.12	3037.74	594.25	49.43	5.68	12.26	90.17
48	1.01	16.68	55.15	3041.47	595.46	49.46	5.69	12.28	90.10
49.61	1.01	16.68	55.15	3041.47	595.46	49.46	5.69	12.28	90.10

Table 17: Overall Factor of Safety for Vertical Post - Case 5

CASE V: TRANSVERSE FRAME BRACING ARMS & FLOOR BEAMS ARE SOLID PROFILES ONLY (DIAGONALS ARE INCORPORATED INTO ANALYSIS)					
Effective Height of Bracing Arm	Effective Length Factor for Top Chord	Overall Slenderness for Top Chord	Allowable Compressive Stress for Top Chord	Allowable Compressive Force for Top Chord	Overall Factor of Safety for Top Chord
Inches	k	$\left\{\frac{\pi \times E}{F_e}\right\}^{0.5} > S_2 = 66$	$F_c(ksi) = \frac{51000}{\left(\frac{\pi \times E}{F_e}\right)}$	P_c (kips)	$\frac{P_c \text{ (kips)}}{P_u \text{ (kips)}}$
71.63	1.31	100.43	5.06	31.72	0.72
76.02	1.23	94.24	5.74	36.02	0.82
80.01	1.17	89.71	6.34	39.76	0.90
82.90	1.13	86.64	6.79	42.62	0.97
84.61	1.09	83.70	7.28	45.66	1.04
86.52	1.06	81.97	7.59	47.61	1.08
87.91	1.05	80.89	7.80	48.90	1.11
89.31	1.04	79.91	7.99	50.10	1.14
89.84	1.03	79.12	8.15	51.11	1.16
90.02	1.02	78.65	8.24	51.71	1.18
90.37	1.02	78.50	8.28	51.92	1.18
90.55	1.02	78.34	8.31	52.12	1.18
90.73	1.01	78.27	8.33	52.22	1.19
90.73	1.01	78.19	8.34	52.33	1.19
90.73	1.01	78.19	8.34	52.33	1.19

L	Iy	A	ry	Pu
98.42	10.44	6.27	1.29	44 Kips

Table 18: Overall Slenderness for Vertical Post - Case 6

CASE VI: FLEXURAL TORSIONAL BUCKLING - OVERALL SLENDERNESS										
Bracing Arm Effective Length	ky	Fey	(Fey+Fet)	$(Fey+Fet)^2$	4B(Fey)(Fet)	$[(Fey+Fet)^2 - 4B(Fey)(Fet)]^{0.50}$	$(Fey+Fet) - [(Fey+Fet)^2 - 4B(Fey)(Fet)]^{0.50}$	Fe	$\pi[E/Fe]^{0.50}$
inches									
22	1.39	8.93	47.40	2246.32	318.63	43.91	3.49	7.53	115.07
24	1.31	9.99	48.46	2348.75	356.78	44.63	3.83	8.27	109.81
26	1.24	11.18	49.65	2464.94	399.06	45.45	4.20	9.05	104.94
28	1.18	12.23	50.70	2570.02	436.45	46.19	4.50	9.72	101.29
30	1.15	12.96	51.43	2644.99	462.65	46.72	4.71	10.17	99.01
32	1.12	13.65	52.12	2716.88	487.44	47.22	4.91	10.58	97.05
34	1.09	14.33	52.80	2788.34	511.75	47.71	5.09	10.98	95.27
36	1.08	14.81	53.28	2838.61	528.67	48.06	5.22	11.25	94.12
38	1.06	15.16	53.63	2876.29	541.25	48.32	5.31	11.45	93.30
40	1.06	15.35	53.82	2897.13	548.17	48.47	5.36	11.56	92.86
42	1.06	15.19	53.66	2879.74	542.40	48.35	5.32	11.47	93.23
44	1.05	15.65	54.12	2928.78	558.64	48.68	5.43	11.72	92.22
46	1.04	15.75	54.22	2939.44	562.15	48.76	5.46	11.78	92.01
48	1.04	15.81	54.28	2946.57	564.50	48.81	5.48	11.81	91.87
49.61	1.04	15.85	54.32	2950.15	565.68	48.83	5.48	11.83	91.80

Table 19: Overall Factor of Safety for Vertical Post - Case 6

CASE VI: TRANSVERSE FRAME FLOOR BEAMS ARE SOLID PROFILES ONLY
(DIAGONALS ARE INCORPORATED INTO ANALYSIS)

Effective Height of Bracing Arm	Effective Length Factor for Top Chord	Overall Slenderness for Top Chord	Allowable Compressive Stress for Top Chord	Allowable Compressive Force for Top Chord	Overall Factor of Safety for Top Chord
Inches	k	$\left\{\frac{\pi \times E}{F_e}\right\}^{0.5} > S_2 = 66$	$F_c(ksi) = \frac{51000}{\left(\frac{\pi \times E}{F_e}\right)}$	P_c (kips)	$\frac{P_c\ (kips)}{P_u\ (kips)}$
54.99	1.39	106.20	4.52	28.37	0.64
62.46	1.31	100.43	5.06	31.72	0.72
68.93	1.24	95.04	5.65	35.42	0.80
73.89	1.18	90.96	6.16	38.67	0.88
79.17	1.15	88.39	6.53	40.94	0.93
82.55	1.12	86.17	6.87	43.09	0.98
84.78	1.09	84.15	7.20	45.18	1.03
86.86	1.08	82.83	7.43	46.63	1.06
88.61	1.06	81.89	7.61	47.71	1.08
89.67	1.06	81.38	7.70	48.30	1.10
90.02	1.06	81.80	7.62	47.81	1.09
90.37	1.05	80.64	7.84	49.20	1.12
90.55	1.04	80.40	7.89	49.50	1.12
90.73	1.04	80.23	7.92	49.70	1.13
90.73	1.04	80.15	7.94	49.80	1.13

L	Iy	A	ry	Pu
98.42	10.44	6.27	1.29	44 Kips

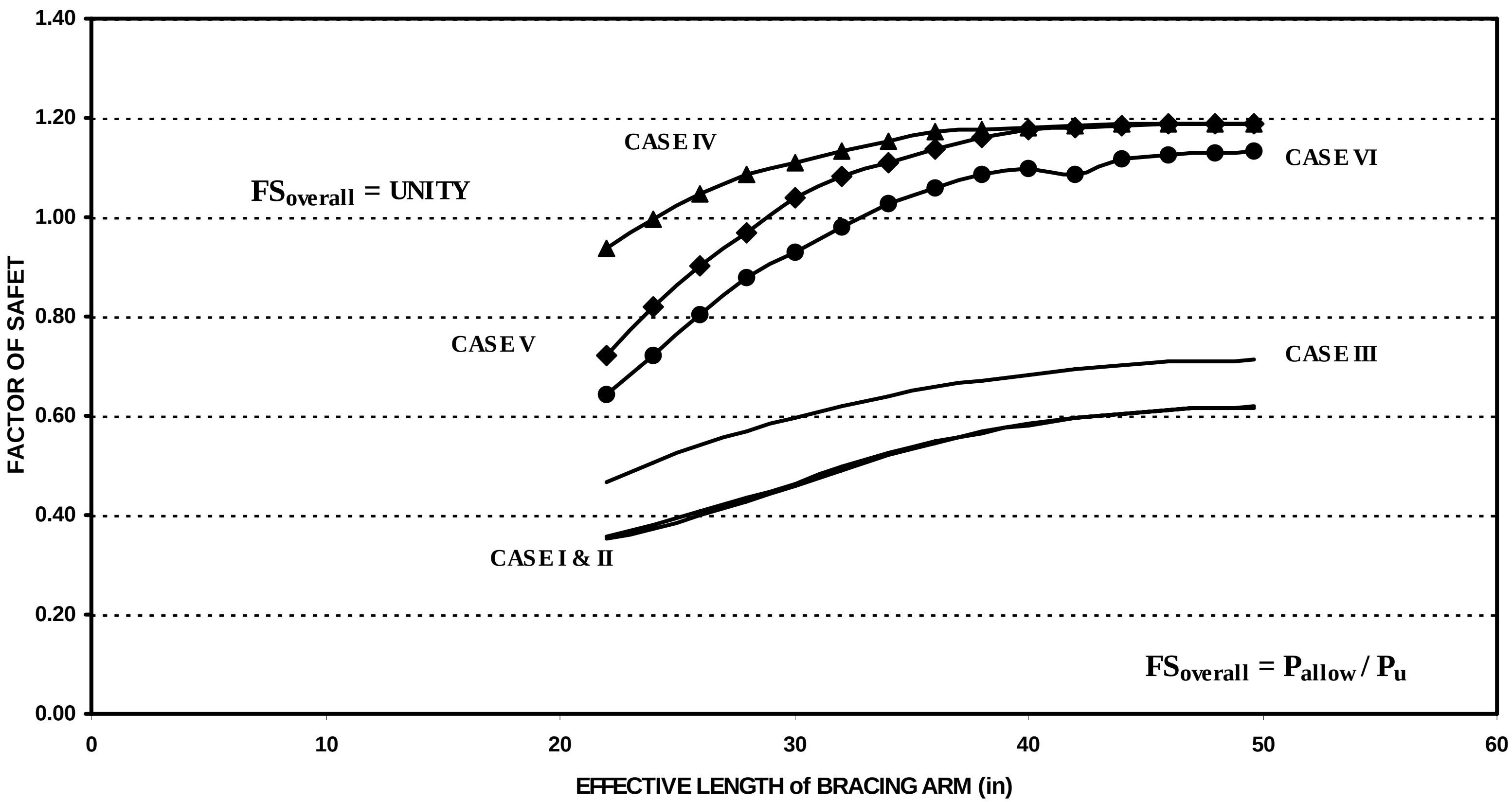

Figure 33: Vertical Post Composite Member – Effect of Bracing Arm on Factor of Safety

APPENDIX D

PEDESTRIAN & BICYCLE RAILING

COMBINED BIAXIAL BENDING AND AXIAL COMPRESSION

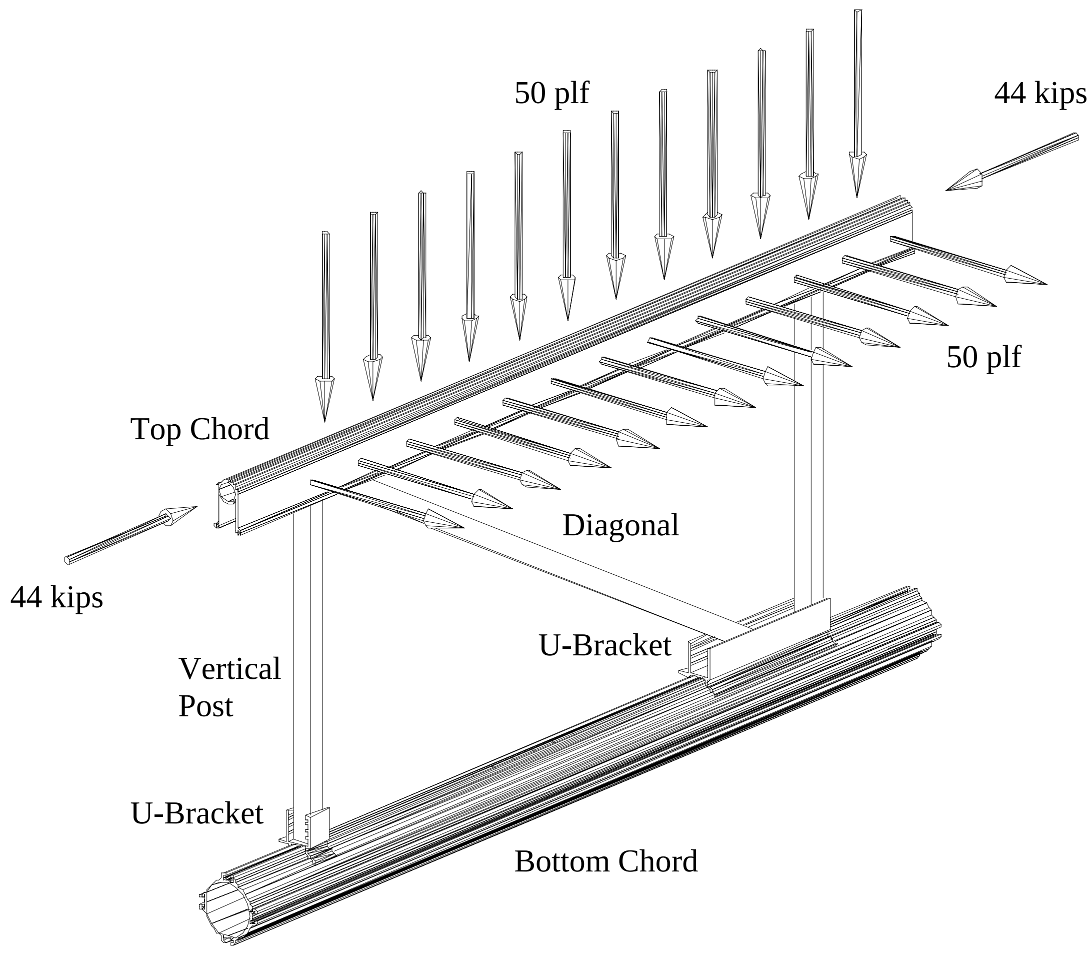

Figure 34: Typical Truss Panel – Pedestrian Railing
Biaxial Bending and Axial Compression

Analysis for Combined Stresses on Pedestrian/Bicycle Railing (Top Chord)

A. Average Compressive Stress on Top Chord

1. $f_a = P_u / A = 44 \text{ kips} / 6.273 \text{ in}^2 = 7.01 \text{ ksi}$

B. ADM Section 4.1.1 Combined axial compression and biaxial bending

1. When fa/Fa is less than or equal to 0.15, a member subjected to axial compression and bending moment loads shall be proportioned in accordance with two individual interaction equations that incorporate these two loading conditions into one correlation.
2. In consideration of the highest allowable compressive stresses from Cases IV, V, and VI based on flexural-torsional buckling:

    i. $F_{15} = 0.15 \times F_a = 0.15 (8.34 \text{ ksi}) = 1.25 \text{ ksi}$

    Note: The imposed axial compressive stress (fa = 7.01 ksi) won't ever be for any of these cases less than or equal to 15% of the allowable compressive stress (Fa). Therefore, both interactions equations must be evaluated as stated in the Aluminum Specifications.

3. Analysis for Biaxial Bending

    i. Maximum Bending Moment:

    $M_{max} = (w \times L^2) / 8 = [50 \text{ plf } (8.202 \text{ ft})^2]/8 = 421 \text{ Lbs x ft}$

    @ midpoint between Vertical Posts.

ii. Maximum Bending Stresses (compression about strong axis):

$f_{bx} = (M_{max} \text{ x } c)/I_{xx}$

f_{bx} = [(421Lbs x ft)(12 in/ft)(2.00 in)]/11.97 in^4 = 846 psi

iii. Maximum Bending Stresses (compression about weak axis):

$f_{by} = (M_{max} \text{ x } c)/I_{yy}$

f_{by} = [(421 Lbs x ft)(12 in/ft)(1.70 in)]/10.44 in^4 = 822 psi

iv. C_m Values:

Cm_x = 0.60 for member whose ends are prevented from sway.

Cm_y = 0.85 for members whose ends are not prevented from sway.

v. Allowable Compressive Stress for Beams based on Lateral Buckling about strong axis (X-X Axis); Section 3.4.14 Compression on extreme fibers (gross section) for members with tubular portions:

- Overall Slenderness:
  - → Torsional Constant, J = 0.881 in^4
  - → Section Modulus, Sc = I_{xx}/c = 11.97 in^4/2.00 in

    = 5.985 in^3

    Note: The value for Torsional Constant as well as Section Modulus was obtained by considering the equivalent channel profile for the top chord, which represents the profile lower bound.
  - → {(Lb x S_c)/0.50 x $[(I_{yy})(J)]^{0.50}$} = {(98.42 in)(5.985 in^3)/(0.50) x [(10.44 in^4)(0.881 in^4)]} = 388

- Allowable Bending Stress (Compression – Inelastic Buckling)

  For $S1 = 146 < (L_b \times S_c)/0.50 \times [(I_{yy})(J)]^{0.50} = 388 < S2 = 1700$

  → $F_b = 23.9 - 0.24 \times \{(L_b \times S_c)/0.50 \times [(I_{yy})(J)]^{0.50}\}^{0.50}$

  → $F_b = 23.9 - 0.24\ (388)^{0.50} = 19.20$ ksi

vi. Allowable Compressive Stress for Beams based on Local Buckling about strong axis (X-X Axis):

- Section 3.4.18, Compression in components of beam under bending in its own plane (gross section), flat plates supported along both edges:

  → Plate Slenderness,

  $b/t = [1.535 - (0.942\ in/2)] / 0.315\ in$

  $= 3.37 < S1 = 46$

  → Allowable Bending Stress (Compression - Full Yielding)

  For $b/t < S1$, $F_b = 28$ ksi

- Section 3.4.16, Compression in components of beams under uniform compression (gross section), flat plates supported along both edges.

  → Plate Slenderness,

  $b/t = 3.406\ in / 0.942\ in = 3.62 < S1 = 22$

  → Allowable Bending Stress (Compression - Full Yielding)

  For $b/t < S1$, $Fb = 21$ ksi

vii. Allowable Compressive Stress for Beams based on Local Buckling about weak axis (Y-Y Axis):

Note: Since lateral buckling is not a failure mode when considering bending about the weak axis, then local buckling represents the only limit state to be evaluated.

- Section 3.4.15, Compression in Components under uniform compression (gross section), flat plates supported along one edge:

  → Plate Slenderness,

  b/t = 4.863 in/0.315 = 15.43 > S2 = 10

  → Allowable Bending Stress (Compression - Elastic Buckling)

  For b/t < S2, F_b = 182/(b/t) = 182/(15.43) = 11.79 ksi

- Section 3.4.16.1, Compression in components of beams under bending in its own plane (gross section), flat plates supported along both edges:

  → Plate Slenderness,

  b/t 3.406 in/0.942 in = 3.62 < S1 = 46

  → Allowable Bending Stress (Compression - Full Yielding)

  For b/t < S1, F_b = 28 ksi

4. Example Evaluation for First Interaction Equation

i. Elastic Buckling Stress, Fe

- $F_{ex} = [(3.14156)^2 \text{ x } E]/[n_u(k \text{ x } L)/r_{xx}]^2$

  $= [(3.14156)^2(10100 \text{ ksi})]/\{[2.2(1.34)(98.42 \text{ in})/1.38 \text{ in}]^2\} = 4.93$ ksi

- $F_{ey} = [(3.14156)^2 \text{ x } E]/[n_u(k \text{ x } L)/r_{yy}]^2$

  $= [(3.14156)^2(10100 \text{ ksi})]/\{[2.2(1.34)(98.42 \text{ in})/1.29 \text{ in}]^2\} = 4.31 \text{ ksi}$

ii. First Interaction Equation

- Axial Component, $f_a/F_a = 7.01 \text{ ksi}/ 4.80 \text{ ksi} = 1.46 > 1.00$ (Not Ok)

- Bending Component about Strong Axis,

  → $f_{bx} = 0.85$ ksi $F_{bx} = 19.20$ ksi

  → $(C_m \text{ x } f_{bx})/\{F_{bx}[1-(f_a/F_{ex})]\}$

  $= [(0.60)(0.85 \text{ ksi})]/\{19.20 \text{ ksi}[1-(7.01 \text{ ksi}/4.93 \text{ ksi})]\} = -0.06$

- Bending Component about Weak Axis,

  → $f_{by} = 0.82$ ksi $F_{bx} = 11.79$ ksi

  → $(C_m \text{ x } f_{by})/\{F_{by}[1-(f_a/F_{ey})]\}$

  $= [(0.85)(0.82 \text{ ksi})]/\{11.79 \text{ ksi}[1-(7.01 \text{ ksi}/4.31 \text{ ksi})]\} = -0.09$

Note: It can be concluded from the previous evaluation that the average compressive stress on the railing has the greatest influence concerning the response of the bridge railing to combined-stresses. In this particular case each individual component represent an inadequate state of stress in this member due to the high level of compressive forces induced by the design loads.

Table 20: Elastic Buckling Stress – Case I

CASE I					
Bracing Arm Effective Length	k	(kL/rx)^2	Fex	(kL/ry)^2	Fey
22	1.88	17971.54	2.52	20566.67	2.20
24	1.82	16937.43	2.68	19383.23	2.34
26	1.76	15710.28	2.88	17978.89	2.52
28	1.70	14711.40	3.08	16835.76	2.69
30	1.64	13714.31	3.30	15694.69	2.89
32	1.59	12815.26	3.54	14665.81	3.09
34	1.54	12075.89	3.75	13819.68	3.28
36	1.51	11571.28	3.92	13242.20	3.42
38	1.48	11097.65	4.08	12700.18	3.57
40	1.46	10839.95	4.18	12405.27	3.65
42	1.44	10591.12	4.28	12120.51	3.74
44	1.43	10439.93	4.34	11947.48	3.79
46	1.42	10321.30	4.39	11811.72	3.84
48	1.42	10233.64	4.43	11711.41	3.87
49.61	1.42	10204.67	4.44	11678.25	3.88

rx	1.38	ry	1.29	E	10100
pi	3.14159	nu	2.2	L	98.42

Table 21: Elastic Buckling Stress – Case II

CASE II					
Bracing Arm Effective Length	k	(kL/rx)^2	Fex	(kL/ry)^2	Fey
22	1.87	17704.31	2.56	20260.85	2.24
24	1.81	16632.53	2.72	19034.31	2.38
26	1.75	15491.71	2.92	17728.75	2.56
28	1.69	14513.27	3.12	16609.02	2.73
30	1.63	13580.19	3.34	15541.20	2.92
32	1.58	12694.08	3.57	14527.13	3.12
34	1.54	12001.81	3.78	13734.89	3.30
36	1.50	11501.79	3.94	13162.67	3.44
38	1.48	11130.51	4.07	12737.78	3.56
40	1.46	10808.37	4.19	12369.13	3.66
42	1.44	10560.62	4.29	12085.60	3.75
44	1.43	10410.08	4.35	11913.32	3.80
46	1.42	10291.96	4.40	11778.14	3.85
48	1.42	10204.67	4.44	11678.25	3.88
49.61	1.41	10175.83	4.45	11645.24	3.89

rx	1.38	ry	1.29	E	10100
pi	3.14159	nu	2.2	L	98.42

Table 22: Elastic Buckling Stress – Case III

CASE III					
Bracing Arm Effective Length	k	(kL/rx)^2	Fex	(kL/ry)^2	Fey
22	1.63	13535.91	3.35	15490.53	2.93
24	1.56	12456.81	3.64	14255.60	3.18
26	1.52	11676.71	3.88	13362.86	3.39
28	1.47	11064.94	4.09	12662.75	3.58
30	1.44	10560.62	4.29	12085.60	3.75
32	1.41	10147.10	4.47	11612.37	3.90
34	1.39	9839.00	4.61	11259.77	4.02
36	1.37	9570.92	4.73	10952.98	4.14
38	1.36	9364.26	4.84	10716.48	4.23
40	1.34	9188.88	4.93	10515.78	4.31
42	1.33	9042.45	5.01	10348.20	4.38
44	1.33	8946.76	5.06	10238.70	4.43
46	1.32	8875.99	5.10	10157.70	4.46
48	1.32	8829.27	5.13	10104.24	4.48
49.61	1.32	8806.05	5.15	10077.67	4.50

rx	1.38	ry	1.29	E	10100
pi	3.14159	nu	2.2	L	98.42

Table 23: Elastic Buckling Stress – Case IV

CASE IV					
Bracing Arm Effective Length	k	(kL/rx)^2	Fex	(kL/ry)^2	Fey
22	1.14	6658.64	6.80	7620.17	5.95
24	1.11	6265.55	7.23	7170.31	6.32
26	1.08	5944.63	7.62	6803.05	6.66
28	1.06	5732.01	7.90	6559.72	6.91
30	1.05	5612.22	8.07	6422.64	7.05
32	1.04	5484.74	8.26	6276.75	7.22
34	1.03	5394.73	8.40	6173.75	7.34
36	1.02	5306.93	8.54	6073.26	7.46
38	1.02	5274.55	8.59	6036.21	7.51
40	1.02	5263.83	8.61	6023.93	7.52
42	1.02	5242.47	8.64	5999.50	7.55
44	1.01	5231.84	8.66	5987.33	7.57
46	1.01	5221.25	8.68	5975.21	7.58
48	1.01	5221.25	8.68	5975.21	7.58
49.61	1.01	5221.25	8.68	5975.21	7.58

rx	1.38	ry	1.29	E	10100
pi	3.14159	nu	2.2	L	98.42

Table 24: Elastic Buckling Stress – Case V

CASE V					
Bracing Arm Effective Length	k	(kL/rx)^2	Fex	(kL/ry)^2	Fey
22	1.31	8714.09	5.20	9972.42	4.54
24	1.23	7657.61	5.92	8763.39	5.17
26	1.17	6925.43	6.54	7925.48	5.72
28	1.13	6450.34	7.02	7381.78	6.14
30	1.09	6009.42	7.54	6877.20	6.59
32	1.06	5756.42	7.87	6587.67	6.88
34	1.05	5600.45	8.09	6409.17	7.07
36	1.04	5462.03	8.30	6250.76	7.25
38	1.03	5350.56	8.47	6123.19	7.40
40	1.02	5285.31	8.57	6048.52	7.49
42	1.02	5263.83	8.61	6023.93	7.52
44	1.02	5242.47	8.64	5999.50	7.55
46	1.01	5231.84	8.66	5987.33	7.57
48	1.01	5221.25	8.68	5975.21	7.58
49.61	1.01	5221.25	8.68	5975.21	7.58

rx	1.38	ry	1.29	E	10100
pi	3.14159	nu	2.2	L	98.42

Table 25: Elastic Buckling Stress – Case VI

CASE VI					
Bracing Arm Effective Length	k	(kL/rx)^2	Fex	(kL/ry)^2	Fey
22	1.39	9757.40	4.64	11166.39	4.06
24	1.31	8714.09	5.20	9972.42	4.54
26	1.24	7790.87	5.82	8915.89	5.08
28	1.18	7123.53	6.36	8152.18	5.56
30	1.15	6720.01	6.74	7690.40	5.89
32	1.12	6378.31	7.10	7299.35	6.21
34	1.09	6075.28	7.46	6952.57	6.52
36	1.08	5880.88	7.70	6730.10	6.73
38	1.06	5744.20	7.89	6573.67	6.89
40	1.06	5671.64	7.99	6490.64	6.98
42	1.06	5732.01	7.90	6559.72	6.91
44	1.05	5565.35	8.14	6369.00	7.11
46	1.04	5530.59	8.19	6329.22	7.16
48	1.04	5507.59	8.23	6302.90	7.19
49.61	1.04	5496.15	8.24	6289.80	7.20

rx	1.38	ry	1.29	E	10100
pi	3.14159	nu	2.2	L	98.42

Table 26: Interaction Equation for Combined Stresses – Pedestrian Railing (Case 1)

Case I							
Bracing Arm Effective Length	F_a	f_a / F_a	F_{ex}	$\frac{C_{mx} \bullet f_{bx}}{F_{bx}(1-f_a/F_{ex})}$	F_{ey}	$\frac{C_{my} \bullet f_{by}}{F_{by}(1-f_a/F_{ey})}$	Interaction Equation
22	2.47	2.84	2.52	-0.01	2.20	-0.03	2.80
24	2.62	2.68	2.68	-0.02	2.34	-0.03	2.64
26	2.82	2.49	2.88	-0.02	2.52	-0.03	2.44
28	3.01	2.33	3.08	-0.02	2.69	-0.04	2.27
30	3.23	2.17	3.30	-0.02	2.89	-0.04	2.11
32	3.45	2.03	3.54	-0.03	3.09	-0.05	1.96
34	3.66	1.92	3.75	-0.03	3.28	-0.05	1.83
36	3.82	1.84	3.92	-0.03	3.42	-0.06	1.75
38	3.98	1.76	4.08	-0.04	3.57	-0.06	1.66
40	4.07	1.72	4.18	-0.04	3.65	-0.06	1.62
42	4.17	1.68	4.28	-0.04	3.74	-0.07	1.57
44	4.23	1.66	4.34	-0.04	3.79	-0.07	1.55
46	4.28	1.64	4.39	-0.04	3.84	-0.07	1.52
48	4.31	1.63	4.43	-0.05	3.87	-0.07	1.51
49.61	4.33	1.62	4.44	-0.05	3.88	-0.07	1.50

fa	7.01
Cmx	0.60
fbx	0.85
Fbx	19.20
Cmy	0.85
fby	0.82
Fby	11.79

Table 27: Interaction Equation for Combined Stresses – Pedestrian Railing (Case 2)

Case II							
Bracing Arm Effective Length	F_a	f_a / F_a	F_{ex}	$\frac{C_{mx} \cdot f_{bx}}{F_{bx}(1-f_a/F_{ex})}$	F_{ey}	$\frac{C_{my} \cdot f_{by}}{F_{by}(1-f_a/F_{ey})}$	Interaction Equation
22	2.50	2.80	2.56	-0.02	2.24	-0.03	2.76
24	2.66	2.63	2.72	-0.02	2.38	-0.03	2.59
26	2.86	2.45	2.92	-0.02	2.56	-0.03	2.40
28	3.05	2.30	3.12	-0.02	2.73	-0.04	2.24
30	3.26	2.15	3.34	-0.02	2.92	-0.04	2.09
32	3.48	2.01	3.57	-0.03	3.12	-0.05	1.94
34	3.68	1.90	3.78	-0.03	3.30	-0.05	1.82
36	3.84	1.83	3.94	-0.03	3.44	-0.06	1.73
38	3.97	1.77	4.07	-0.04	3.56	-0.06	1.67
40	4.09	1.72	4.19	-0.04	3.66	-0.06	1.61
42	4.18	1.68	4.29	-0.04	3.75	-0.07	1.57
44	4.24	1.65	4.35	-0.04	3.80	-0.07	1.54
46	4.29	1.64	4.40	-0.04	3.85	-0.07	1.52
48	4.33	1.62	4.44	-0.05	3.88	-0.07	1.50
49.61	4.34	1.62	4.45	-0.05	3.89	-0.07	1.50

fa	7.01
Cmx	0.60
fbx	0.85
Fbx	19.20
Cmy	0.85
fby	0.82
Fby	11.79

Table 28: Interaction Equation for Combined Stresses – Pedestrian Railing (Case 3)

Case III							
Bracing Arm Effective Length	F_a	f_a / F_a	F_{ex}	$\frac{C_{mx} \cdot f_{bx}}{F_{bx}(1-f_a/F_{ex})}$	F_{ey}	$\frac{C_{my} \cdot f_{by}}{F_{by}(1-f_a/F_{ey})}$	Interaction Equation
22	3.27	2.15	3.35	-0.02	2.93	-0.04	2.08
24	3.55	1.98	3.64	-0.03	3.18	-0.05	1.90
26	3.79	1.85	3.88	-0.03	3.39	-0.06	1.76
28	3.99	1.76	4.09	-0.04	3.58	-0.06	1.66
30	4.18	1.68	4.29	-0.04	3.75	-0.07	1.57
32	4.35	1.61	4.47	-0.05	3.90	-0.07	1.49
34	4.48	1.56	4.61	-0.05	4.02	-0.08	1.43
36	4.61	1.52	4.73	-0.06	4.14	-0.08	1.38
38	4.71	1.49	4.84	-0.06	4.23	-0.09	1.34
40	4.80	1.46	4.93	-0.06	4.31	-0.09	1.30
42	4.87	1.44	5.01	-0.07	4.38	-0.10	1.27
44	4.93	1.42	5.06	-0.07	4.43	-0.10	1.25
46	4.97	1.41	5.10	-0.07	4.46	-0.10	1.24
48	4.99	1.41	5.13	-0.07	4.48	-0.10	1.23
49.61	5.00	1.40	5.15	-0.07	4.50	-0.11	1.22

fa	7.01
Cmx	0.60
fbx	0.85
Fbx	19.20
Cmy	0.85
fby	0.82
Fby	11.79

Table 29: Interaction Equation for Combined Stresses – Pedestrian Railing (Case 4)

Case IV							
Bracing Arm Effective Length	F_a	f_a / F_a	F_{ex}	$\frac{C_{mx} \cdot f_{bx}}{F_{bx}(1-f_a/F_{ex})}$	F_{ey}	$\frac{C_{my} \cdot f_{by}}{F_{by}(1-f_a/F_{ey})}$	Interaction Equation
22	6.59	1.07	6.80	-0.86	5.95	-0.33	-0.13
24	6.99	1.00	7.23	0.88	6.32	-0.54	1.35
26	7.36	0.95	7.62	0.33	6.66	-1.11	0.17
28	7.62	0.92	7.90	0.24	6.91	-3.82	-2.67
30	7.78	0.90	8.07	0.20	7.05	10.27	11.38
32	7.95	0.88	8.26	0.18	7.22	2.09	3.14
34	8.08	0.87	8.40	0.16	7.34	1.33	2.36
36	8.21	0.85	8.54	0.15	7.46	0.99	1.99
38	8.26	0.85	8.59	0.14	7.51	0.90	1.90
40	8.28	0.85	8.61	0.14	7.52	0.88	1.87
42	8.31	0.84	8.64	0.14	7.55	0.83	1.81
44	8.33	0.84	8.66	0.14	7.57	0.81	1.79
46	8.34	0.84	8.68	0.14	7.58	0.79	1.77
48	8.34	0.84	8.68	0.14	7.58	0.79	1.77
49.61	8.34	0.84	8.68	0.14	7.58	0.79	1.77

fa	7.01
Cmx	0.60
fbx	0.85
Fbx	19.20
Cmy	0.85
fby	0.82
Fby	11.79

Table 30: Interaction Equation for Combined Stresses – Pedestrian Railing (Case 5)

Case V							
Bracing Arm Effective Length	F_a	f_a / F_a	F_{ex}	$\frac{C_{mx} \cdot f_{bx}}{F_{bx}(1-f_a/F_{ex})}$	F_{ey}	$\frac{C_{my} \cdot f_{by}}{F_{by}(1-f_a/F_{ey})}$	Interaction Equation
22	5.06	1.39	5.20	-0.08	4.54	-0.11	1.20
24	5.74	1.22	5.92	-0.14	5.17	-0.17	0.91
26	6.34	1.11	6.54	-0.37	5.72	-0.26	0.48
28	6.79	1.03	7.02	18.10	6.14	-0.41	18.72
30	7.28	0.96	7.54	0.38	6.59	-0.91	0.43
32	7.59	0.92	7.87	0.24	6.88	-2.99	-1.82
34	7.80	0.90	8.09	0.20	7.07	7.54	8.64
36	7.99	0.88	8.30	0.17	7.25	1.83	2.88
38	8.15	0.86	8.47	0.15	7.40	1.13	2.15
40	8.24	0.85	8.57	0.15	7.49	0.93	1.93
42	8.28	0.85	8.61	0.14	7.52	0.88	1.87
44	8.31	0.84	8.64	0.14	7.55	0.83	1.81
46	8.33	0.84	8.66	0.14	7.57	0.81	1.79
48	8.34	0.84	8.68	0.14	7.58	0.79	1.77
49.61	8.34	0.84	8.68	0.14	7.58	0.79	1.77

fa	7.01
Cmx	0.60
fbx	0.85
Fbx	19.20
Cmy	0.85
fby	0.82
Fby	11.79

Table 31: Interaction Equation for Combined Stresses – Pedestrian Railing (Case 6)

Case VI							
Bracing Arm Effective Length	F_a	f_a / F_a	F_{ex}	$\frac{C_{mx} \bullet f_{bx}}{F_{bx}(1-f_a/F_{ex})}$	F_{ey}	$\frac{C_{my} \bullet f_{by}}{F_{by}(1-f_a/F_{ey})}$	Interaction Equation
22	4.52	1.55	4.64	-0.05	4.06	-0.04	1.46
24	5.06	1.39	5.20	-0.08	4.54	-0.05	1.26
26	5.65	1.24	5.82	-0.13	5.08	-0.07	1.04
28	6.16	1.14	6.36	-0.26	5.56	-0.10	0.78
30	6.53	1.07	6.74	-0.66	5.89	-0.14	0.28
32	6.87	1.02	7.10	2.11	6.21	-0.20	2.92
34	7.20	0.97	7.46	0.45	6.52	-0.35	1.07
36	7.43	0.94	7.70	0.30	6.73	-0.63	0.61
38	7.61	0.92	7.89	0.24	6.89	-1.51	-0.35
40	7.70	0.91	7.99	0.22	6.98	-5.57	-4.44
42	7.62	0.92	7.90	0.24	6.91	-1.72	-0.56
44	7.84	0.89	8.14	0.19	7.11	1.89	2.98
46	7.89	0.89	8.19	0.18	7.16	1.31	2.39
48	7.92	0.89	8.23	0.18	7.19	1.09	2.16
49.61	7.94	0.88	8.24	0.18	7.20	1.01	2.07

fa	7.01
Cmx	0.60
fbx	0.85
Fbx	19.20
Cmy	0.85
fby	0.82
Fby	11.79

APPENDIX E

ALOWABLE TENSILE CAPACITY OF BOTTOM CHORD

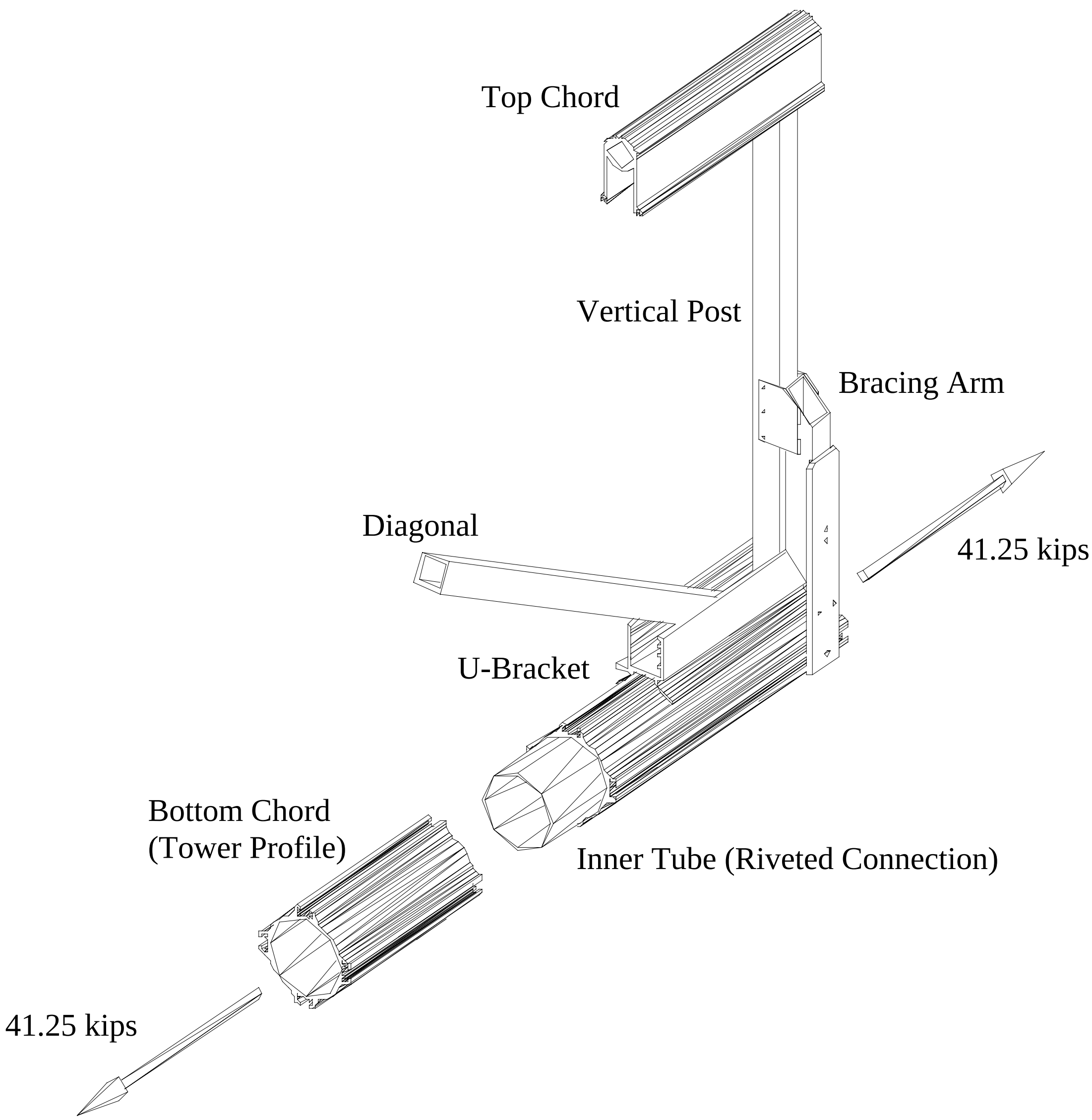

Figure 35: Allowable Tensile Capacity of
Bottom Chord @ Splice Connection

Allowable Tensile Capacity of Bottom Chord

A. Allowable Tensile Stress, F_t (6061-T6 Aluminum Alloy Extrusions)

1. F_t = min [F_{tu}/n_u or F_{ty}/n_y]

   = min [(38 ksi/2.2 or 35 ksi/1.85]

   = min [17.27 ksi or 18.92 ksi]

   F_t = 17.27 ksi

   Note: Ultimate Strength governs The Tensile Capacity for this alloy.

   Since the ratio of the factor of safety on the yield and ultimate allowable tensile stresses is (1.85/2.20) = 0.84, the allowable tensile stress for alloys with a yield strength greater than 84% of the ultimate strength are governed by tensile ultimate strength.

2. Allowable Tensile Capacity @ Splice Connection

   i. Tower Profile (Bottom Chord)

   - A_{eff} = A_{total} - (d_r x t)

     = A_{total} - n(d_r + 0.04d_r) x t

     = 9.038 in^2 - 8[0.256 in + (0.04)(0.256 in)](0.236 in)

     = 8.535 in^2

   - T_a = F_t x A_{net} = 17.27 ksi (8.535 in^2) = 147.5 kips

   ii. Inner Tube (Splice)

   - A_{eff} = A_{total} - (d_r x t) = A_{total} - n(d_r + 0.04d_r) x t

     = 7.845 in^2 - 8[0.256 in + (0.04)(0.256 in)](0.0.354 in) = 7.091 in^2

- $T_a = F_t \times A_{net} = 17.27$ ksi $(7.091\ in^2) = 122.5$ kips

3. Bearing Capacity @ Splice Connection - Tower Profile

    i. Section 3.4.5, Bearing on Rivets and Bolts:

    - Ratio = edge distance/fastener diameter

        = 1.260 in/0.256 in = 4.92 > 2.00

        Note: No reduction is necessary to be applied to the allowable bearing stress.

    ii. Allowable Bearing Stress, F_{br}

    - $F_{br} = 2F_{tu}/n_u = 2(35ksi)/2.2 = 31.82$ ksi

    iii. Allowable Bearing Capacity of Tower Profile

    - P_b = 4 rows x n x F_{br} x A_{net}

        = 4(8)(31.82 ksi)(0.256in +0.010 in)(0.236 in)

        = 64 Kips

4. Bearing Capacity @ Splice Connection – Inner Tube

    i. Section 3.4.5, Bearing on Rivets and Bolts:

    - Ratio = edge distance/fastener diameter

        = 0.886 in/0.256 in = 3.383 > 2.00

        Note: No reduction is necessary to be applied to the allowable bearing stress.

    ii. Allowable Bearing Stress, F_{br}

    - $F_{br} = 2F_{tu}/n_u = 2(35ksi)/2.2 = 31.82$ ksi

iii. Allowable Bearing Capacity of Tower Profile

- $P_b = 4 \text{ rows x n x } F_{br} \text{ x } A_{net}$

  $= 4(8)(31.82 \text{ ksi})(0.256\text{in} + 0.010 \text{ in})(0.354 \text{ in})$

  $= 95.9$ Kips

5. Tensile Fracture Capacity @ Net Section

i. Tower Profile

- $A_{net} = A_{total} - A_{holes}$

  $= A_{total} - n(d_h + 0.04d_r) \text{ x t}$

  $= 9.038 \text{ in}^2 - 8[0.400 \text{ in} + (0.04)(0.400 \text{ in})](0.236 \text{ in})$

  $= 8.253 \text{ in}^2$

- $P_f = 17.27 \text{ ksi } (8.253 \text{ in}^2) = 142$ kips

ii. Inner Tube

- $A_{net} = A_{total} – A_{holes}$

  $= A_{total} - n(d_h + 0.04d_r) \text{ x t}$

  $= 7.845 \text{ in}^2 - 8[0.400 \text{ in} + (0.04)(0.400 \text{ in})](0.354 \text{ in})$

  $= 6.667 \text{ in}^2$

- $P_f = 17.27 \text{ ksi } (6.667 \text{ in}^2) = 115.1$ kips

6. Shear Capacity of Rivets (6061-T6 Aluminum Alloy Rivets)

i. $P_{shear} = 4 \text{ rows x 8 rivets/row x } (F_{shear}/n_u) \text{ x } A_r$

$= 4(8)(25 \text{ ksi})[(3.14156/4)(0.256 \text{ in})^2]$

$= 15.6 \text{ kips} < T_u = 31.2$ kips (<u>Not Adequate</u>)

ii. Solution A – Increase the number of rivets per row

- N_{req} = T_u/[8 rivets/row x (F_v/n_u) x A_r

  = 32 kips/[(8)(25 ksi)(3.14156/4)(0.256 in)^2)]

  = 8.2 rivets/row (Use 9 rivets/row minimum)

iii. Solution B – Increase the river diameter

- d_{req} =[T_u/4 rows x (F_v/n_u) x (3.14156/4)]$^{0.50}$

  = [32 kips/(4)(25 ksi)(3.14156/4)]$^{0.50}$

  = 0.370 inches (Use 3/8" Diam. Rivets)

APPENDIX F

ALOWABLE TENSILE CAPACITY OF DIAGONAL MEMBERS

A. Allowable Tensile Stress, Ft (6061-T6 Aluminum Alloy Extrusions)

1. Ft = min [F_{tu}/n_u or F_{ty}/n_y]

   = min [(38 ksi/2.2 or 35 ksi/1.85]

   = min [17.27 ksi or 18.92 ksi]

   Ft = 17.27 ksi

   Note: Tensile Capacity for this alloy is governed by Ultimate Strength since the ratio of the factor of safety on the yield and ultimate allowable tensile stresses is (1.85/2.20) = 0.84, the allowable tensile stress for alloys with a yield strength greater than 84% of the ultimate strength are governed by tensile ultimate strength.

2. Allowable Bearing Strength @ End Connection for Bolt Group A & B

   (Bolt Group A = 4 Bolts and Bolt Group B = 2 Bolts)

i. Section 3.4.5 Bearing on Rivets and Bolts:

- Ratio = edge distance/fattener diameter

  = 0.945 in/0.480 = 1.969 < 2.00

  Note: A reduction to the allowable bearing stress is required. For ratios smaller than 2.00, the allowable bearing stress shall be multiplied by the following correlation (Reduction Factor):

- Correlation (Reduction Factor):

  → edge distance/2 x bolt diameter = 0.945 in/2(0.480 in)

  = 0.984

  Note: This reduction to the allowable bearing stress shall be applicable for both Bolt Groups A & B.

ii. Allowable Bearing Stress, F_{br}

- $F = [(2 \times F_{tu})/n_u] \times$ Reduction Factor

  = [2(35 ksi)/2.2](0.984)

  = 31.31 ksi

iii. Allowable Bearing Capacity @ End Connection

- Bolt Group A:

  → $P_{br} = F_{br} \times n \times (d_b + 1/16") \times t$

  = 31.31 ksi (8)(0.480 in + 0.0625 in)(0.315 in)

  = 42.8 kips

- Bolt Group B:

→ $P_{br} = F_{br}$ x n x (d_b + 1/16") x t

= 31.31 ksi (4)(0.480 in + 0.0625 in)(0.315 in)

= 21.4 kips

Note: "n" represents the number of bearing surfaces @ the end connection of the diagonal member.

iv. Tensile Fracture @ Net Section

- Net Effective Area - Failure Path "AC" for Bolt Group A

→ $A_{net} = A_{total}$ - n(d_b + 1/16") x t

= 3.028 in^2 - 4(0.480 in + 0.0625 in)(0.315 in)

= 2.344 in^2

- Net Effective Area - Failure Path "ABC" for Bolt Group A

→ $A_{net} = A_{total}$ - n(d_b + 1/16") x t + 4[(s^2)/4g]

= 3.028 in^2 - 6(0.480 in + 0.0625 in)(0.315 in)

+ 4[(0.787 in)^2]/4(0.709 in)

= 2.995 in^2

Note: Bolt Group A - Failure Path "AC" controls.

- Net Effective Area - Failure Path "B" for Bolt Group B

→ $A_{net} = A_{total}$ - n(d_b + 1/16") x t

= 3.028 in^2 - 2(0.480 in + 0.0625 in)(0.315 in)

= 2.686 in^2

v. Allowable Tensile Force (Fracture @ Net Section)

- Bolt Group A

  → $T = A_{net} \times F_t = 2.344 \text{ in}^2 (17.27 \text{ ksi}) = 40.5 \text{ kips}$

- Bolt Group B

  → $T = A_{net} \times F_t = 2.686 \text{ in}^2 (17.27 \text{ ksi}) = 46.4 \text{ kips}$

vi. Block Shear Strength

- Effective Areas for Bolt Group A:

  → $A_{nt} = 4\{[(0.709 \text{ in})^2 + (0.787 \text{ in})^2]^{0.50}\} \times (0.315 \text{ in})$

  $= 1.335 \text{ in}^2$

  → $A_{nv} = 1.654 \text{ in}(0.315 \text{ in})(4) = 2.083 \text{ in}^2$

- Effective Areas for Bolt Group B:

  → $A_{nv} = (1.654 \text{ in} + 0.709 \text{ in})(0.315 \text{ in})(4) = 2.977 \text{ in}^2$

vii. Tensile and Shear Capacities

- Bolt Group A:

  → $F_{tu} \times A_{nt} = 38 \text{ ksi } (1.335 \text{ in}^2) = 50.70 \text{ kips}$

  → $F_{su} \times A_{nv} = 24 \text{ ksi } (2.083 \text{ in}^2) = 49.9 \text{ kips}$

  Note: $F_{tu} \times A_{nt} > F_{su} \times A_{nv}$

  → $P_{sr} = [F_{sy} \times A_{gv} + F_{tu} \times A_{nt}]/n_u$

  $= [(20 \text{ ksi})(2.083 \text{ in}^2) + (38 \text{ ksi})(1.335 \text{ in})]/2.2 = 42 \text{ kips}$

- Bolt Group B:

  → $F_{su} \times A_{nv} = 24 \text{ ksi } (2.997 \text{ in}^2) = 71.90 \text{ kips}$

→ $P_{sr} = (F_{su} \text{ x } A_{nv})/n_u = 71.90 \text{ kips}/2.20 = 32.70\text{kips}$

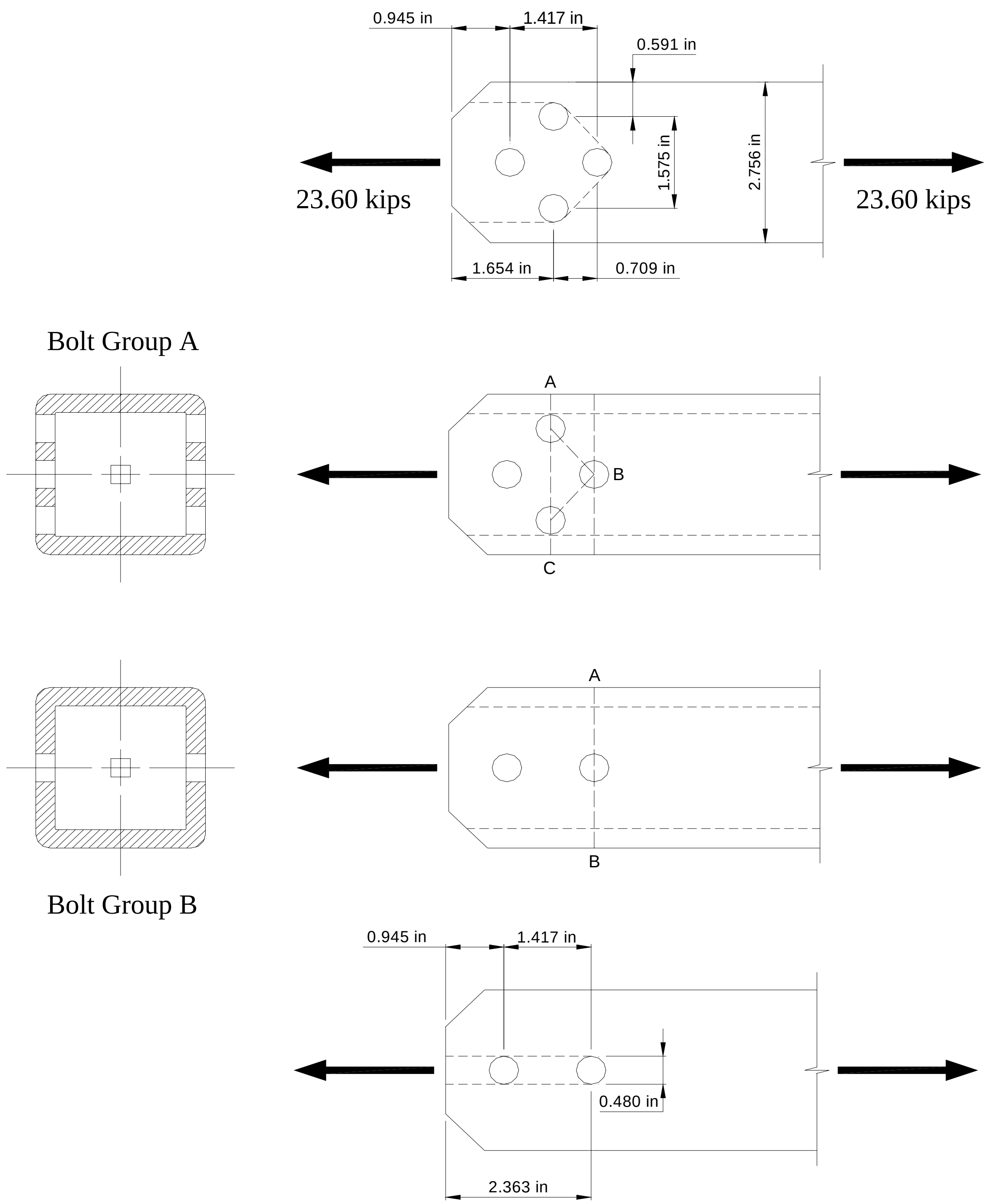

Figure 36: Typical Bolt Groups on Diagonal Members

APPENDIX G

ALOWABLE FLEXURAL CAPACITY OF FLOOR BEAMS

A. Allowable Tensile Stress, Ft (6061-T6 Aluminum Alloy Extrusions)

1. F_t = min [F_{tu}/n_u or F_{ty}/n_y]

   = min [(38 ksi/2.2 or 35 ksi/1.85]

   = min [17.27 ksi or 18.92 ksi]

   F_t = 17.27 ksi

   Note: The ratio of the factor of safety on the yield and ultimate allowable tensile stresses is (1.85/2.20) = 0.84, therefore the allowable tensile stress with yield strength greater than 84% of the ultimate strength is governed by tensile ultimate strength.

2. Bending Compression (Hollow Cross Section)

   i. Lateral Torsional Buckling

   - Torsional Constant, J

     $J = [4 \text{ x } A_o^2]/[\text{Sum } (S_i/t_i)]$

     $= \{4[(2.756 \text{ in} - 0.315 \text{ in})^2]^2\}/[4(2.756 \text{ in}/0.315 \text{ in})] = 4.06 \text{ in}^4$

- Section Modulus for Compression Side, S_c

  $S_c = I_{xx}/c = 23\ in^4/(1.673\ in + 1.378\ in) = 7.54\ in^3$

- Critical Slenderness

  $[L_b \times S_c] / 0.50[I_{yy} \times J]^{0.50} = (98.42\ in)(7.54\ in^3) \div$

  $\{0.50[(6.04\ in^4)(4.06\ in^4)]^{0.50}\} = 300$

- Allowable Bending Stress, F_b

  → Section 3.4.14 Compression in beams extreme fibers (gross section):

  For $S_1 = 146 < [L_b \times S_c]/0.50[I_{yy} \times J]^{0.50} = 300 < S_2 = 1700$

  $F_b = 23.9 - 0.24 \times \{[L_b \times S_c]/0.50[I_{yy} \times J]^{0.50}\}^{0.50}$

  $= 23.9 - 0.24\ (300)^{0.50} = 19.70$ ksi

ii. Local Buckling Stress

- Plate Slenderness, b/t

  $b/t = 2.756\ in / 0.315\ in = 8.75$

- Allowable Bending Stress, F_b

  → Section 3.4.16 Beam components under uniform compression (gross section), flat plates supported along both edges:

  For $b/t = 8.75 < S_1 = 22$ $\quad F_b = 21$ ksi

→ Section 3.4.18 Components of beams under bending in its own plane (gross section) flat plates supported along both edges:

For $b/t = 8.75 < S_1 = 46$ $F_b = 28$ ksi

iii. Conclusion:

For lateral torsional buckling the allowable bending stress in compression controls ($F_b = 19.70$ ksi)

3. Internal Bending Stress caused by External Design Forces, f_b (Hollow Cross Section)

   i. Load Case 1 - H5-44 Vehicle Load, $W_v = 10$ kips

   - Reaction Force = 0.40(10 kips) = 4 kips
   - Maximum Bending Moment, M_{max}

     → $M_{max} = (P \times L)/4 + (w \times L^2)/8$

     $= 4 \text{ kips } (8.202 \text{ ft})/4 + [0.07 \text{ klf } (8.202 \text{ ft})^2]/8$

     $= 5.03 \text{ kips} \times \text{ft}$

   - Maximum Internal Bending Stress, f_b

     → $f_b = (M_{max} \times c)/I_{xx}$

     $= (5.03 \text{ kips} \times \text{ft})(12 \text{ in/ft})(1.673 \text{ in} + 1.378 \text{ in})/23 \text{ in}^4$

     $= 8.00$ ksi

   ii. Load Case 2 - Pedestrian Live Load

   - w = 85 psf x (8.222 ft) = 699plf Say 700 plf

- Maximum Bending Moment, M_{max}

  → $M_{max} = (w \times L^2)/8 = [(700 + 62)plf\ (8.202\ ft)^2]/8$

  $= (6407\ Lbs \times ft)(1\ kip/\ 1000\ lbs) = 6.41\ kips \times ft$

- Maximum Internal Bending Stress, f_b

  → $f_b = (M_{max} \times c)/I_{xx}$

  $= (6.41\ kips \times ft)(12\ in/ft)(1.673\ in + 1.378\ in)/23\ in^4$

  $= 10.20\ ksi$

iii. Conclusion: The bending stresses from either load combination is lower as compared to the allowable bending stress for lateral torsional buckling.

4. Deflection Analysis (Double Hollow Cross Section)

   i. Deflection for Uniformly Distributed Dead Load, w

   - $D = (5)(5.167E\text{-}3\ kips/in)[(98.42\ in)^4]\ /\ (384)(10100\ ksi)(23\ in^4)$

     $= 0.027\ in$

   ii. Deflection for H5-44 Truck Live Load, P

   - $D = (4\ kips)(24\ in)[3(98.42\ in)^2 - 4(24\ in)^2] \div$

     $[(24)(10100\ ksi)(23in^4)] = 0.461\ in$

   iii. Deflection for Pedestrian Live Load, w_p

   - $D = (5)(5.833E\text{-}2\ kips/in)[(98.42\ in)^4]/(384)(10100\ ksi)(23\ in^4)$

     $= 0.307\ in$

iv. Total Deflection

- Load Case 1 = H5-44 Truck Live Load + Dead Load

  D = 0.461 in + 0.027 in

  = 0.488 in >> L/500 = 98.42 in/500 = 0.197 in (<u>Not Adequate</u>)

- Load Case 2 = Pedestrian Live Load + Dead Load

  D = 0.307 in + 0.027 in

  = 0.334 in >> L/500 = 98.42 in/500 = 0.197 in (<u>Not Adequate</u>)

5. Deflection Analysis (Double Solid Cross Section)

i. New Moment of Inertia, I_{xx}

- I_{xx} = 2 x [(1/12)(2.756 in)^4] + (2.756 in)^2(1.673 in)^2]

  = 52.1 in^4

ii. Deflection for Uniformly Distributed Dead Load, w

- D = (5)(5.167E-3 kips/in)[(98.42 in)^4]/(384)(10100 ksi)(52.1 in^4)

  = 0.012 in

iii. Deflection for H5-44 Truck Live Load, P

- D = (4 kips)(24 in)[3(98.42 in)^2 - 4(24 in)^2] ÷

  [(24)(10100 ksi)(52.1in^4)] = 0.203 in

iv. Pedestrian Live Load, w_p

- D = (5)(5.833E-2 kips/in)[(98.42 in)^4]/(384)(10100 ksi)(52.1 in^4)

  = 0.135 in

v. Total Deflection

- Load Case 1 = H5-44 Truck Live Load + Dead Load

  D = 0.203 in + 0.012 in

  = 0.215 in > L/500 = 98.42 in/500 = 0.197 in (Not Adequate)

- Load Case 2 = Pedestrian Live Load + Dead Load

  D = 0.135 in + 0.012 in

  = 0.147 in < L/500 = 98.42 in/500 = 0.197 in (Adequate)

6. Conclusion: For double-solid floor beams the allowable deflection remains in permissible levels (Load Case 2 – Pedestrian Live Load). Internal stresses induced by either load case results in a higher moment of inertia about the weak axis (Iyy) and so lower internal stresses. The overall slenderness for lateral torsional buckling will become lower and the allowable bending stress for compression will result even higher.

7. Bending Compression based on Equivalent Rectangular Cross Section

   i. Lateral Torsional Buckling

   - Section 3.4.13 Compression in beam extreme fibers (gross section):

     → Equivalent Thickness, te

     $I_{eq} = (1/12) \text{ x } t_e \text{ x } d^3 = 52.1 \text{ in}^4$

     $t_e = [(52.1 \text{ in}^4)(12)/(6.102 \text{ in}^3)] = 2.753 \text{ in}$

   - Critical Slenderness

     $(d/t)[(L_d/d)]^{0.50} = (6.10 \text{ in})(2.753 \text{ in})[(98.42 \text{ in})/6.10 \text{ in})]^{0.50} = 8.8$

For $(d/t)[(L_d/d)]^{0.50} = 8.89 < S_1 = 13.0$ $F_c = 28$ ksi

- Applied Bending Stress, f_b

$fb = (M_{max} \times c)/I_{xx}$

$= (5.03 \text{ kips} \times \text{ft})(12 \text{ in/ft})(1.673 \text{ in} + 1.378 \text{ in})/52.1 \text{ in}^4$

$= 3.53$ ksi

ii. Local Buckling is not applicable for solid extrusions.

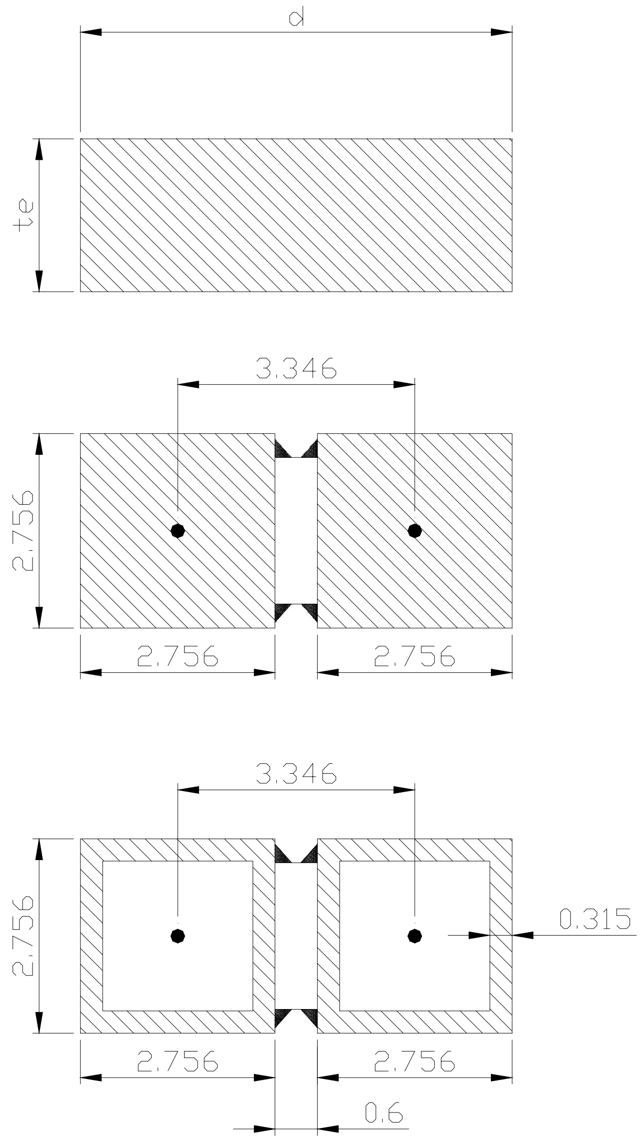

Figure 37: Typical & Equivalent Cross Section for Floor Beam

APPENDIX H

ALOWABLE COMPRESSIVE CAPACITY OF VERTICAL POST

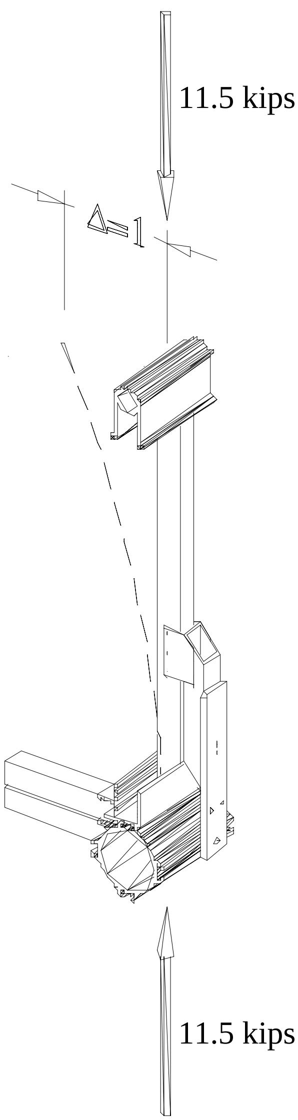

Figure 38: Vertical Post Layout

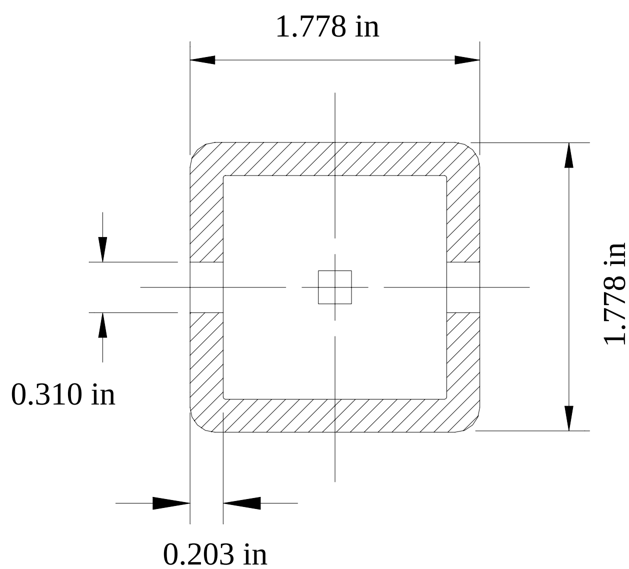

Figure 39: Vertical Post Cross-Section

Allowable Compressive Capacity of Vertical Post

A. Slenderness Ratio:

i. Overall Flexural Buckling

- $(k \times L)/r = 1.0(55.12 \text{ in}).0.999 \text{ in} = 55.2$

ii. Local Buckling

- $b/t = 2.756 \text{ in}/0.315 \text{ in} = 8.75$

B. Allowable Compressive Stress

i. Overall Flexural Buckling

- Section 3.4.7, Compression in all column (gross section)

  For $S_1 = 0 < (k \times L)/r = 55.2 < S_2 = 66$

  $F_c = 20.2 - 0.126[(k \times L)/r] = 20.2 - 0.126(55.2) = 13.2$ ksi

ii. Local Buckling

- Section 3.4.9, Compression in components of columns (gross section)

  For $S_1 = 8.4 < b/t = 8.75 < S_2$ 33

  $F_c = 23.1 - 0.25(b/t) = 23.1 - 0.25(8.75) = 20.9$ ksi

C. Effect of Local Buckling on member performance

i. This design restriction is not applicable to this member given that the slenderness ratio for the plate element does not exceeds the Slenderness Limit S_2. Therefore, there won't be any elastic local buckling in this member.

D. Conclusion: Overall Flexural Buckling is the failure mode that controls the design of this member, $F_c = 13.2$ ksi

E. Allowable Compressive Force, P_c

i. $P_c = 13.2 \text{ ksi } (3.028 \text{ in}^2) = 39.9$ kips

ii. $P_u = 11.5$ kips FS = 39.9 kips/11.5 kips = 3.47

APPENDIX I

ALOWABLE CAPACITY OF TYPICAL CONNECTIONS

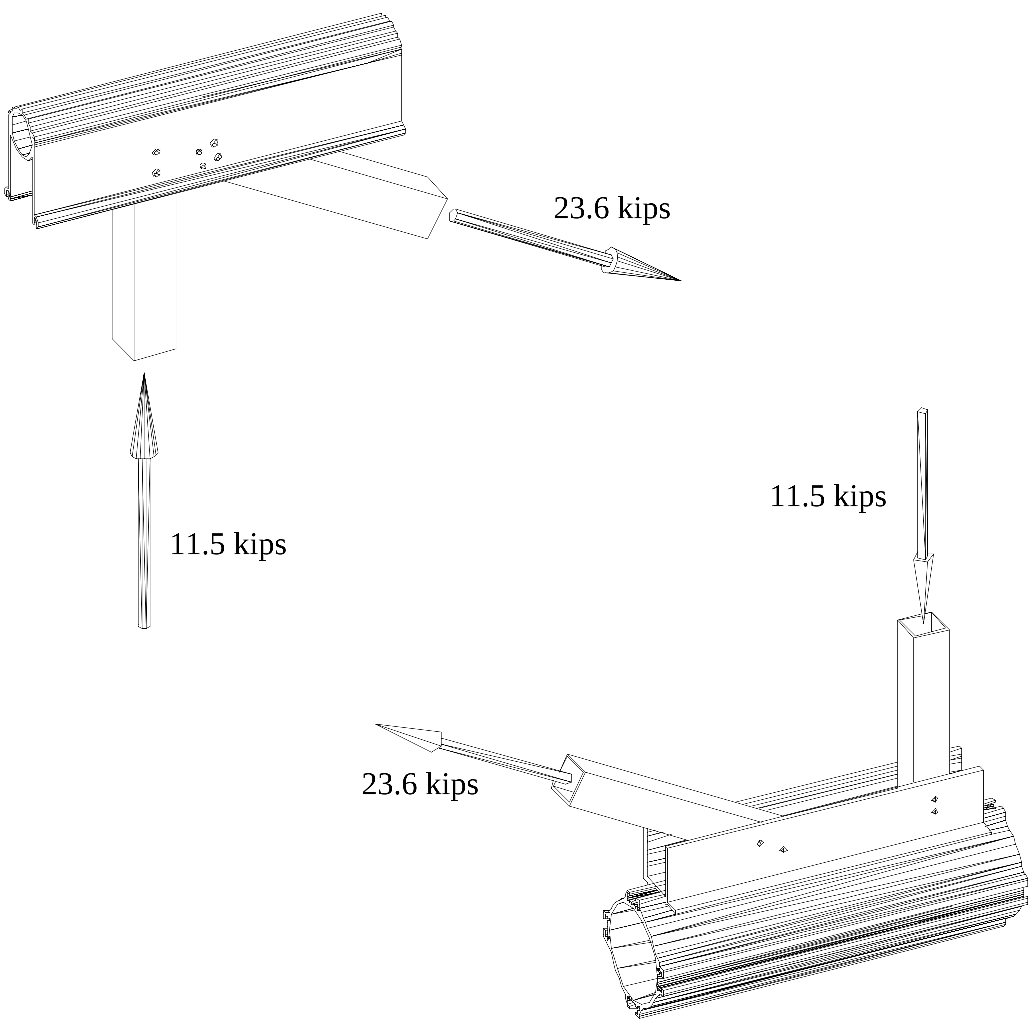

Figure 40: Diagrams for Typical Connections

Typical Bolted Connections

A. Bolted Connection between Top Chord and Diagonal Members

i. Bearing Capacity of Bolt Group A (4 Bolts)

- Allowable Bearing Stress Reduction Factor

→ Ratio = edge distance/fastener diameter

$= 3.117 \text{ in} / 0.480 \text{ in} = 6.49 < 2.00$

Note: Reduction factor does not apply.

- Allowable Bearing Stress for 6061-T6 Aluminum Alloy, F_{br}

→ $F_{br} = 2 \times F_{tu} / n_u = 2 \text{ (35 ksi)} / 2.20 = 31.82 \text{ ksi}$

- Allowable Bearing Force, P_{br}

→ $P_{br} = F_{br} \times A_{br}$

$= (4)(31.82 \text{ ksi})(0.480 \text{ in})(0.315 \text{ in}) = 38.5 \text{ kips}$

ii. Bearing Capacity of Bolt Group B (2 Bolts)

- Allowable Bearing Stress Reduction Factor

→ Ratio = edge distance/fastener diameter

$= 3.117 \text{ in} / 0.480 \text{ in} = 6.49 < 2.00$

Note: Reduction factor does not applies

- Allowable Bearing Stress for 6061-T6 Aluminum Alloy, F_{br}

→ $F_{br} = 2 \times F_{tu} / n_u = 2 \text{ (35 ksi)} / 2.20 = 31.82 \text{ ksi}$

- Allowable Bearing Force, P_{br}

  → $P_{br} = F_{br} \times A_{br}$

  $= (2)(31.82 \text{ ksi})(0.480 \text{ in})(0.315 \text{ in}) = 19.24 \text{ kips}$

iii. Block Shear of Bolt Group A (4 Bolts)

- $P_{sr} = 41.99$ kips

  Note: The load carrying capacity of the Top Chord against this failure mode is equivalent to the one on the Diagonal Members given that the bolt layout is identical as well as the wall thickness of the free standing flat plates on the Top Chord.

iv. Block Shear of Bolt Group B (2 Bolts)

- $P_{sr} = 19.24$ kips

  Note: The load carrying capacity of the Top Chord against this failure mode is similar to the one on the Diagonal Members since the bolt layout is identical as well as the wall thickness of the free standing flat plates on the Top Chord.

B. Bolted Connection between Diagonal Members and U-Bracket A

i. Bearing Capacity of Bolt Group A (4 Bolts)

- Allowable Bearing Stress Reduction Factor

  → Ratio = edge distance/fastener diameter

  $= 2.900 \text{ in} / 0.480 \text{ in} = 6.04 < 2.00$

  Note: Reduction factor does not apply.

- Allowable Bearing Stress for 6061-T6 Aluminum Alloy, F_{br}

  → $F_{br} = 2 \times F_{tu} / n_u = 2$ (35 ksi) / 2.20 = 31.82 ksi

- Allowable Bearing Force, P_{br}

  → $P_{br} = F_{br} \times A_{br}$

  = (4)(2)(31.82 ksi)(0.480 in)(0.354 in) = 43.25 kips

ii. Bearing Capacity of Bolt Group B (2 Bolts)

- Allowable Bearing Stress Reduction Factor

  Ratio = edge distance/fastener diameter

  = 2.900 in / 0.480 in = 6.04 < 2.00

  Note: Reduction factor does not apply.

- Allowable Bearing Force, Pbr

  → $P_{br} = F_{br} \times A_{br}$

  = (2)(2)(31.82 ksi)(0.480 in)(0.354 in) = 21.70 kips

C. Bolted Connection between U-Bracket A and Bottom Chord

i. Bearing Capacity of Bolt Group C on U-Bracket (6 Bolts)

- Allowable Bearing Stress Reduction Factor

  → Ratio = edge distance/fastener diameter

  = 0.984 in / 0.480 in = 2.05 < 2.00

  Note: Reduction factor does not apply.

- Allowable Bearing Force, Pbr

  → $P_{br} = F_{br} \times A_{br}$

  = (6)(31.82 ksi)(0.480 in)(0.289 in) = 26.50 kips

ii. Bearing Capacity of Bolt Group C on Bottom Chord (6 Bolts)

- $P_{br} = F_{br} \times A_{br}$

  $= (6)(31.82 \text{ ksi})(0.480 \text{ in})(0.236 \text{ in}) = 21.60 \text{ kips}$

D. Bolted Connection between U-Bracket B and Bottom Chord

i. Bearing Capacity of Bolt Group C on U-Bracket (4 Bolts)

- Allowable Bearing Stress Reduction Factor

  → Ratio = edge distance/fastener diameter

  $= 0.984 \text{ in} / 0.480 \text{ in} = 2.05 < 2.00$

  Note: Reduction factor does not apply.

- Allowable Bearing Force, P_{br}

ii. Bearing Capacity of Bolt Group C on Bottom Chord (4 Bolts)

- $P_{br} = F_{br} \times A_{br}$

  $= (4)(31.82 \text{ ksi})(0.480 \text{ in})(0.236 \text{ in}) = 14.40 \text{ kips}$

  Note: The load carrying capacity of the bolted connections in between the U-Brackets (A & B) and the Bottom Chord has to be compared with the horizontal component of the corresponding maximum tensile forces applied to the Diagonal Members.

APPENDIX J

ALOWABLE CAPACITY OF ABUTMENT CONNECTIONS

Load Carrying Capacity of Bridge Main Supports

A. AASHTO Design Requirements for Single Span Bridges (Earthquakes)

Section 4.5 is a design provision obtained from AASHTO Standard Specifications for Highway Bridges, Seismic Design. It states that a detailed seismic analysis is not required for single span bridges. However, connections between the bridge span and the abutments shall be designed longitudinally and transversally to resists a force with a magnitude equivalent to the gravity reaction (dead load) at the abutment support times the Acceleration Coefficient at the site.

Section 3.2 provides contour maps from the United States and its territories where these Acceleration Coefficients can be determined. These contour values are expressed as percentages and the corresponding multiplier can be obtained by dividing these coefficients by 100. These values of horizontal ground acceleration are determined in rock with a 90% probability of not being exceeded in 50 years as stated by the United States Geological Survey, 1988.

B. Abutment Support I (Longitudinal Direction)

i. Bearing Capacity of Standing Plates

- Allowable Bearing Stress Reduction Factor

→ Ratio = edge distance/fastener diameter

= 2.953 in / 0.728 in = 4.06 < 2.00

Note: Reduction factor does not apply.

ii. Allowable Bearing Stress for 6061-T6 Aluminum Alloy, Fbr

- $F_{br} = 2 \times F_{tu} / n_u = 2\,(35\text{ ksi}) / 2.20 = 31.82\text{ ksi}$

iii. Allowable Bearing Force, P_{br}

- $P_{br} = F_{br} \times A_{br}$

$= 31.82\text{ ksi}\,(0.625\text{ in})(0.787\text{ in})(2) = 23.6\text{ kips}$

iv. Weld Shear Capacity

- Shear Strength of Filler Alloy

→ For 4043 Aluminum Alloy, Fv = 4.4 ksi

→ For 5356 Aluminum Alloy, Fv = 7.0 ksi

Note: These allowable shear values are for bridge type structures.

v. Weld Shear Capacity

- Shear Strength of Base Metal

→ For Tension Failure, $F_v = 1.41\,(24\text{ ksi})(0.90)/2.34(1.0) = 13\text{ ksi}$

→ For Shear Failure, Fv = 1.41 (15 ksi)/2.34 = 9 ksi

Conclusion: Allowable shear stress is controlled by the shear capacity of the filler alloy selected to make the welds.

Note: In the case of this particular support some of the fillet welds are loaded longitudinally and others are loaded transversely. In order to avoid any confusion the Aluminum Specifications conservatively use the longitudinal shear strength of the controlling material. This is due to the fact that similar to steel, aluminum fillet welds are rather strong when loaded transversely than longitudinally.

vi. Allowable Shear Force on Weld Group, P_w

- F_w = [(0.787 in)(4) + (5.906 in)(4) + (0.591 in)(4) + (3.937 in)(4)](4.4 ksi)
- $P_w = F_w$ x w x (0.707)

  = 197.5 Kips/in (0.250 in)(0.707) = 34.9 kips

vii. Abutment Support I (Longitudinal Direction)

- In this particular orientation only shear forces will be transmitted through the bridge support into the abutments. Therefore, only the fillet welds capacity needs to be evaluated.

viii. Allowable Shear Force on Weld Group, P_w

- F_w = [(0.787 in)(4) + (5.906 in)(4) + (0.591 in)(2) + (3.937 in)(2)](4.4 ksi)
- $P_w = F_w$ x w x (0.707)

  = 157.6 Kips/in (0.250 in)(0.707) = 27.8 kips

ix. Bearing Capacity of Base Plate (either direction)

- Allowable Bearing Stress Reduction Factor

  → Ratio = 1.575 in / 0.630 in = 2.50 > 2.00

  Note: No reduction is required.

- Allowable Bearing Force, P_{br}

  → P_{br} = (4)(31.82 ksi)(0.625in)(0.394 in) = 31.34 kips

C. Abutment Support II (Longitudinal Direction)

   i. In this particular orientation the bridge support is designed with a slotted hole on both gusset plates to accommodate any longitudinal displacement. In addition, there are no stop-bars along this direction and consequently the bridge is able to slide back and forth upon any disturbance, either thermally or physically. In case of an overload of the support along this direction, the bearing capacity (P_{br} = 23.6 kips) is equivalent to that as provided by Abutment Support I.

D. Abutment Support II (Transverse Direction)

   i. In this particular orientation only shear forces will be transmitted through the bridge support into the abutments. Therefore, only the fillet welds capacity needs to be evaluated.

   ii. Allowable Shear Force on Weld Group, Pw

   - F_w = [(0.787 in)(4) + (5.906 in)(4) + (0.591 in)(2) + (3.937 in)(2)](4.4 ksi)
   - P_w = 157.6 Kips/in (0.250 in)(0.707) = 27.8 kips

   iii. Bearing Capacity of Base Plate (either direction)

   - Allowable Bearing Stress Reduction Factor

     Ratio = 1.575 in / 0.630 in = 2.50 > 2.00

     <u>Note</u>: No reduction is required.

   iv. Allowable Bearing Force, P_{br} = (4)(31.82 ksi)(0.625in)(0.394 in) = 31.34 kip

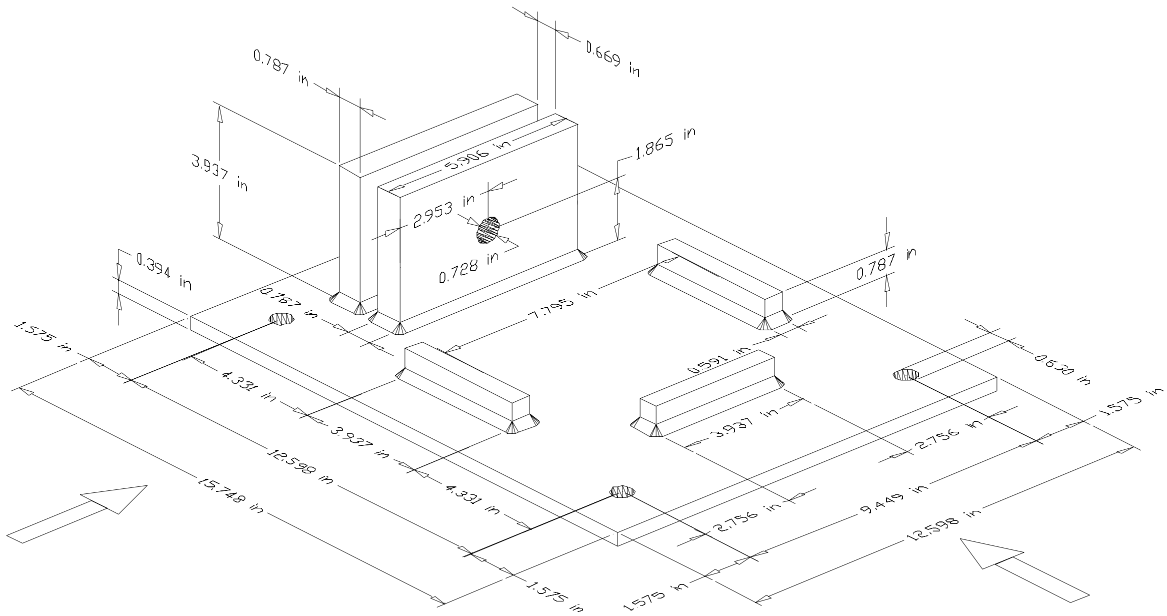

(a)

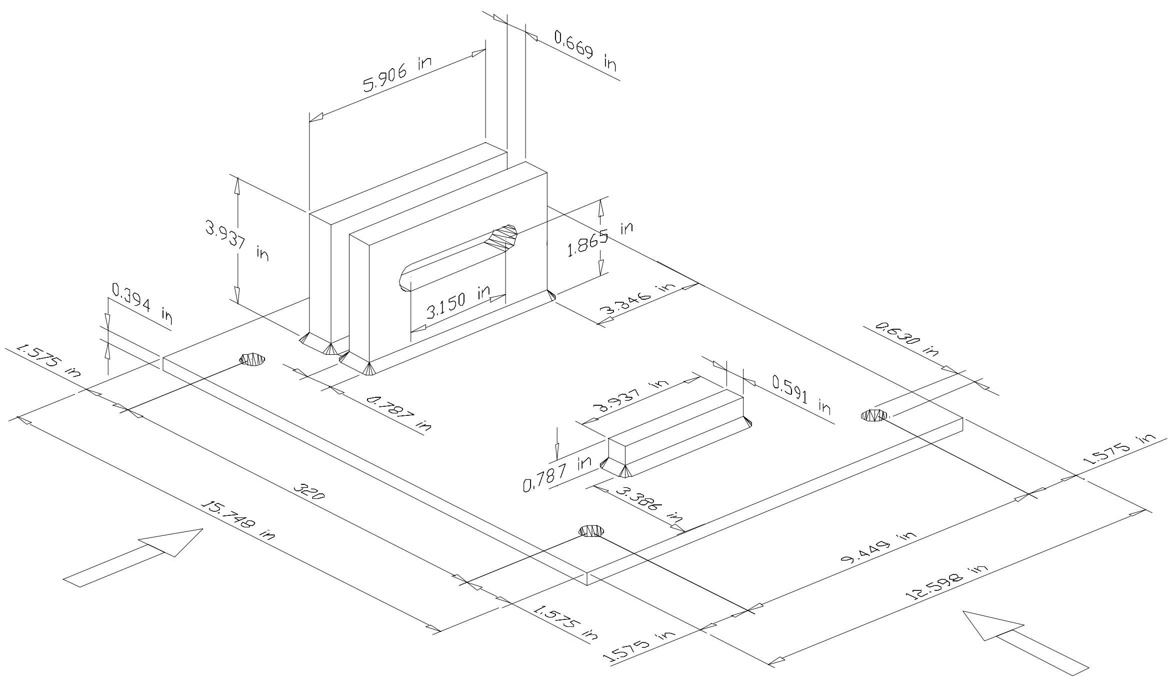

(b)

Figure 41: Bridge Supports: (a) Abutment Support I (b) Abutment Support II

APPENDIX K

EFFECTIVE MOMENT OF INERTIA OF COMPOSITE SECTION

VS. EFFECTIVE LENGTH OF BRACING ARM

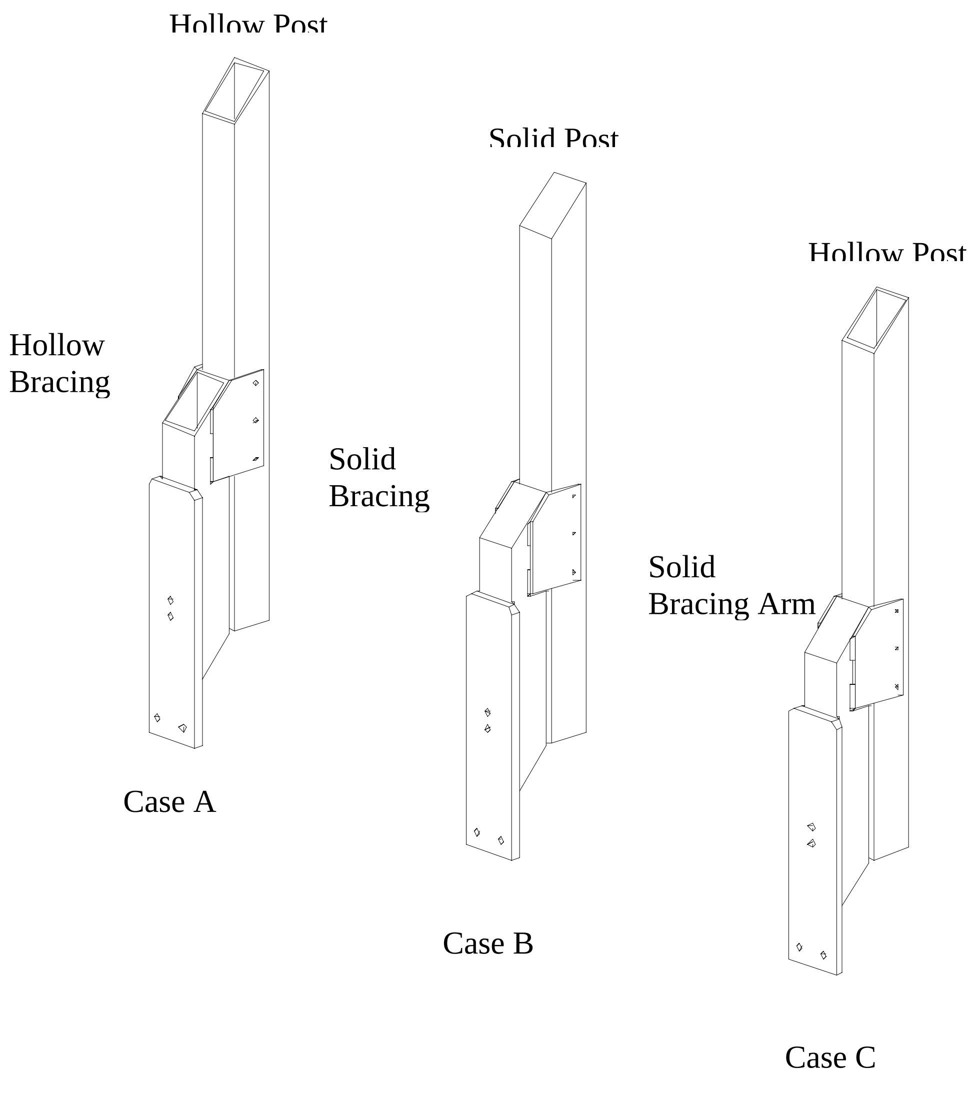

Figure 42: Composite Section

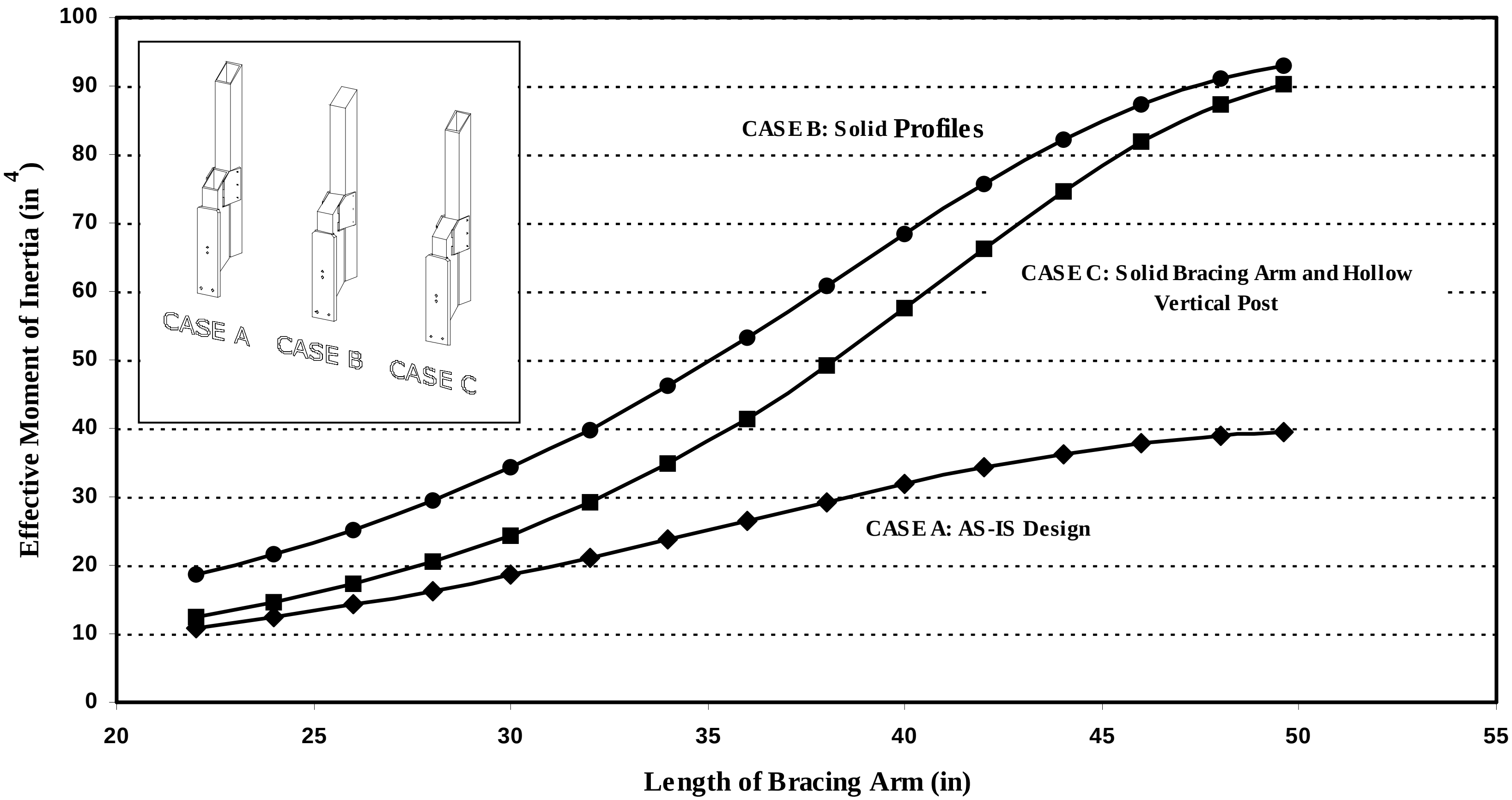

Figure 43: Vertical Post Composite Member – Effect
of Bracing Arm on Effective Moment of Inertia

APPENDIX L

ELASTIC TRANSVERSE FRAME STIFFNESS VS.

EFFECTIVE LENGTH OF BRACING ARM

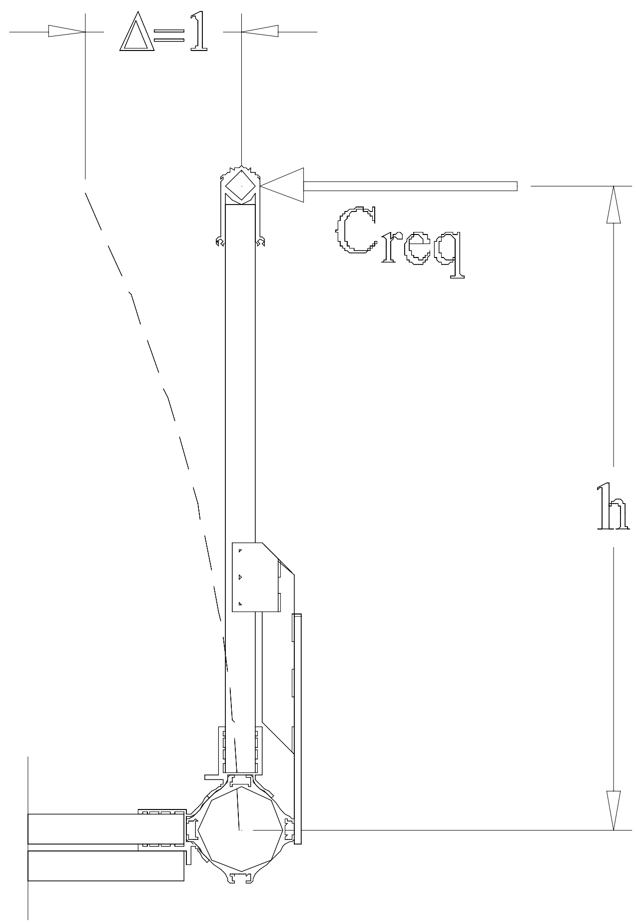

Figure 44: Elastic Transverse Frame Stiffness – Sectional View

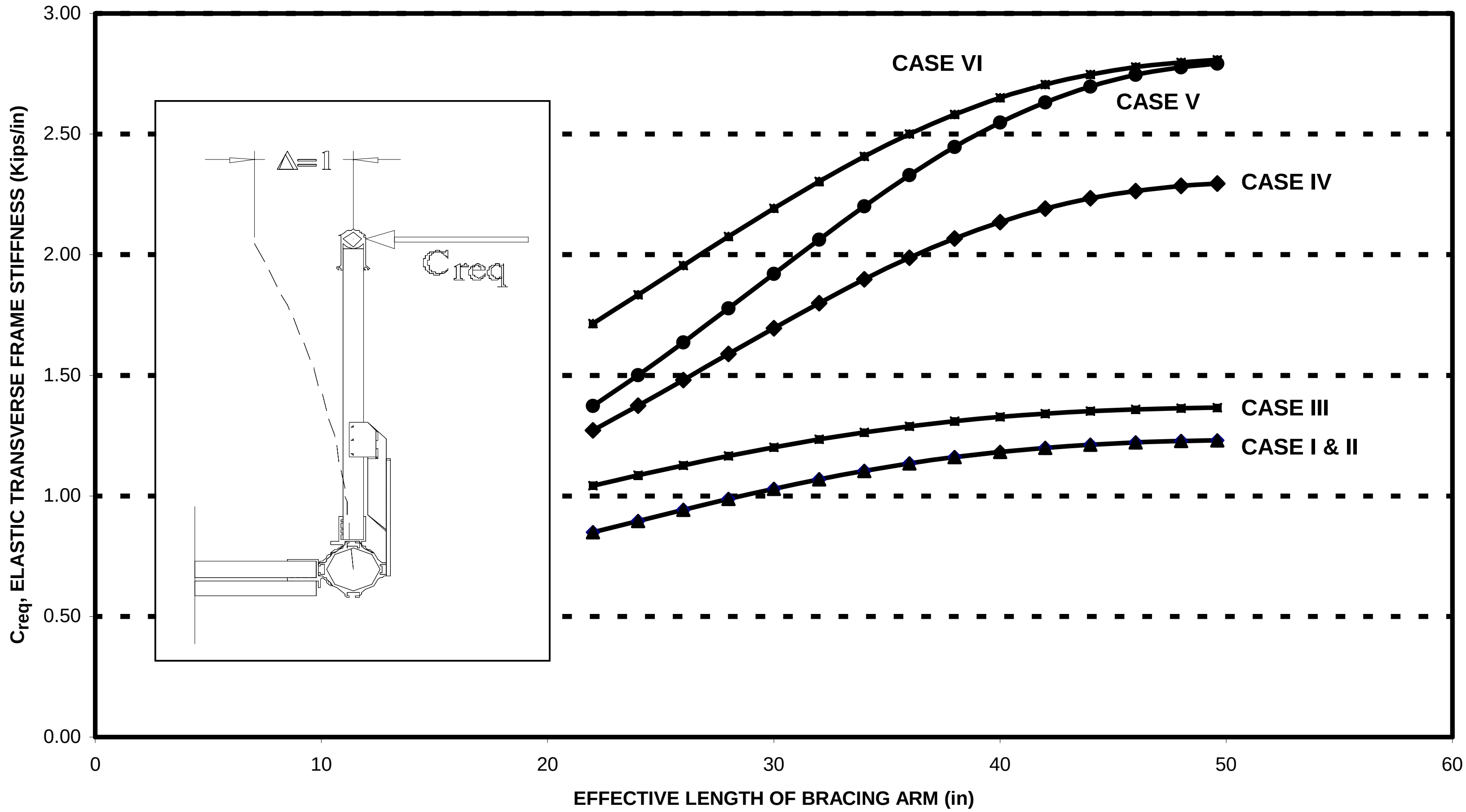

Figure 45: Vertical Post Composite Member – Effect of Bracing
Arm on Truss Lateral Stiffness

APPENDIX M

EFFECTIVE LENGTH FACTOR VS.

EFFECTIVE LENGTH OF BRACING ARM

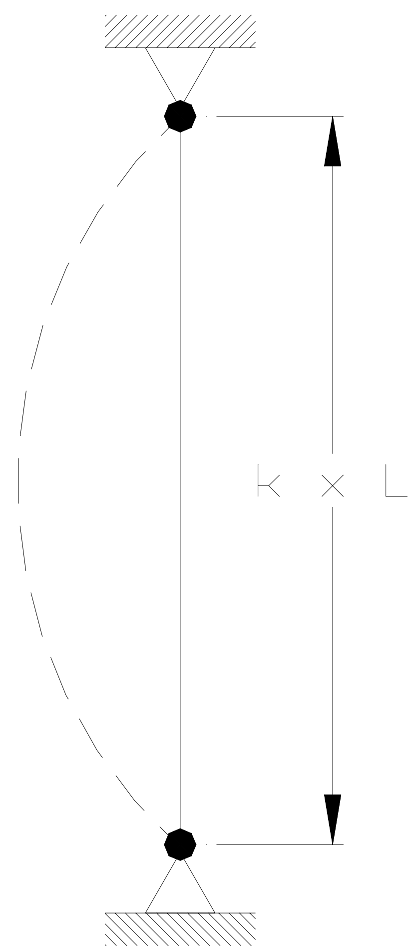

Figure 46: Composite Section – Column Line Diagram

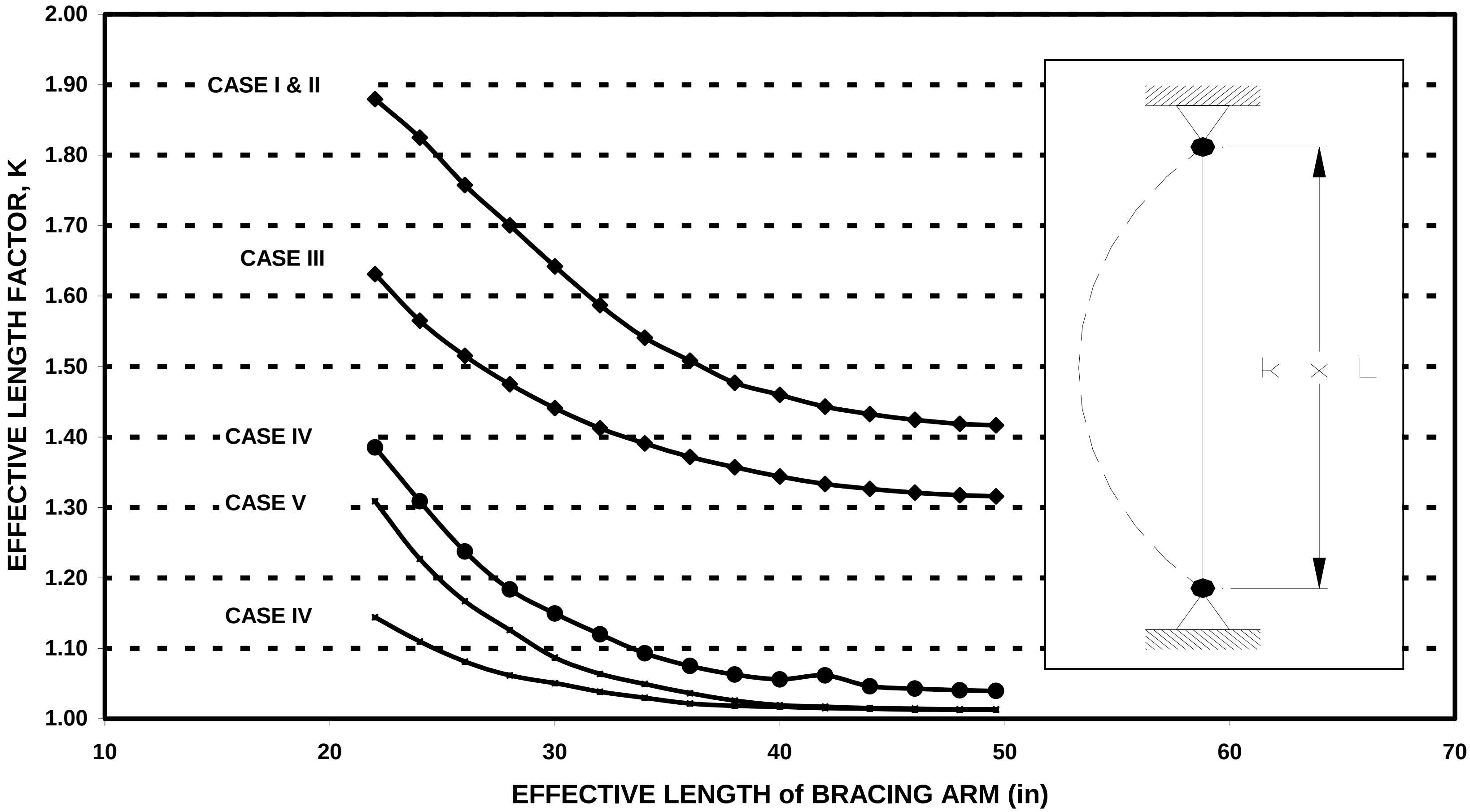

Figure 47: Vertical Post Composite Member – Effect of Bracing Arm on Column Effective Length Factor, k

APPENDIX N

OVERALL FACTOR OF SAFETY VS.

EFFECTIVE LENGTH OF BRACING ARM

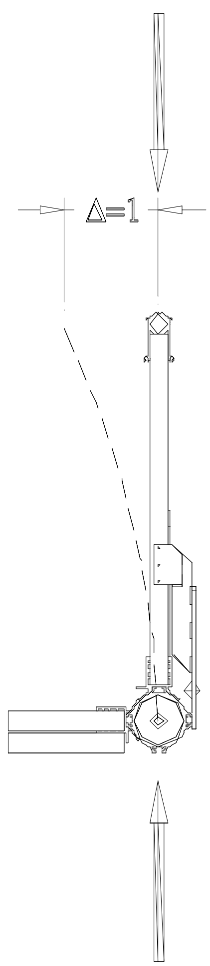

$FS = P_{ALLOW} / P_U$

- FS = Factor of Safety
- P_{ALLOW} = AA ADM Nominal Capacity
- P_U = Ultimate External Load

Figure 48: Vertical Post Composite Member – Factor of Safety

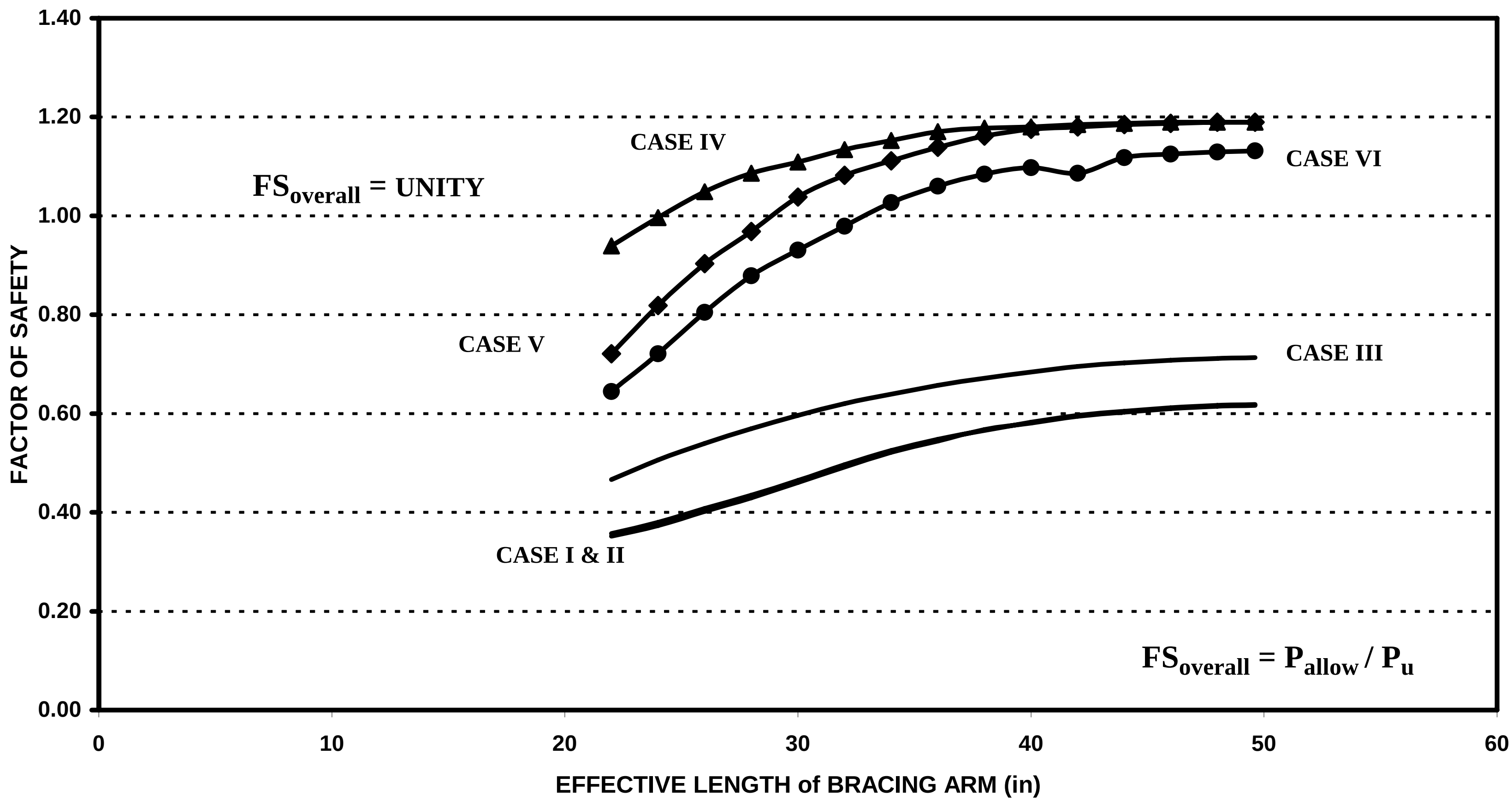

Figure 49: Vertical Post Composite Member – Effect of Bracing Arm on Top Cord Compressive Capacity (Factor of Safety)

APPENDIX O

DEFLECTION AND VIBRATION ANALYSIS

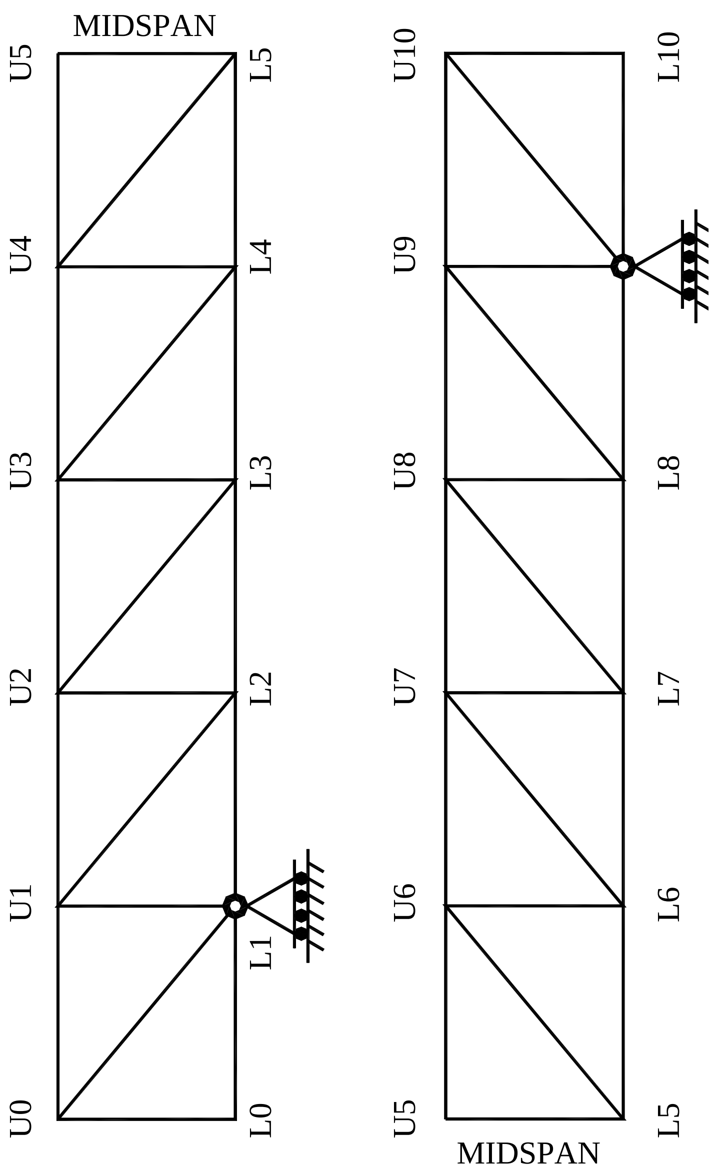

Figure 50: Bridge Layout

Table 32: Maximum Induced Forces on Truss Members – Deflection Analysis (Based on Controlling Load Combination)

Truss Frame consist of 10 Panels

Member Desidnation	Member Forces	Resultants (kips)	Live Load	Dead Load	D+.05L
Top Chord					
U0U1	0.893	2.947	2.590	0.366	0.495
U1U2	5.357	17.678	15.535	2.196	2.968
U2U3	9.822	32.413	28.484	4.027	5.441
U3U4	12.500	41.250	36.250	5.125	6.925
U4U5	13.393	44.197	38.840	5.491	7.420
Bottom Chord					
L0L1	0.000	0.000	0.000	0.000	0.000
L1L2	0.893	2.947	2.590	0.366	0.495
L2L3	5.357	17.678	15.535	2.196	2.968
L3L4	9.822	32.413	28.484	4.027	5.441
L4L5	12.500	41.250	36.250	5.125	6.925
Diagonal					
U0L1	1.023	3.376	2.967	0.419	0.567
U1L2	7.163	23.638	20.773	2.937	3.968
U2L3	5.116	16.883	14.836	2.098	2.834
U3L4	3.070	10.131	8.903	1.259	1.701
U4L5	1.023	3.376	2.967	0.419	0.567
Vertical Post					
U0L0	0.500	1.650	1.450	0.205	0.277
U1L1	3.500	11.550	10.150	1.435	1.939
U2L2	2.500	8.250	7.250	1.025	1.385
U3L3	1.500	4.950	4.350	0.615	0.831
U4L4	0.500	1.650	1.450	0.205	0.277
U5L5	0.000	0.000	0.000	0.000	0.000

Notes:

1. Member Forces come from Truss Analysis
2. Resultants (kips) = Member Forces x 3.30 kips
3. Live Load (kips) = Member Forces x 2.90 kips
4. Dead Load (kips) = Member Forces x 0.410 kips
5. D + 0.05L = Dead Load + 5%(Live Load) = Member Forces x 0.554 kips
6. Bridge has (8) Truss Panel in between Supports and (2) Panel overhang at the ends.

Table 33: Deflection Analysis based on Original Bridge Design

CASES I, II, V, & VI • Deflection under Live Load (ONLY)					
Truss Frame consisit of 10 Panels					
Member Desidnation	Memebers Length, L	Memebers Area, A	Member Live Force, F_L	Member Virtual Forces, F_v	$F_v(F_L L/A)$
	in	in^2	kips	kips	$kips^2/in$
Top Chord (TUBULAR PROFILE WITH FLAT PALTES)					
U0U1	98.42	6.273	-2.590	0.000	0.000
U1U2	98.42	6.273	-15.535	-0.893	217.660
U2U3	98.42	6.273	-28.484	-1.786	798.155
U3U4	98.42	6.273	-36.250	-2.678	1523.094
U4U5	98.42	6.273	-38.840	-3.571	2176.075
U5U6	98.42	6.273	-38.840	-3.571	2176.075
U6U7	98.42	6.273	-36.250	-2.678	1523.094
U7U8	98.42	6.273	-28.484	-1.786	798.155
U8U9	98.42	6.273	-15.535	-0.893	217.660
U9U10	98.42	6.273	-2.590	0.000	0.000
					9429.968
Bottom Chord (TOWER PROFILE)					
L0L1	98.42	9.038	0.000	0.000	0.000
L1L2	98.42	9.038	2.590	0.000	0.000
L2L3	98.42	9.038	15.535	0.893	151.071
L3L4	98.42	9.038	28.484	1.786	553.975
L4L5	98.42	9.038	36.250	2.678	1057.133
L5L6	98.42	9.038	36.250	2.678	1057.133
L6L7	98.42	9.038	28.484	1.786	553.975
L7L8	98.42	9.038	15.535	0.893	151.071
L8L9	98.42	9.038	2.590	0.000	0.000
L9L10	98.42	9.038	0.000	0.000	0.000
					3524.359
Diagonal (HOLLOW SQUARE TUBE)					
U0L1	112.81	3.028	2.9667	0.000	0.000
U1L2	112.81	3.028	20.7727	1.023	791.699
U2L3	112.81	3.028	14.8364	1.023	565.452
U3L4	112.81	3.028	8.903	1.023	339.316
U4L5	112.81	3.028	2.9667	1.023	113.068
U5L6	112.81	3.028	2.9667	1.023	113.068
U6L7	112.81	3.028	8.903	1.023	339.316
U7L8	112.81	3.028	14.8364	1.023	565.452
U8L9	112.81	3.028	20.7727	1.023	791.699
U9L10	112.81	3.028	2.9667	0.000	0.000
					3619.071
Vertical Post (HOLLOW SQUARE TUBE)					
U0L0	55.12	3.028	-1.450	0.000	0.000
U1L1	55.12	3.028	-10.150	-0.500	92.382
U2L2	55.12	3.028	-7.250	-0.500	65.987
U3L3	55.12	3.028	-4.350	-0.500	39.592
U4L4	55.12	3.028	-1.450	-0.500	13.197
U5L5	55.12	3.028	0.000	-0.500	0.000
U6L6	55.12	3.028	0.000	-0.500	0.000
U7L7	55.12	3.028	-1.450	-0.500	13.197
U8L8	55.12	3.028	-4.350	-0.500	39.592
U9L9	55.12	3.028	-7.250	-0.500	65.987
U10L10	55.12	3.028	-10.150	-0.500	92.382
U11L11	55.12	3.028	-1.450	0.000	0.000
					422.320

	$\Sigma F_v(FL/A)$	16995.718
E=10100 ksi	$\Delta_{midspan}$ (in)	1.683
E=10000 ksi	$\Delta_{midspan}$ (in)	1.700
	Δ_{max}(in) = 1.575	NOT OK!

Table 34: Deflection Analysis using Tower Profile as Top Chord

CASES I, II, V, & VI • Deflection under Live Load (ONLY)					
Truss Frame consisit of 10 Panels					
Member Desidnation	Memebers Length, L	Memebers Area, A	Member Live Forces, F	Member Virtual Forces, F_v	$F_V(FL/A)$
	in	in^2	kips	kips	$kips^2/in$
Top Chord (TOWER PROFILE)					
U0U1	98.42	9.038	-2.5897	0.000	0.000
U1U2	98.42	9.038	-15.5353	-0.893	151.071
U2U3	98.42	9.038	-28.4838	-1.786	553.975
U3U4	98.42	9.038	-36.25	-2.678	1057.133
U4U5	98.42	9.038	-38.8397	-3.571	1510.347
U5U6	98.42	9.038	-38.8397	-3.571	1510.347
U6U7	98.42	9.038	-36.25	-2.678	1057.133
U7U8	98.42	9.038	-28.4838	-1.786	553.975
U8U9	98.42	9.038	-15.5353	-0.893	151.071
U9U10	98.42	9.038	-2.5897	0.000	0.000
					6545.053
Bottom Chord (TOWER PROFILE)					
L0L1	98.42	9.038	0.000	0.000	0.000
L1L2	98.42	9.038	2.590	0.000	0.000
L2L3	98.42	9.038	15.535	0.893	151.071
L3L4	98.42	9.038	28.484	1.786	553.975
L4L5	98.42	9.038	36.250	2.678	1057.133
L5L6	98.42	9.038	36.250	2.678	1057.133
L6L7	98.42	9.038	28.484	1.786	553.975
L7L8	98.42	9.038	15.535	0.893	151.071
L8L9	98.42	9.038	2.590	0.000	0.000
L9L10	98.42	9.038	0.000	0.000	0.000
					3524.359
Diagonal (HOLLOW SQUARE TUBE)					
U0L1	112.81	3.028	2.9667	0.000	0.000
U1L2	112.81	3.028	20.7727	1.023	791.699
U2L3	112.81	3.028	14.8364	1.023	565.452
U3L4	112.81	3.028	8.903	1.023	339.316
U4L5	112.81	3.028	2.9667	1.023	113.068
U5L6	112.81	3.028	2.9667	1.023	113.068
U6L7	112.81	3.028	8.903	1.023	339.316
U7L8	112.81	3.028	14.8364	1.023	565.452
U8L9	112.81	3.028	20.7727	1.023	791.699
U9L10	112.81	3.028	2.9667	0.000	0.000
					3619.071
Vertical Post (HOLLOW SQUARE TUBE)					
U0L0	55.12	3.028	-1.450	0.000	0.000
U1L1	55.12	3.028	-10.150	-0.500	92.382
U2L2	55.12	3.028	-7.250	-0.500	65.987
U3L3	55.12	3.028	-4.350	-0.500	39.592
U4L4	55.12	3.028	-1.450	-0.500	13.197
U5L5	55.12	3.028	0.000	-0.500	0.000
U6L6	55.12	3.028	0.000	-0.500	0.000
U7L7	55.12	3.028	-1.450	-0.500	13.197
U8L8	55.12	3.028	-4.350	-0.500	39.592
U9L9	55.12	3.028	-7.250	-0.500	65.987
U10L10	55.12	3.028	-10.150	-0.500	92.382
U11L11	55.12	3.028	-1.450	0.000	0.000
					422.320

	$\Sigma F_V(FL/A)$	14110.803
E=10100 ksi	$\Delta_{midspan}$ (in)	1.397
E=10000 ksi	$\Delta_{midspan}$ (in)	1.411
	Δ_{max}(in) = 1.575	OK!

Table 35: Deflection Analysis based on Solid Diagonal and Post

CASES III & IV • Deflection under Live Load (ONLY)					
Truss consisit of 10 Panels					
Member Desidnation	Memebers Length, L	Memebers Area, A	Member Live Forces, F	Member Virtual Forces, F_v	$F_V(FL/A)$
	in	in^2	kips	kips	$kips^2/in$
Top Chord (TUBULAR PROFILE WITH FLAT PALTES)					
U0U1	98.42	6.273	-2.590	0.000	0.000
U1U2	98.42	6.273	-15.535	-0.893	217.660
U2U3	98.42	6.273	-28.484	-1.786	798.155
U3U4	98.42	6.273	-36.250	-2.678	1523.094
U4U5	98.42	6.273	-38.840	-3.571	2176.075
U5U6	98.42	6.273	-38.840	-3.571	2176.075
U6U7	98.42	6.273	-36.250	-2.678	1523.094
U7U8	98.42	6.273	-28.484	-1.786	798.155
U8U9	98.42	6.273	-15.535	-0.893	217.660
U9U10	98.42	6.273	-2.590	0.000	0.000
					9429.968
Bottom Chord (TOWER PROFILE)					
L0L1	98.42	9.038	0.000	0.000	0.000
L1L2	98.42	9.038	2.590	0.000	0.000
L2L3	98.42	9.038	15.535	0.893	151.071
L3L4	98.42	9.038	28.484	1.786	553.975
L4L5	98.42	9.038	36.250	2.678	1057.133
L5L6	98.42	9.038	36.250	2.678	1057.133
L6L7	98.42	9.038	28.484	1.786	553.975
L7L8	98.42	9.038	15.535	0.893	151.071
L8L9	98.42	9.038	2.590	0.000	0.000
L9L10	98.42	9.038	0.000	0.000	0.000
					3524.359
Diagonal (SOLID SQUARE)					
U0L1	112.81	4.808	2.967	0.000	0.000
U1L2	112.81	4.808	20.773	1.023	498.599
U2L3	112.81	4.808	14.836	1.023	356.113
U3L4	112.81	4.808	8.903	1.023	213.695
U4L5	112.81	4.808	2.967	1.023	71.209
U5L6	112.81	4.808	2.967	1.023	71.209
U6L7	112.81	4.808	8.903	1.023	213.695
U7L8	112.81	4.808	14.836	1.023	356.113
U8L9	112.81	4.808	20.773	1.023	498.599
U9L10	112.81	4.808	2.967	0.000	0.000
					2279.232
Vertical Post (SOLID SQUARE)					
U0L0	55.12	4.808	-1.450	0.000	0.000
U1L1	55.12	4.808	-10.150	-0.500	58.181
U2L2	55.12	4.808	-7.250	-0.500	41.558
U3L3	55.12	4.808	-4.350	-0.500	24.935
U4L4	55.12	4.808	-1.450	-0.500	8.312
U5L5	55.12	4.808	0.000	-0.500	0.000
U6L6	55.12	4.808	0.000	-0.500	0.000
U7L7	55.12	4.808	-1.450	-0.500	8.312
U8L8	55.12	4.808	-4.350	-0.500	24.935
U9L9	55.12	4.808	-7.250	-0.500	41.558
U10L10	55.12	4.808	-10.150	-0.500	58.181
U11L11	55.12	4.808	-1.450	0.000	0.000
					265.970

	$\Sigma F_V(FL/A)$	15499.529
E=10100 ksi	$\Delta_{midspan}$ (in)	1.535
E=10000 ksi	$\Delta_{midspan}$ (in)	1.550
	Δ_{max}(in) = 1.575	OK!

Vibration Analysis

The fundamental frequency of a pedestrian bridge with no imposed live load should be greater that 3.0 hertz (Hz) to evade throughout its service life the first harmonic. In case the fundamental frequency cannot comply with such design requirement, or if the second harmonic is a potential issue of interest then an appraisal for the structural dynamic performance shall be carried out on the bridge.

In conformance to such limitation, the overall design of the bridge structure shall be so as to provide elements proportioned with the intention that the fundamental frequency results greater than:

$$F \geq 2.86 \ln (180/W)$$

where "ln " correspond to the natural logarithm and W is the actual weight (kips) of the supported pedestrian bridge, which also must include the dead load and any allowance for actual pedestrian live loads present. Alternatively, the minimum supported structure weight (W) shall be larger than:

$$W \geq 180\, e^{(-0.35\, f)}$$

where "f" is the fundamental frequency of the structure (hertz).

Calculations for Cases I, II, V, and VI:

A. Fundamental Frequency;

i. $f = 0.18\,[(32.2\ \text{ft/s}^2) / (0.20\ \text{in})(1\ \text{ft}/12\ \text{in})] = 7.91\ \text{Hz} > 3.0\ \text{Hz}$ (<u>Adequate</u>)

B. Assuming a higher harmonic frequency is a concern:

i. W = 2[(2)(10.579) + (2)(3.544) + 21.475 + 3.554] plf x 82.02 ft

= 8.74 kips

ii. f = 2.86 ln (180/8.74) = 8.65 Hz

C. Assuming an allowance for any possible live load (LL); W = DL + 0.05LL

i. W = 8.74 kips + 2[0.05(350 plf)(82.02 ft)/1000]

= 10.18 kips

ii. f = 2.86 ln (180/10.18) = 8.22 Hz (<u>Adequate</u>)